AD-A188 858 A MOMENT APPROACH TO MODELING NEGATIVE ION SOURCES(U) 1/2
AIR FORCE INST OF TECH WRIGHT-PATTERSON AFB OH SCHOOL
OF ENGINEERING D E BELL DEC 87 AFIT/GEP/ENP/87D-2
UNCLASSIFIED F/G 20/7 NL

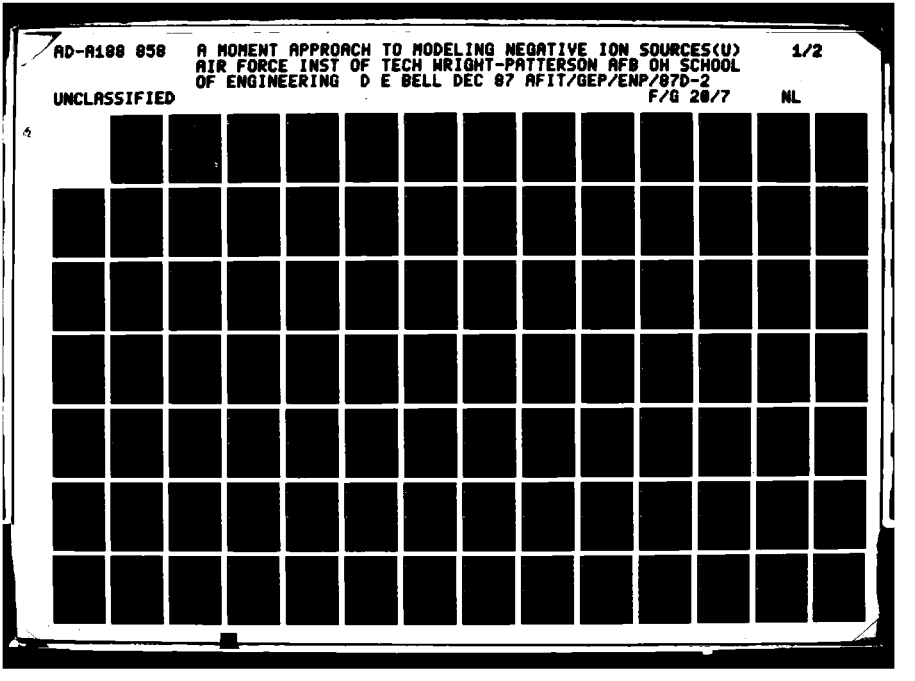

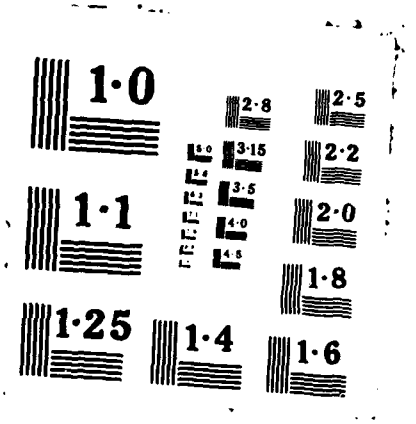
1·0
1·1
1·25
1·4
1·6
1·8
2·0
2·2
2·5
2·8
3·15
3·5
4·0
4·5

A MOMENT APPROACH TO MODELING NEGATIVE ION SOURCES

THESIS

David E. Bell, B.S.
Second Lieutenant, USAF

AFIT/GEP/ENP/87D-2

DEPARTMENT OF THE AIR FORCE
AIR UNIVERSITY
AIR FORCE INSTITUTE OF TECHNOLOGY

Wright-Patterson Air Force Base, Ohio

AFIT/GEP/ENP/87D-2

A MOMENT APPROACH TO MODELING NEGATIVE ION SOURCES

THESIS

David E. Bell, B.S.
Second Lieutenant, USAF

AFIT/GEP/ENP/87D-2

Approved for public release; distribution unlimited

AFIT/GEP/ENP/87D-2

A MOMENT APPROACH TO MODELING NEGATIVE ION SOURCES

THESIS

Presented to the Faculty of the School of Engineering

of the Air Force Institute of Technology

Air University

In Partial Fulfillment of the

Requirements for the Degree of

Master of Science (Engineering Physics)

David E. Bell, B.S.

Second Lieutenant, USAF

December 1987

ACKNOWLEDGEMENTS

I would like to thank my thesis advisor, Dr. William F. Bailey, for motivating this study and for his immense help and extremely useful suggestions throughout the study. I would also like to thank him for his advice in areas unrelated to this thesis. Next, I would like to express my gratitude to Lt. Col. Howard Evans and to Dr. Alan Garscadden for their helpful suggestions and comments on this manuscript. I would also like to express my gratitude to Maj. James Lupo, who wrote the graphics routines that I used to produce the figures in this thesis.

Finally, my deepest appreciation and love goes to my wife, Leticia, who has given me so much support throughout this study. She was always there with words of encouragement when I needed them and extreme patience when I would get carried away with my work. Without her support, this thesis could never have been completed.

TABLE OF CONTENTS

ABSTRACT

Relativistic neutral particle beams (NPBs) offer the potential for highly lethal space-based weapon systems and decoy discriminators. These uses of NPBs have motivated extensive theoretical and experimental studies of negative ion sources. Negative ion sources are divided into two categories: surface sources - such as the Penning discharge, and volume sources - such as the magnetic multicusp discharge. The negative ion beam required as input to a NPB system should be of high current and low emittance. Surface sources produce a high current, high emittance negative ion beam; whereas, volume sources produce a low current, low emittance beam. Due to the use of reactive elements, such as cesium, in surface sources, they have a much shorter useful lifetime than volume sources. While current limitations may preclude the use of volume sources in NPB weapon systems, they are excellent candidates for use in NPB discrimination systems. Thus, a typical volume source was chosen as the topic of this thesis.

This study considers negative ion production in a magnetic multicusp ion source. A self-consistent model based on Maxwellian moments of the Boltzmann equation is presented. The departure of the electron energy distribution from a Maxwellian is also discussed and incorporated. The results of this model for discharge currents ranging from 1-100 A, for pressures ranging from 1-100 mTorr, and for voltages ranging from 20-100 V are compared to previous studies and

used to formulate scaling laws. The scaling laws predicted for the negative ion density are seen to be supported by previous experimental observations. Finally, the scaling laws are used to predict the optimum operating regime for a magnetic multicusp ion source.

CHAPTER I - INTRODUCTION

The use of neutral particle beams in heating of fusion plasmas and in weapons research has motivated considerable interest in the study of sources that produce beams of negative ions with high brightness and low emmitance. One such source of interest is the magnetic multicusp ion source. Many experimental and theoretical studies have been conducted on this type of source in order to determine the processes involved in the volume production of negative hydrogen ions and in order to optimize the ion production. Before these studies are discussed, a typical magnetic multicusp ion source will be described.

The Magnetic Multicusp Ion Source

The magnetic multicusp ion source (MMIS) was originally developed to improve the containment of a collisionless quiescent plasma [1]. A source of this type consists of a metal container with some wire filaments on one wall (see Fig. 1). The container is filled with low pressure H_2 gas (1-40 mTorr, typically) and a current is passed through the filaments causing thermionic emission of electrons. The filaments (cathode) are typically biased negative with respect to the chamber walls (anode) in order to accelerate the emitted electrons through the hydrogen gas, creating a plasma.

What makes a MMIS special is that the outer walls of the

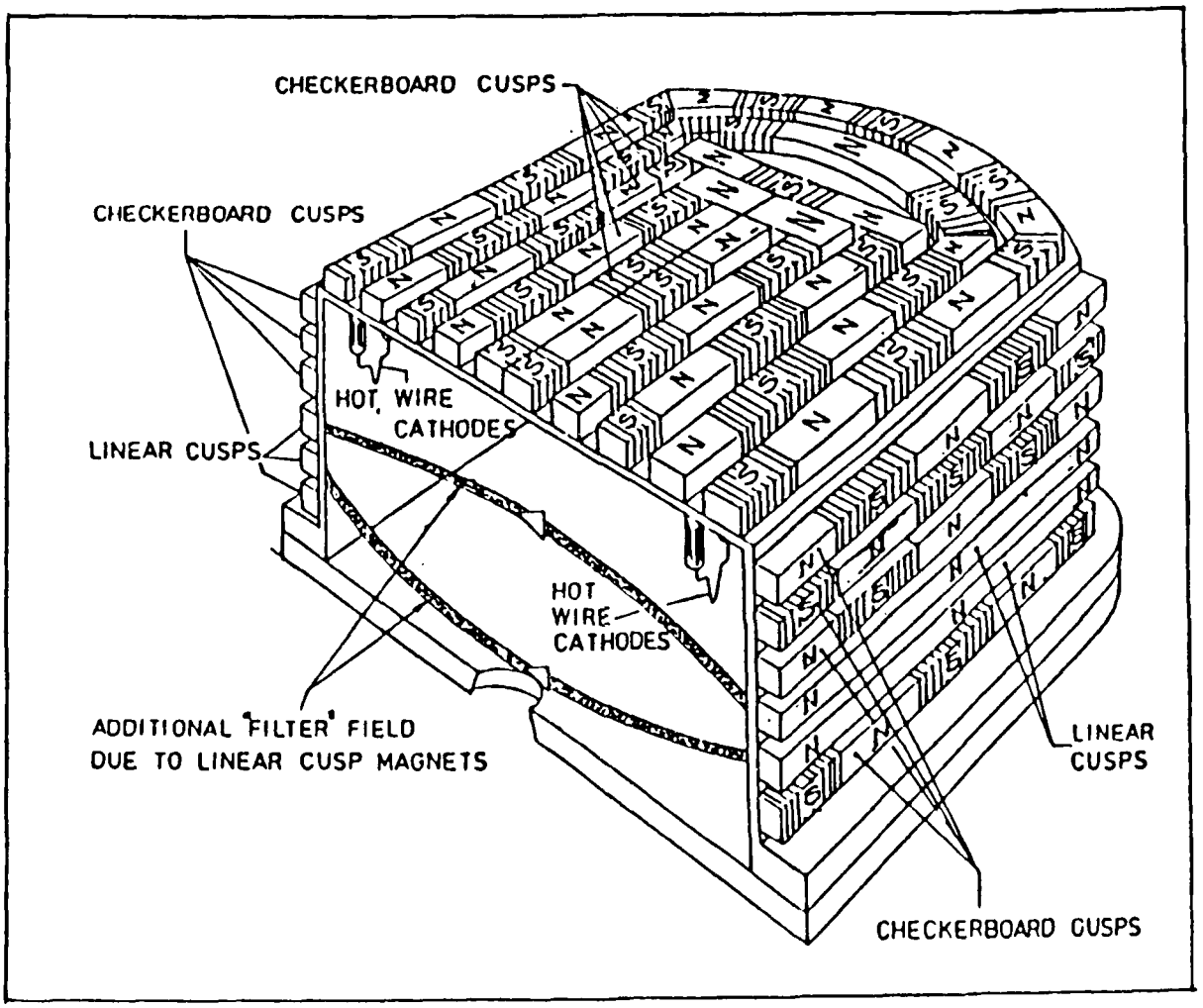

Fig. 1 - Diagram of a typical magnetic multicusp ion source with tandem filter. [4:215]

chamber are covered by a checkerboard array of permanent magnets. Without the magnets the electrons are quickly accelerated into the walls of the chamber and lost from the plasma. This results in a low ionization efficiency for the electrons. With the magnets in place, a complex multipole (or multicusp - hence, the name) magnetic field exists at the wall. This field tends to reflect the energetic electrons back into the plasma [2:1822]. Thus the ionization efficiency of the electrons is improved. This can be verified by looking at the electron containment time; it is found [3] that with the magnets in place the containment time is much improved.

It has been proposed that negative hydrogen ions are produced by these energetic electrons in a two-step process [5:223]. First, the energetic electrons ($E \geq 20$ eV) collide with molecular hydrogen and electronically excite the hydrogen. The excited hydrogen then undergoes an electronic-vibrational transition, producing vibrationally excited hydrogen. This vibrationally excited hydrogen then collides with slow electrons ($E \leq 2$ eV). The electrons undergo dissociative attachment onto the hydrogen, producing H^-. Thus we have the two processes:

$$e_{fast} + H_2[X^1\Sigma^+_g(v=0)] \rightarrow H_2[B^1\Sigma^+_u, C^1\Pi_u, \ldots, v'] + e \rightarrow H_2[X^1\Sigma^+_g(v'')] + e + h\nu \qquad (1)$$

$$e_{slow} + H_2(v'') \rightarrow H^- + H \qquad (2)$$

The negative ions produced can be lost through several

processes which include detachment induced by energetic electrons and mutual neutralization with positive ions. In order to reduce losses caused by the energetic electrons, a linear cusp of permanent magnets is added to the walls of the chamber, as shown in Fig. 1. These magnets introduce a sheet of magnetic field into the plasma separating the discharge region into two sections. The first is called the production region and is adjacent to the filaments. In this region, the energetic electrons produce the vibrationally excited H_2. The neutral species and the thermal electrons then drift across the magnetic field into the extraction region. It is here that the dissociative attachment occurs. The energetic electrons are unable to pass through the magnetic field; hence the naming of this field as the filter field. A MMIS with such a filter field is often referred to as a tandem discharge.

Further optimization of a MMIS is the subject of several studies that have been performed [2,6-9]. In particular, much work has been concentrated on consistently modeling the plasma discharge. Bretagne, *et al*, [10] numerically solved the Boltzmann equation to calculate the electron energy distribution function in the H_2 discharge. This allowed them to determine scaling laws for H^- production in terms of discharge current, discharge voltage, and neutral gas pressure. These detailed calculations produced good agreement with experimental data; however, they are very tedious to perform.

Problem and Scope

The present study is concerned with a simplified approach to modeling the magnetic multicusp H_2 discharge using Maxwellian moments of the Boltzmann equation. A preliminary study of this approach [11] has yielded results consistent with both experimental data and detailed theoretical calculations. This thesis takes a more self-consistent approach towards modeling a MMIS using moment equations. This approach will make it easier to determine scaling laws for H^- production in terms of the plasma parameters, thus allowing the optimum operating regime of the MMIS to be determined.

Approach

This research began with a compilation of the cross-section data for the relevant processes within the hydrogen discharge. This data was then transformed into average collision rates (cm^3/sec) assuming a Maxwellian distribution. Next, the density and energy moments of the Boltzmann equation were developed with consideration to the plasma chemistry. These time-dependent, coupled equations were then solved numerically, yielding the time evolution of the electron temperature and the densities of the electrons and ions. The resulting data were compared to experimental and theoretical data for verification of the model. Finally, scaling laws with discharge parameters were determined.

CHAPTER II - THE MOMENT APPROACH

In this chapter, the reactive and non-reactive kinetics of the hydrogen discharge will be presented. Based on the identified processes, Maxwellian moments of the Boltzmann equation will then be developed. Finally, the numerical solution of the moment equations will be examined.

Processes Occurring in a Hydrogen Discharge

In considering the relevant reactions occurring in the hydrogen discharge, it is necessary to look at production and loss mechanisms for all of the species being considered. In this study these species were: electrons (e), negative hydrogen ions (H^-), positive hydrogen ions (both H_2^+ and H^+), and vibrationally excited hydrogen molecules ($H_2(v)$). In addition, the electron temperature was modeled.

All of the reactions will be characterized by a rate coefficient, $R_i(E)$ (in cm^3/sec), that indicates the rate at which the reaction proceeds for an interaction energy E.

Reaction rates are given by the expression

$$R_i(E) = \sigma_i(E)\, v(E) \qquad (3)$$

where R_i is the reaction rate for process i, σ_i is the cross-section for an interaction energy E for process i, and v is the relative velocity of interaction written in terms of energy. Since the reactions dealt with here are between electrons and heavier particles, it is assumed that the interaction energy is simply the electron energy.

In using Maxwellian moments of the Boltzmann equation, it will be necessary to use an average value for the reaction rates, $\langle R_i \rangle$. This averaging is done over a Maxwell-Boltzmann distribution:

$$\langle R_i \rangle = \frac{\int \sigma_i(E)\, v(E)\, f_{MB}(E)\, dE}{n_e} \qquad (4)$$

with

$$f_{MB}(E) = 2/\sqrt{\pi}\; n_e\; (T_e)^{-3/2}\; \sqrt{E}\; e^{-E/T_e} \qquad (5)$$

where T_e is the electron temperature (in eV) and n_e is the electron density (in cm^{-3}).

The cross-section data used for most of the reactions considered in this paper are experimental. This prevented the need to make complex theoretical calculations for this moment approach. References to the source of cross-section data is given in the form [data-XX:XXX] after the reaction is introduced. For those cases that pre-calculated reaction rate data is used, the reference is in the form [rate-XX:XXX].

Production and loss of H^-

It has been indicated [6:1247] that the primary production mechanism for H^- in a MMIS is through dissociative attachment of low energy electrons onto vibrationally excited H_2. Another contributing process [12:L22] is the dissociative recombination of an electron onto H_2^+ (in this study

this will be called polarized dissociation to differentiate it from dissociative recombination resulting in neutral products). These two reactions can be written as:

Dissociative Attachment (att) [rate-13:918]

$$e + H_2(v) \rightarrow H + H^- \quad (6)$$

Polarized Dissociation (pdiss) [data-14:1572]

$$e + H_2^+ \rightarrow H^+ + H^- \quad (7)$$

Four loss mechanisms of H^- are considered. The first three are collisional detachment processes [15:73]. These are detachment by an electron, associative detachment with atomic hydrogen, and detachment by atomic hydrogen. The fourth process is mutual neutralization with H^+. These reactions can be written as:

Electron Detachment (edet) [data-16:1347]

$$e + H^- \rightarrow H + 2e \quad (8)$$

Associative Detachment (adet) [rate-17:231]

$$H + H^- \rightarrow e + H_2 \quad (9)$$

Hydrogen Detachment (hdet) [rate-17:232]

$$H + H^- \rightarrow 2H + e \quad (10)$$

Mutual Neutralization (mneut) [data-18:437,19:L370]

$$H^+ + H^- \rightarrow H + H \quad (11)$$

These six reactions constitute the production and loss mechanisms for H^- ions that will be considered in this paper.

The cross-sections for Eqns. 7, 8, and 11 are shown in Fig. 2.

Production and loss of electrons

Looking at the electron energy distribution function (EEDF) for a typical MMIS, shown in Fig. 3 (from Bretagne, *et al*), it is seen that there are two distinct regions to the distribution. For low energies, the distribution is characteristic of a Maxwellian distribution of electrons. For higher energies, the distribution becomes non-Maxwellian. This indicates that electrons in the discharge can be divided into two species: fast electrons (E > 10 eV) and slow electrons (E < 10 eV). In this study, the slow electrons (which are dominant) are the species primarily considered. The fast electrons are treated as a production mechanism for the slow electrons, for vibrationally excited hydrogen, and for positive hydrogen ions. Handling the electrons in this manner makes it possible to use Maxwellian moments of the Boltzmann equation and get good results, even with the distribution being non-Maxwellian. The fast electrons will be treated in a later section. This section will deal with the slow electrons only.

Slow electrons are produced through five reactions. The first three are the detachment processes listed in the previous section (Eqns. 8-10). The other two are ionization

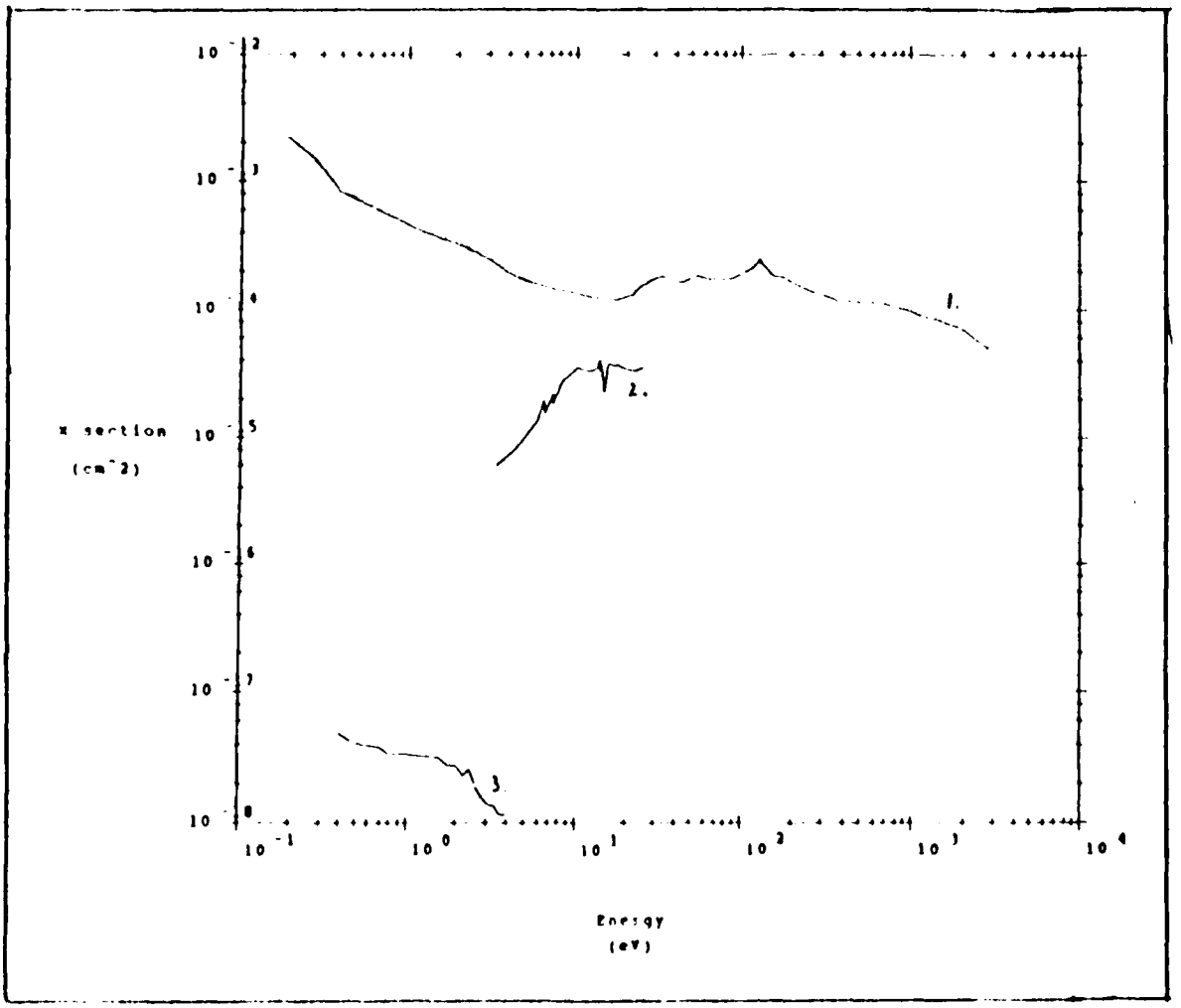

Fig. 2 - Cross-section data used for calculating negative ion density. 1 - mneut, 2 - edet, 3 - pdiss.

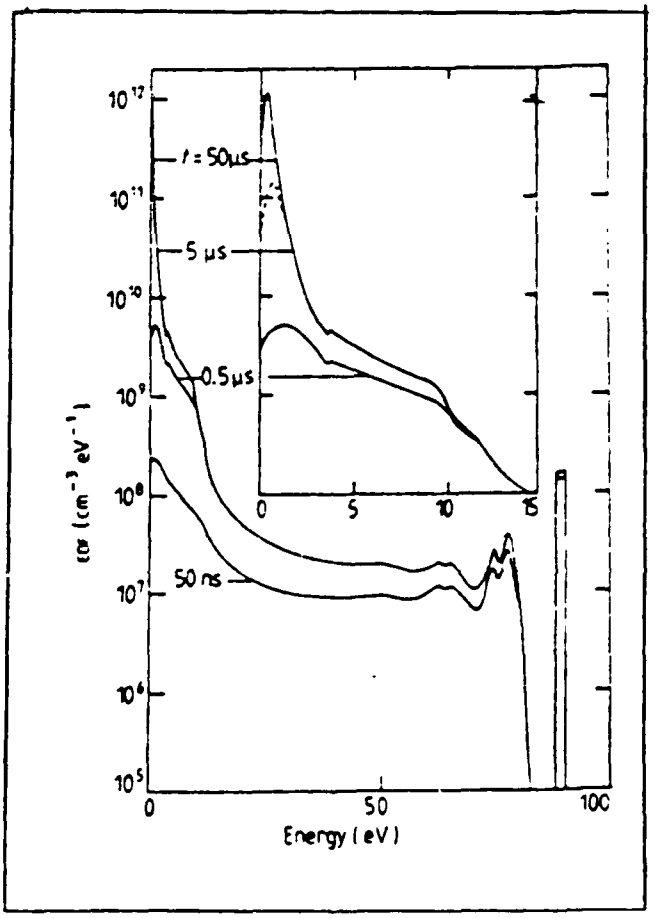

Fig. 3 - EEDF calculated by Bretagne, *et al*, [10:816] for a 40 mTorr, 90 V, 10 A discharge with 56% dissociation.

reactions:

H_2 Ionization (h2ion) [data-20:1471]

$$H_2 + e \rightarrow H_2^+ + 2e \qquad (12)$$

H Ionization (hion) [data-21:1948]

$$H + e \rightarrow H^+ + 2e \qquad (13)$$

In addition to these reactions, slow electrons are produced when the fast electrons undergo ionizing collisions. This production term will be considered when the fast electrons are studied.

Electrons are lost through five processes also. These are dissociative attachment (Eqn. 6), polarized dissociation (Eqn. 7), three-body recombination of both H^+ and H_2^+, and dissociative recombination. These last three reactions are written:

H_2^+ Recombination (h2rec)

$$H_2^+ + 2e \rightarrow H_2 + e \qquad (14)$$

H^+ Recombination (hrec)

$$H^+ + 2e \rightarrow H + e \qquad (15)$$

Dissociative Recombination (drec) [data-22:241]

$$H_2^+ + e \rightarrow H + H \qquad (16)$$

For the three-body recombination rates, the equation given by Golant, *et al*, [23:68] was used. This equation is

$$\langle R_{rec} \rangle = a \frac{e^{10}}{\sqrt{m_e}} \frac{n_e}{T_e^{4.5}} \approx 8.75 \times 10^{-27} T_e^{-4.5} n_e \qquad (17)$$

where α is a coefficient of the order of unity, e is the electron charge, and m_e is the electron mass.

The cross-sections for Eqns. 12, 13, and 16 are shown in Fig. 4.

Production and loss of H_2^+

Positive hydrogen ions are produced through two ionization processes. The first is through ionization (Eqn. 12) by the slow electrons. The second is through ionization caused by the fast electrons. This second process will be considered in the section where fast electrons are dealt with.

The loss processes considered for H_2^+ are dissociative recombination (Eqn. 16), polarized dissociation (Eqn. 7), and three-body recombination (Eqn. 14).

Production and loss of H^+

Positive ions of atomic hydrogen are produced through the processes of ionization (Eqn. 13) and polarized dissociation (Eqn. 7). They are lost through three-body recombination (Eqn. 15) and mutual neutralization (Eqn. 11).

Production and loss of vibrationally excited H_2

Vibrationally excited hydrogen molecules are produced through E-V processes, as was indicated in Chapter I. It has been determined through isotope studies [6:1247] that vibrational levels with $6 \leq v \geq 10$ are the primary contributors to the production of H^- through dissociative attachment in a

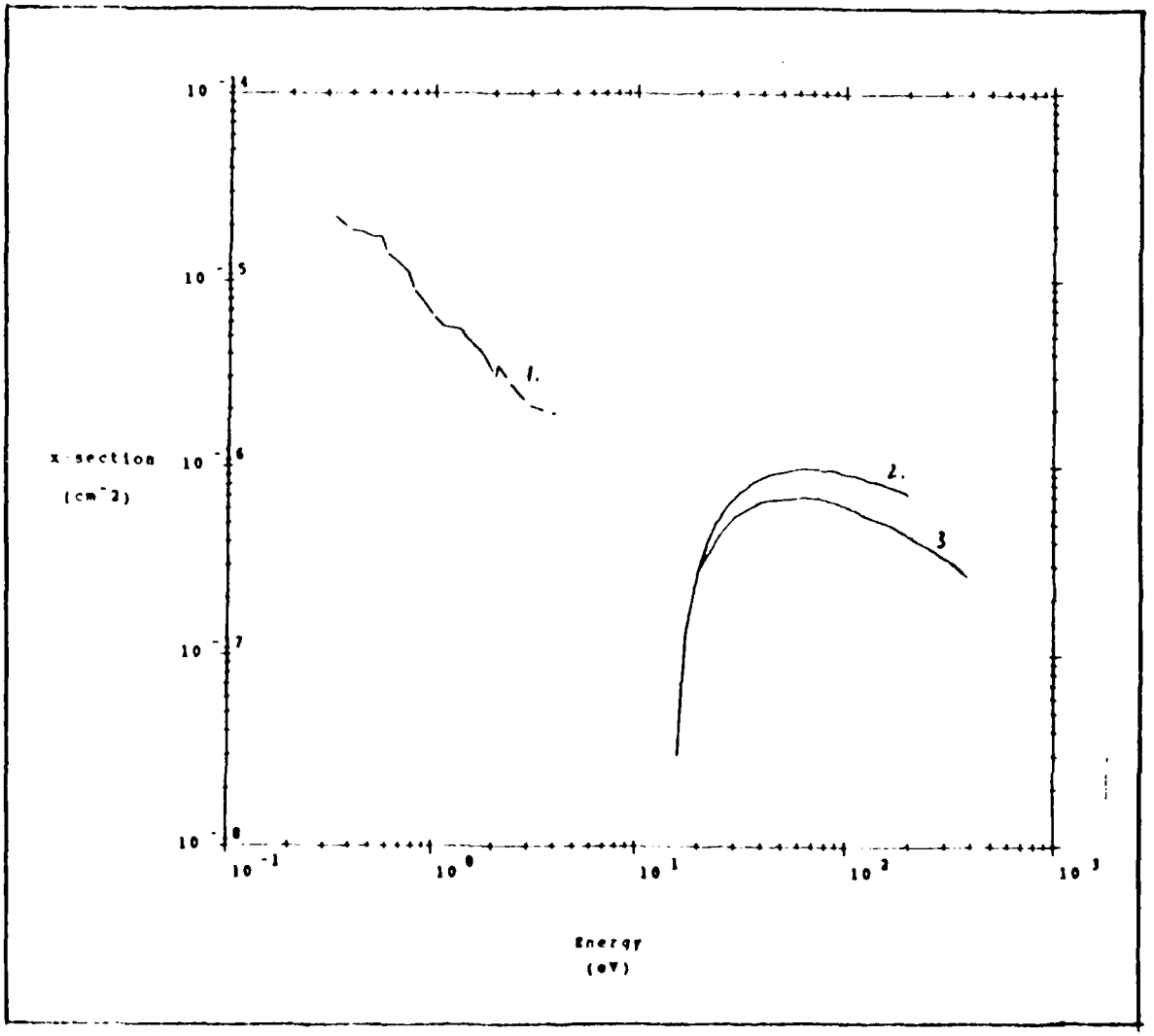

Fig. 4 - Cross-sections used for calculating electron density. 1 - drec, 2 - h2ion, 3 - hion

MMIS. These levels are populated by fast electrons electronically exciting H_2 and then the hydrogen undergoing radiative relaxation into a vibrationally excited state (Eqn. 1) [24:51]. A typical vibrational distribution is shown in Fig. 5. It is seen that these levels lie along a plateau of the distribution, indicating that the vibrational densities for levels 6 to 10 are approximately equal. If the average reaction rates for dissociative attachment are now looked at (see Fig. 6), it is seen that the reaction rate increases for increasing vibrational level. Combining a knowledge of the vibrational distribution with the average reaction rates for dissociative attachment it is apparent that only the vibrational levels between 6 and 10 should contribute, as was indicated.

For this work a representative population $H_2(v)$, which represents an average value for the vibrational densities between v=6 and v=10, is used. In addition, for the average reaction rate for dissociative attachment, the average for the reaction rates between v=6 and v=10 is used.

The electronic excitations used to populate this average vibrational level are:

$$e + H_2(X) \rightarrow e + H_2(B'^1\Sigma^+_u) \quad \text{[data-25:1511]} \quad (18)$$

$$e + H_2(X) \rightarrow e + H_2(B''^1\Sigma^+_u) \quad \text{[data-25:1511]} \quad (19)$$

$$e + H_2(X) \rightarrow e + H_2(D^1\Pi_u) \quad \text{[data-25:1511]} \quad (20)$$

$$e + H_2(X) \rightarrow e + H_2(D'^1\Pi_u) \quad \text{[data-25:1511]} \quad (21)$$

$$e + H_2(X) \rightarrow e + H_2(E\text{-}F^1\Sigma^+_g) \quad \text{[data-25:1511]} \quad (22)$$

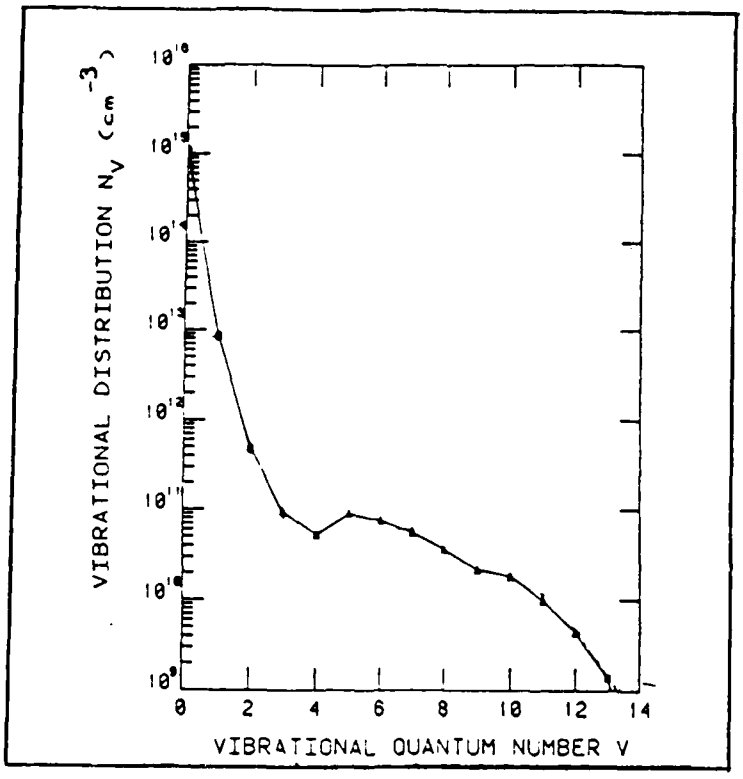

Fig. 5 - Typical vibrational population distribution in a multicusp source (from Gorse, *et al* [27]).

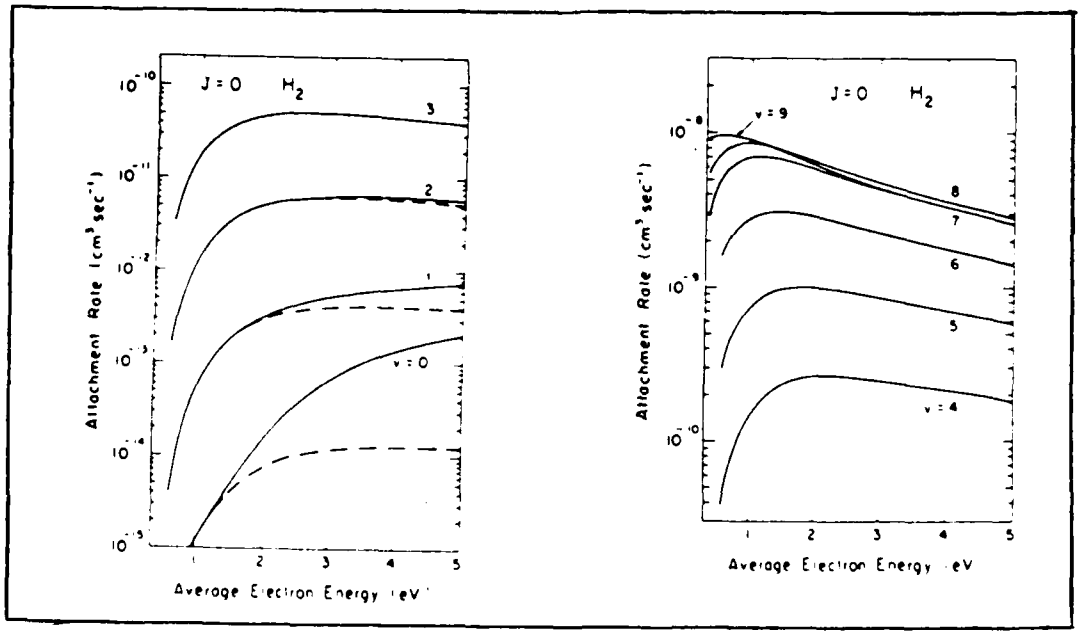

Fig. 6 - Rate of dissociative attachment as a function of vibrational level (from Wadehra [13:918]).

$$e + H_2(X) \rightarrow e + H_2(a^3\Sigma^+_g) \quad \text{[data-26:1886]} \quad (23)$$

$$e + H_2(X) \rightarrow e + H_2(b^3\Sigma^+_u) \quad \text{[data-26:1886]} \quad (24)$$

$$e + H_2(X) \rightarrow e + H_2(c^3\Pi_u) \quad \text{[data-26:1886]} \quad (25)$$

It is assumed in this work that each of these excitations will proceed to relax into a vibrational state, producing $H_2(v)$. The cross-sections for these reactions are given in Fig. 7. The choice of which electronic excitations to use was guided by the work of Bretagne, *et al* [10:814].

Vibrationally excited hydrogen is considered to be lost through three processes in this study. It is lost through dissociative attachment, through wall collisions, and through vibrational-translational (V-T) relaxation.

V-T relaxation is given by the reaction [27:4]

$$H_2(v) + H \rightarrow H_2(v=0) + H \quad (26)$$

The rate coefficient for the $v=1 \rightarrow v=0$ reaction is given by [27:4]

$$\langle R_{VT} \rangle \approx 1.5 \times 10^{-10} e^{-.1603/T_g} \text{ cm}^3/\text{sec} \quad (27)$$

where T_g is the gas temperature in eV. Gorse, *et al*, say that the rate coefficients for higher vibrational levels have a v^3 dependence at low gas temperature, and are linear with v at high gas temperature. In this study, a gas temperature of about 450 K was used, thus the linear dependence of $\langle R_{VT} \rangle$ was assumed. Since levels between 6 and 10 are considered, $\langle R_{VT} \rangle$ given in Eqn. 27 was multiplied by the average value of v, i.e.- by a factor of 8.

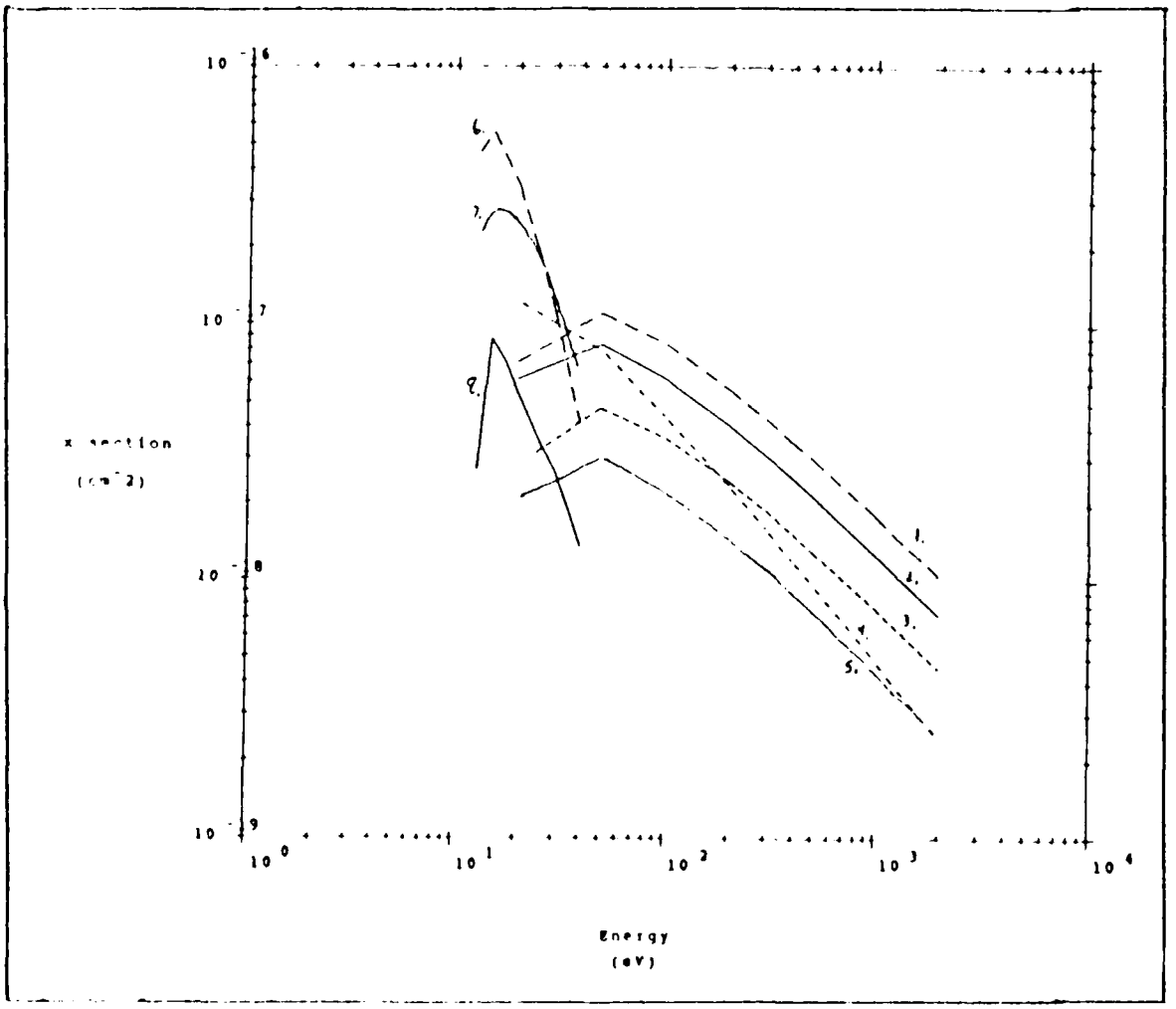

Fig. 7 - Electronic excitation cross-sections used to calculate vibrational population. 1 - $D^1\Pi_u$, 2 - $B'^1\Sigma^+_u$, 3 - $D'^1\Pi_u$, 4 - E-$F^1\Sigma^+_g$, 5 - $B''^1\Sigma^+_u$, 6 - $c^3\Pi_u$, 7 - $b^3\Sigma^+_u$, 8 - $a^3\Sigma^+_g$.

For wall losses of $H_2(v)$, it was assumed that 10 collisions with the walls were necessary to bring the excited hydrogen back to the v=0 state. The frequency of wall collisions can be written (assuming free-flight to the wall) as the ratio of H_2 velocity to the average distance to the wall, or, in terms of the gas temperature,

$$\nu_{vibwall} = 1.56 \times 10^6 \frac{\sqrt{T_g/2}}{L} \qquad (28)$$

where L is the average distance to the walls of the discharge. Thus the frequency of loss of vibrationally excited hydrogen to the walls is $\nu_{vibwall}/10$.

The fast electrons

It has already been indicated that the electron distribution can be divided into two distinct portions. The low energy part of the distribution can be approximated by a Maxwellian distribution of electrons. In this part of the distribution, the electrons are dominated by electron-electron collisions and a thermal distribution exists. The high energy portion of the distribution is where electron-neutral collisions dominate.

The problem is in how to approximate the high energy tail of the distribution. These high energy electrons are produced by electrons being thermionically emitted from the filaments in the discharge. These emitted electrons then undergo ionizing collisions in the plasma producing high energy, or secondary, electrons, and positive hydrogen ions.

The strength of the source (number of secondary electrons produced per second per unit volume) is given by

$$S_o = \frac{I}{e\, V_{ol}} \frac{V}{2\, E_I} \qquad (29)$$

where I is the discharge current, V_{ol} is the plasma volume, V is the discharge voltage, and E_I is the ionization energy for H_2 (in Volts). It is assumed that each emitted electron will have an ionizing collision with H_2, producing H_2^+ and a secondary electron. With this assumption, the classical Thomson theory of ionization is used to determine the distribution of secondary electrons. According to this theory (see Appendix A) the secondary electron distribution is given by

$$f_{thom}(E) = \frac{E_I\ (1 + E_I/V)}{(E + E_I)^2} \qquad 0 \le E \le V \qquad (30)$$

To determine the actual tail of the EEDF, a balance between the source production and collisional and wall losses is considered. If $f_{tail}(E)$ is the distribution of fast electrons, $\nu_{coll}(E)$ is the rate of electron impact collision, and $\nu_{wall}(E)$ is the rate of loss of electrons to the walls, then we have the balance

$$S_o\, f_{thom}(E) + \Pi'(E) = \qquad (31)$$
$$\nu_{coll}(E)\, f_{tail}(E) + \nu_{wall}(E)\, f_{tail}(E)$$

or

$$f_{tail}(E) = \frac{S_o\, f_{thom}(E) + \Pi'(E)}{\nu_{coll}(E) + \nu_{wall}(E)} \qquad 0 \le E \le V\text{-}E_I \qquad (32)$$

with

$$\nu_{coll}(E) = n_o \Sigma_i [\sigma_i(E)\, v(E)] \quad (33)$$

$$\Pi'(E) = n_o \Sigma_i [\sigma_i(E+E_i)\, v(E+E_i)\, f_{tail}(E+E_i)] \quad (34)$$

and [10:813]

$$\nu_{wall}(E) = v(E)\, A/V_{ol}\, (1 - V_p/E)/4 \quad (35)$$

where n_o is the neutral number density, the summation is over all of the electron collisional processes, v(E) is the electron velocity in terms of energy, E_i is the threshold energy for process i, Π' represents the production of a fast electron at an energy of E due to losses from the distribution at higher energies, A is the effective wall loss area of the MMIS chamber (which takes into account the magnetic shielding of the walls), and V_p is the plasma potential. This is the distribution that will be used in this study for the tail of the EEDF.

If the probability of an electron not undergoing a wall collision before it has the chance to undergo any other type of collision is given by [11:22]

$$P(E) = 1 - \frac{\nu_{wall}(E)}{\nu_{coll}(E) + \nu_{wall}(E)} \quad (36)$$

then the tail distribution can be written

$$f_{tail}(E) = \frac{S_o\, P(E)\, f_{thom}(E) + P(E)\, \Pi'(E)}{\nu_{coll}(E)} \quad (37)$$

The total EEDF is assumed to be the superposition of the

Maxwellian distribution and the modified Thomson distribution. This superposition comes from being able to consider the electrons as composing two distinct species. In addition, since number density distributions and not probability distributions are being used, the algebraic addition of the two distributions will give us the total distribution:

$$f(E) = f_{MB}(E) + f_{tail}(E) \qquad (38)$$

This distribution is graphed in Fig. 8 (same conditions as in Fig 3). On comparison to Fig. 3, it is seen that approximating the tail of the distribution as a modified Thomson distribution does a good job of representing the EEDF.

For most of the calculations (e.g., the rate coefficients), only the Maxwellian portion of the distribution will be considered. As can be seen from Fig. 8, the tail of the distribution is several orders of magnitude lower than the Maxwellian portion. The tail of the distribution becomes important for the E-V processes that produce $H_2(v)$, since it is the high energy electrons that need to be considered. Thus, for the electronic excitations producing $H_2(v)$ we have

$$\langle R_{elec} \rangle = \frac{\int \sigma_i(E)\, v(E)\, f_{tail}(E)\, dE}{\int f_{tail}(E)\, dE} \qquad (39)$$

We have now dealt with the production and loss of all of the species that are relevant to this study. In addition, we have considered how the fast electrons will enter into the calculations. At this point we will discuss the moment equations that describe a MMIS.

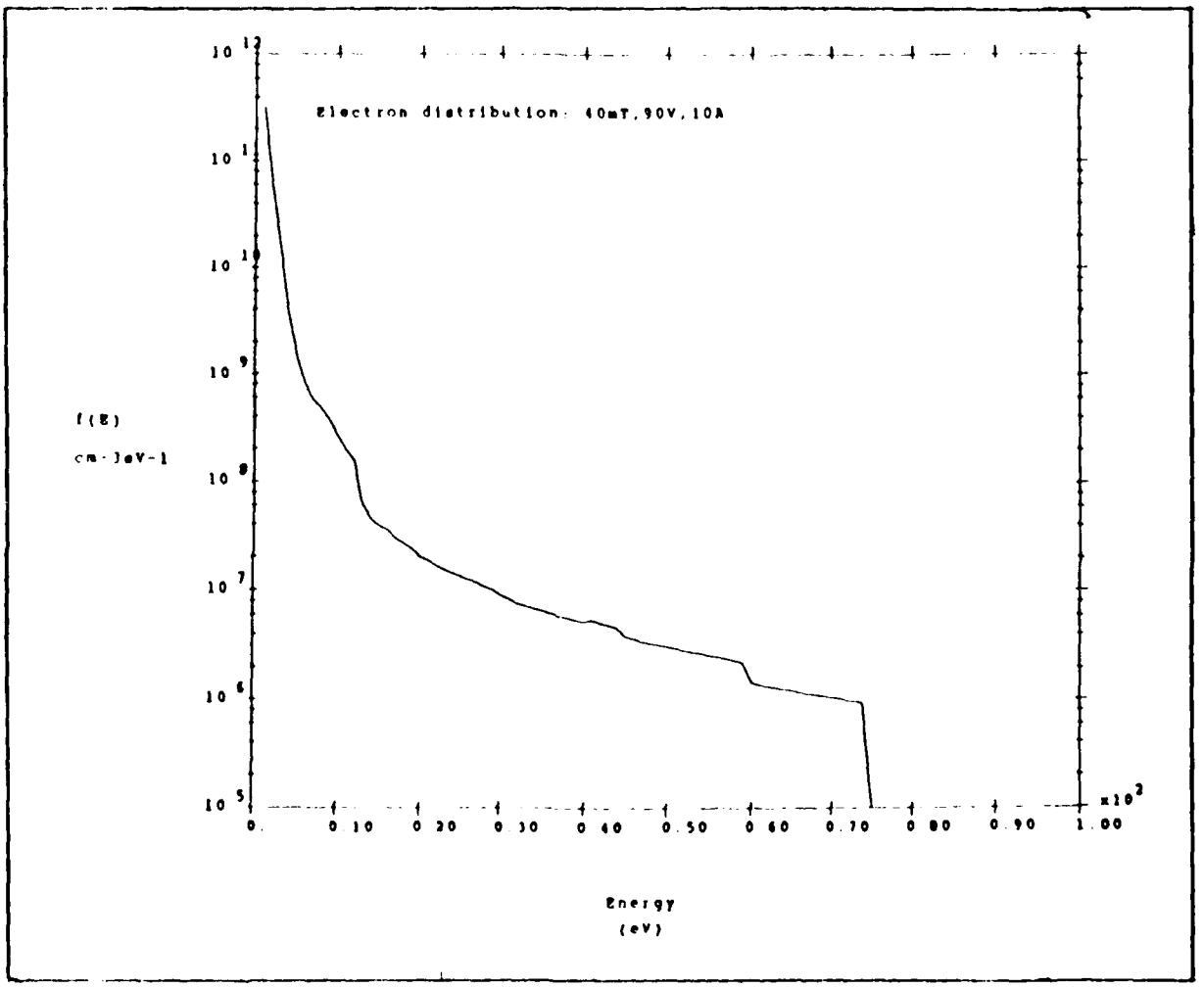

Fig. 8 - EEDF calculated using Eqn. 38 for a 40 mTorr, 90 V, 10 A discharge with 56% dissociation.

The Maxwellian Moments of the Boltzmann Equation

In this study we are concerned with modeling the electron density, the ionic densities, and the electron temperature. To do this, the density moments for the electrons and ions and the energy moment for the electrons will be needed. First we start with the basic moment equations of the Boltzmann equation:

Density Moment (Continuity Equation) [31:28]

$$\frac{\partial N}{\partial t} + \frac{\partial}{\partial x_i}(N\, v_i) = S_{coll} \qquad (40)$$

Energy Moment [31:42]

$$\frac{\partial}{\partial t}(1/2\ N\ m\ v_j\ v_j) + \frac{\partial}{\partial t}(1/2\ N\ m\ \langle w_j\ w_j \rangle) =$$

$$- \frac{\partial}{\partial x_i}(1/2\ N\ m\ v_i\ \langle w_j\ w_j \rangle) - \frac{\partial}{\partial x_i}(1/2\ N\ m\ v_i\ v_j\ v_j)$$

$$- \frac{\partial}{\partial x_i}(1/2\ N\ m\ \langle w_i\ w_j\ w_j \rangle) - \frac{\partial}{\partial x_i}(N\ M\ \langle w_i\ w_j \rangle\ v_j)$$

$$+ N\ \langle F_i\ u_i \rangle + E_{coll} \qquad (41)$$

where N is the species density, v_i is the average directed velocity of the species, m is the mass of the species, w_i is the thermal velocity of the species, $u_i = v_i + w_i$, F_i is the external force acting on the species, S_{coll} and E_{coll} represent the change in density and energy, respectively, due to collisions, angled brackets represent an average over the distribution, and summation over repeated indices is assumed. For this work a Maxwellian distribution is assumed. The densities are assumed to be uniform and isotropic over the

plasma volume. For a MMIS this uniformity is achieved by the magnets shielding the walls. It is also assumed that $F_i = 0$. We are considering the source electrons to be part of S_{coll} and E_{coll} instead of producing an electric field. Also, the magnetic field on the walls is considered to only effect the area of possible wall loss of electrons.

Consider first the continuity equation. For an isotropic distribution $v_i = 0$. Therefore the continuity equation becomes

$$\frac{\partial N}{\partial t} = S_{coll} \tag{42}$$

S_{coll} for the various species is all that needs to be determined for the density moments. The continuity equations for all of the species in the plasma can now be written:

$$\frac{\partial n_-}{\partial t} = S_{coll,H^-} \tag{43}$$

$$\frac{\partial n_e}{\partial t} = S_{coll,e} \tag{44}$$

$$\frac{\partial n_+}{\partial t} = S_{coll,H_2^+} \tag{45}$$

$$\frac{\partial n_{H^+}}{\partial t} = S_{coll,H^+} \tag{46}$$

$$\frac{\partial n_v}{\partial t} = S_{coll,H_2(v)} \tag{47}$$

where n_- is the H^- density, n_+ is the H_2^+ density, n_{H^+} is the H^+ density, and n_v is the $H_2(v)$ density.

Since the distribution of slow electrons is Maxwellian, the energy equation can also be much simplified. Note that

$1/2\ m \langle w_i\ w_i \rangle = 3/2\ T_e$. With this substitution Eqn. 41 can be written (still noting that $v_i = 0$)

$$\frac{\partial}{\partial t}(N\ 3/2\ T_e) = -\frac{\partial}{\partial t}(1/2\ N\ m \langle w_i\ w_j\ w_j \rangle) + E_{coll} \qquad (48)$$

To simplify the equation further the first term on the right hand side needs to be looked at. This term is

$$\langle w_i\ w_j\ w_j \rangle = 1/N \int w_i\ w_j\ w_j\ f_{MB}(u_i)\ du_i \qquad (49)$$

$f_{MB}(u_i)\ du_i$ is an even function of w_i, therefore the integrand of Eqn. 49 is seen to be an odd function of w_i and Eqn. 49 is identically equal to zero for a Maxwellian distribution. Finally, we have (letting $\langle E \rangle = 3/2\ T_e$)

$$\frac{\partial}{\partial t}(n_e \langle E \rangle) = E_{coll} \qquad (50)$$

As in the density equation, only E_{coll} needs to be determined in order to solve the energy equation.

The density equation collision terms

Looking at the plasma reactions involving H^- we see that the collision term for negative ions is given by (the angle brackets on the rate coefficients are left off for ease of expression)

$$S_{coll,H^-} = n_e n_v R_{att} + n_e n_+ R_{pdiss} - n_{H^+} n_- R_{mneut} - n_e n_- R_{edet} - n_H n_- R_{adet} - n_H n_- R_{bdet} \qquad (51)$$

For electrons we have

$$S_{coll,e} = S_o\langle P\rangle + n_e n_o R_{h2ion} + n_e n_H R_{hion} - n_e n_v R_{att}$$
$$- n_e n_+ R_{pdiss} - n_3 n_+ R_{h2rec} - n_e n_H + R_{hrec}$$
$$+ n_e n_- R_{edet} + n_- n_H R_{adet} - n_e n_+ R_{drec} + n_H n_- R_{hdet} \quad (52)$$

Where $\langle P\rangle$ is the average probability of a fast electron not undergoing a wall collision before it has a chance to undergo any impact collision. It is defined by

$$\langle P\rangle = \int P(E)\, f_{thom}(E)\, dE \quad (53)$$

where $P(E)$ was defined in Eqn. 36, and $f_{thom}(E)$ was defined in Eqn. 30.

The collision term for H_2^+ is

$$S_{coll,H2+} = S_o\langle P\rangle + n_e n_o R_{h2ion} - n_e n_+ R_{drec}$$
$$- n_e n_+ R_{pdiss} - n_e n_+ R_{h2rec} \quad (54)$$

The collision term for H^+ is

$$S_{coll,H+} = n_e n_H R_{hion} + n_e n_+ R_{pdiss} - n_{H+} n_e R_{hrec}$$
$$- n_{H+} n_- R_{mneut} \quad (55)$$

The collision term for $H_2(v)$ is

$$S_{coll,H2(v)} = n_f n_o \Sigma R_{elec} - n_e n_v R_{att} - n_v \nu_{vibwall}/10$$
$$- n_H n_v R_{vT} \quad (56)$$

where R_{elec} is given by Eqn. 39, and n_f is given by

$$n_f = \int f_{tail}(E)\, dE \quad (57)$$

and represents the total number of fast electrons.

The energy equation collision term

The collision term of the energy equation must take into account everything that will cause the slow electrons to gain or lose energy. The only energy production mechanism in the system is the source. Superelastic collisions were ignored in this study since several sources [32:1203,11:22] indicated that they have little effect on the average energy and electron density. Energy is lost through electronic excitations, through vibrational excitations, through ionization, in recombination processes, in detachment processes, and through momentum transfer. Thus the collision term in the energy equation can be written as

$$\begin{aligned} E_{coll} = {} & \langle E_s \rangle S_o \langle P \rangle - n_e n_o \sum E_{elec} R_{elec} - n_e n_o E_{vib} R_{vib} \\ & - n_e n_o E_{h2ion} R_{h2ion} - n_e n_n E_{hion} R_{hion} \\ & - n_e n_+ \langle E\, R_{drec}(E) \rangle - n_e n_+ \langle E\, R_{h2rec}(E) \rangle \\ & - n_e n_{n+} \langle E\, R_{hrec}(E) \rangle - n_e n_v \langle E\, R_{att}(E) \rangle \\ & - n_e n_- \langle E\, R_{edet}(E) \rangle - n_- n_n \langle E\, R_{hdet}(E) \rangle \\ & - n_- n_n \langle E\, R_{adet}(E) \rangle - 2(m_e/M) n_e n_o \langle E\, R_{mt}(E) \rangle \end{aligned} \tag{58}$$

where $\langle E_s \rangle$ is the average energy of the source and is defined by

$$\langle E_s \rangle = \frac{\int E\, P(E)\, f_{thom}(E)\, dE}{\int P(E)\, f_{thom}(E)\, dE} \tag{59}$$

E_i is the threshold energy for process i and M is the mass of H_2. The subscript vib refers to the excitation of H_2 from

the v=0 state to the v=1 state. The subscript mt refers to the momentum transfer reaction. For the energy equation, R_{elec} is averaged over the Maxwell-Boltzmann distribution, and not the modified Thomson distribution, since the slow electrons are being considered.

It should be noted that in Eqn. 58 the recombination and detachment terms are averages of the rate coefficients multiplied by the electron energy. As a simplification for this model, this average will be approximated by the average electron energy times the average reaction rate. This will result in a slightly less accurate electron energy, but it will reduce the computations needed. Thus the energy equation collision term actually used in the calculations in this study is

$$\begin{aligned} E_{coll} = {} & \langle E_a \rangle S_o \langle P \rangle - n_e n_o \sum E_{elec} R_{elec} - n_e n_o E_{vib} R_{vib} \\ & - n_e n_o E_{h2ion} R_{h2ion} - n_e n_a E_{hion} R_{hion} \\ & - n_e n_+ \langle E \rangle \langle R_{drec}(E) \rangle - n_e n_+ \langle E \rangle \langle R_{h2rec}(E) \rangle \\ & - n_e n_{a+} \langle E \rangle \langle R_{hrec}(E) \rangle - n_e n_v \langle E \rangle \langle R_{att}(E) \rangle \\ & - n_e n_- \langle E \rangle \langle R_{edet}(E) \rangle - n_- n_a \langle E \rangle \langle R_{hdet}(E) \rangle \\ & - n_- n_a \langle E \rangle \langle R_{adet}(E) \rangle - 2(m_e/M) n_e n_o \langle E \rangle R_{mt} \end{aligned} \qquad (60)$$

Solution of the Coupled Moment Equations

An analytic solution of the moment equations is not possible due to the experimental nature of the cross-section data. It was, therefore, necessary to solve the equations numerically. A complete description of the numerical tech-

niques used and a listing of the actual computer code are included in Appendix B. In this section only a brief summary of the solution process will be presented.

The equations are solved by using a Runge-Kutta-Fehlberg method of orders 4 and 5 [29:129-147]. This is an adaptive routine and is stable for mildly stiff systems of differential equations. The average rate coefficients as a function of the average electron energy are stored in the program in look-up tables. These tables were calculated using cross-section data and integrating (using an adaptive quadrature routine [30:174-175]) over either f_{MB} or f_{tail}.

The program proceeds until a steady state (mathematically determined by the time derivatives in the moment equations equaling zero) is determined to be achieved or until a set time is reached (typically 20 msec), whichever comes first.

In the next chapter the results of this model are compared to various experimental and theoretical calculations.

CHAPTER III - RESULTS AND ANALYSIS

In this chapter the results of the model presented in the previous chapter will be discussed and compared to other experimental and theoretical work. Scaling laws with the discharge parameters will then be presented. These laws will then be used to estimate the best operating conditions for a MMIS.

Comparison of Model to Previous Work

For a preliminary consistency check of the moment model, the output was compared to the theoretical calculations of Bretagne, *et al*, [10], and the experimental data of Péalat, *et al*, [33] for a pressure of 40 mTorr, a discharge voltage of 90 V, a plasma potential of 2 V, and 56% dissociation of H_2 into H. The discharge currents considered were 1-10 A. Table I presents the results obtained.

The electron temperature and electron density calculations are very good for the current range considered. In fact, they are generally better predictions of the experimental data than Bretagne's work. The ratio of n_-/n_e, on the other hand, is as much as an order of magnitude off from the experimental data. This is probably due to my treatment of the vibrational population density. The use of a representative population, instead of using the full set of vibrational master equations, causes a loss of information. This loss of information results in the negative ion density calculation being an order of magnitude estimate.

TABLE I

Comparison of Discharge Parameters

40 mTorr, 90 V, 56% dissociation, V_p = 2 V
T_g = 450 K, V_{01} = 10 l, A = 700 cm², L = 14.3 cm

(a) Present work (b) Experiment [33] (c) Theory [10]

I(A)	T_e (eV)			n_e (10^{11} cm^{-3})			n_-/n_e (10^{-3})		
1	.43[a]	.43[b]	.32[c]	2.5[a]	1.7[b]	1.9[c]	.65[a]	7.0[b]	7.0[c]
3	.50	.65	.42	4.1	5.7	3.8	1.8	4.0	4.1
10	.62	.85	.59	7.1	9.8	6.7	4.8	---	2.7

TABLE II

Comparison at Low Pressure

2 mTorr, 50 V, 5 A, .4% dissociation, V_p = 1.15 V
T_g = 450 K, V_{01} = 8.8 l, A = 830 cm², L = 14.3 cm

(a) Present work (b) Experiment [24] (c) Theory [24]

	n_e (10^{10} cm^{-3})	T_e (eV)	n_- (10^9 cm^{-3})	n_-/n_e (10^{-3})
(a)	26.30	.748	20.12	76.52
(b)	1.1-3.4	.75	3.2	94.1-290.9
(c)	3.43	.40	2.3	67.1

It is seen from Table I that the present model predicts that the ratio of n_-/n_e will increase with current, whereas both Péalat and Bretagne show a decrease with current. This discrepancy can be partially accounted for by the fact that a dissociation of 56% was used at all currents. It will be shown later that the negative ion density is inversely proportional to the atomic hydrogen density. As the current is increased, you have a larger electron density with which H_2 can be dissociated. Therefore, at higher currents, the dissociation should be larger and the total negative ion density should decrease. For a fixed dissociation, however, it will later be seen that the behavior this model predicts has been experimentally observed.

The model was also compared to the work of Gorse, *et al*, [24] at a pressure of 2 mTorr, a voltage of 50 V, a current of 5 A, a plasma potential of 1.15 V, and a dissociation of .4%. The results of this comparison are presented in Table II.

The moment model has predicted the electron temperature extremely well. The electron density and negative ion density calculations, however, are both off by an order of magnitude. The error in the electron density calculation is most likely due to the fact that wall-losses were ignored in the electron continuity equation. For the data in Table II, a plasma potential of 1.15 V was used, compared to 2 V for the data in Table I. At this lower plasma potential, more of the slow electrons can overcome the potential barrier and be

lost to the walls. This increased wall-loss could possibly explain why the observed electron density is lower than calculated by this model. The negative ion density being an order of magnitude too high is then due directly to n_e being an order of magnitude too high, since $n_- \propto n_e$.

With fairly good success of the model for various values of the discharge parameters, the code was then run over the pressure, voltage, and current parameter spaces. The results of these runs were used to determine scaling laws.

Scaling Laws with Discharge Parameters

The scalings of the various particle species are determined by looking at the steady state solutions of the moment equations. These solutions are given by the following coupled set of equations:

$$n_- = \frac{n_e n_v R_{att} + n_e n_+ R_{pdiss}}{n_B R_{mneut} + n_e R_{edet} + n_B (R_{adet} + R_{hdet})} \quad (60)$$

$$n_e = \frac{S_o \langle P \rangle + n_- n_B R_{adet} + n_- n_B R_{hdet}}{X} \quad (61)$$

$$X = n_v R_{att} + n_+ (R_{pdiss} + R_{h2rec} + R_{drec}) + n_{B+} R_{hrec} - n_o R_{h2ion} - n_B R_{hion} - n_- R_{edet}$$

$$n_+ = \frac{S_o \langle P \rangle + n_e n_o R_{h2ion}}{n_e (R_{drec} + R_{h2rec} + R_{pdiss})} \quad (62)$$

$$n_{B+} = \frac{n_e (n_B R_{hion} + n_+ R_{pdiss})}{n_e R_{hrec} + n_- R_{mneut}} \quad (63)$$

$$n_v = \frac{n_f n_o \Sigma R_{elec}}{n_e R_{att} + n_B R_{VT} + \nu_{vibwall}/10} \quad (64)$$

By looking at the relative magnitudes of the various terms in the above equations it is possible to determine the

dominant processes in the steady state. Using the data from running the code between 20-100 V, 1-100 A, 1-100 mTorr, and 56% dissociation, it was found that the densities are given by

$$n_- = \frac{n_e n_v R_{att}}{n_g R_{adet}} \qquad P \geq 4 \text{ mT} \qquad (65)$$

$$n_e \approx n_+ = \left(\frac{S_0 \langle P \rangle}{n_+ R_{drec}} \right)^{1/2} \qquad (66)$$

$$n_{g+} = \frac{n_e n_+ R_{pdiss}}{n_- R_{mneut}} \qquad (67)$$

$$n_v = \frac{n_f n_0 \Sigma R_{elec}}{n_e R_{att} + n_g R_{VT} + \nu_{vibwall}/10} \qquad (68)$$

As indicated, Eqn. 65 is only valid if the pressure, P, is greater than, or about, 4 mTorr. For pressures lower than this, Eqn. 65 will produce an answer with about 12% error. To be more accurate, the polarized dissociation and mutual neutralization terms of Eqn. 60 must be retained. This indicates that at lower pressures, polarized dissociation and mutual neutralization start becoming the dominant production and loss mechanisms for negative hydrogen ions. Thus we have

$$n_- = \frac{n_e n_+ R_{pdiss}}{n_{g+} R_{mneut}} \qquad P < 4 \text{ mT} \qquad (69)$$

If the current is greater than 40 A and the pressure is less than 10 mTorr, then Eqn. 68 can be simplified to

$$n_v = \frac{n_f n_0 \Sigma R_{elec}}{n_e R_{att} + \nu_{vibwall}/10} \qquad \begin{matrix} I \geq 40 \text{ A} \\ P < 10 \text{ mT} \end{matrix} \qquad (70)$$

Using Eqns. 65-70 it will be possible to elucidate

scaling laws with respect to the discharge parameters.

Scaling with current

We will first determine how the electron density scales with current, using Eqn. 66. By refering to Eqns. 53, 36, 35, 33, and 30 it is seen that $\langle P \rangle$ is independent of current. Also, the rate of dissociative recombination is independent of current if you assume that the electron temperature is constant. Eqn. 29 shows that the source strength is directly proportional to the current; therefore, we have

$$n_e \propto I^{1/2} \tag{71}$$

In Fig. 9, a graph of n_e as a function of current is given. From the graph it is obvious that the scaling given by Eqn. 71 is valid for the model. This scaling was also found by Bailey and Jones [11:21].

To determine the scaling of the vibrational population with current we must first see how n_f scales with current. The fast electrons will scale the same as f_{tail} with respect to the discharge parameters (see Eqn. 57). Refering to Eqn. 32 and ignoring the Π' term, it is seen that f_{tail} is directly proportional to current. Likewise, n_f will be directly proportional to the current. R_{elec} and R_{att} are both independent of current; therefore, using Eqn. 70 and ignoring the wall-loss term, we find

$$n_v \propto I^{1/2} \tag{72}$$

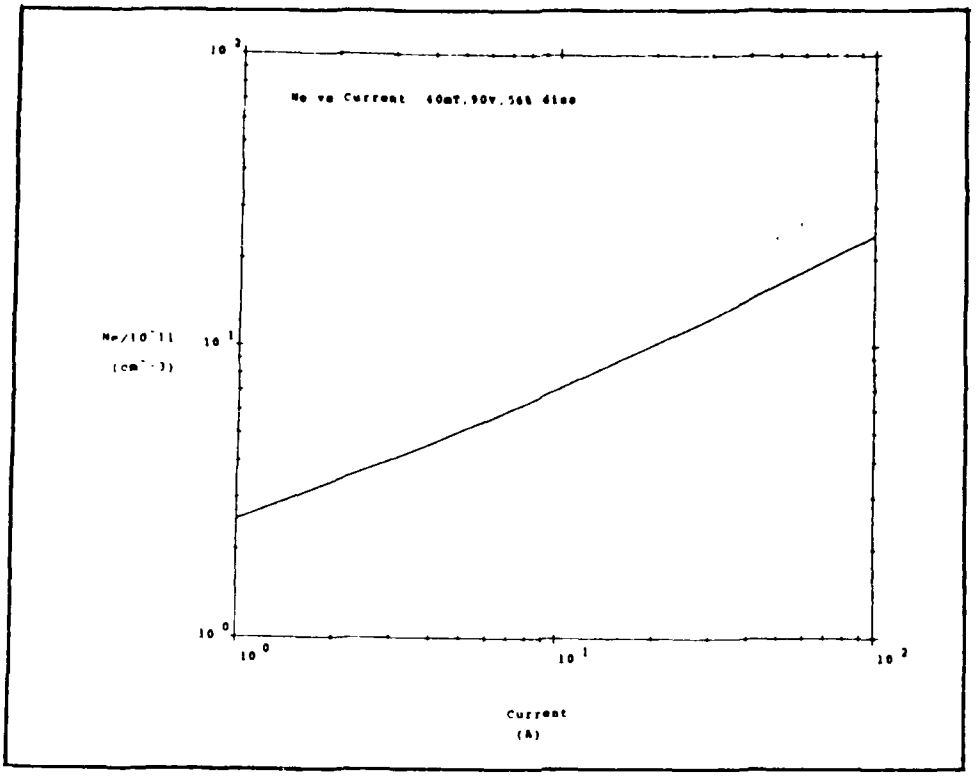

Fig. 9 - Electron density as a function of discharge current for a 40 mTorr, 90 V, 56% dissociation discharge.

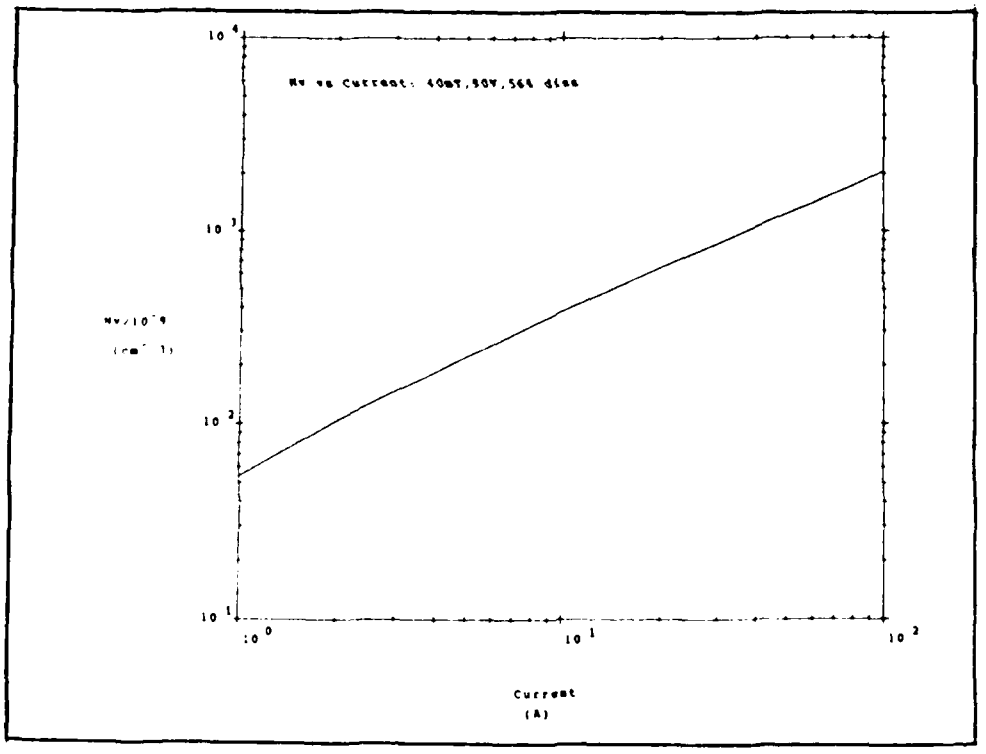

Fig. 10 - Vibrational population as a function of discharge current for the same conditions as in Fig. 9.

Fig. 10 is a graph of n_v as a function of current and shows the dependence given by Eqn. 72.

With a knowledge of how n_e and n_v scale with current it is possible to determine how the negative ion density scales with current. Again assuming that rates are constant and assuming that n_{H^+} is independent of current (we will show this shortly), both Eqn. 65 and Eqn. 69 give

$$n_- \propto I \tag{73}$$

This scaling is seen to hold in Fig. 11, and is verified experimentally by York, *et al* [35:682] and Bacal, *et al* [36:23].

Using the scalings for the electron density and the negative ion density, Eqn. 67 indicates that n_{H^+} should be constant with respect to current changes. Fig. 12 is a graph of n_{H^+} versus current; the density is fairly constant for currents above 10 A. Below 10 A, the inconsistency is due to the fact that the n_{H^+} density had not reached a true steady state when the code output the density. This will be seen when the time evolution of the densities is considered later. The rest of the calculations will not be affected by this lack of steady state since none of the other densities depend on n_{H^+}.

Using Eqns. 71 & 73 it is possible to find the scaling for the ratio of negative ions to electrons. This ratio is important in the extraction of negative ions since a large population of electrons extracted with the negative ions

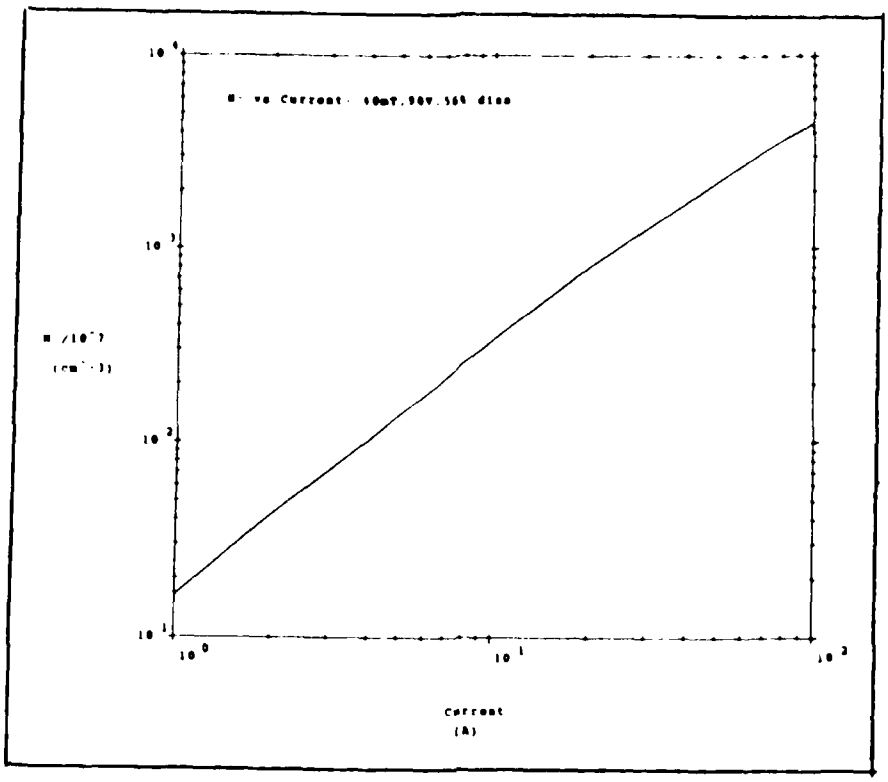

Fig. 11 - Negative ion density as a function of discharge current for the same conditions as in Fig. 9

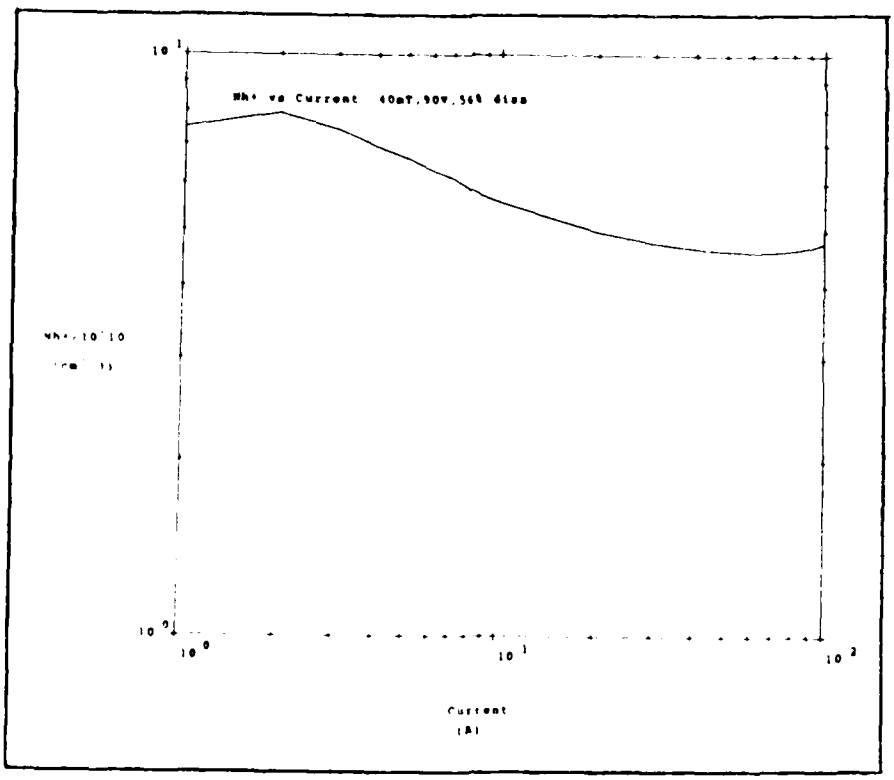

Fig. 12 - H^+ density as a function of discharge current for the same conditions as in Fig. 9.

degrades the quality of the ion source output [34:56]. The ratio scales as

$$\frac{n_-}{n_e} \propto I^{1/2} \tag{74}$$

A graph of this ratio is seen in Fig. 13, confirming the given current scaling.

Next, the scaling of the densities with respect to pressure needs to be examined.

Scaling with pressure

If it is assumed that $\langle P \rangle$ and the rate coefficients are independent of pressure, then Eqn. 66 indicates that the electron density should be independent of pressure. Fig. 14, which is a graph of n_e as a function of pressure, shows that the electron density is basically independent of pressure. The slight increase with pressure that is seen is due to the fact that $\langle P \rangle$ is weakly dependent on pressure (see Fig. 15), since ν_{coll} is a function of pressure.

In order to determine the pressure scaling of n_v, we have to look at the scaling of n_f with pressure. Eqn. 32 indicates that the tail of the distribution scales as $(P + k)^{-1}$, where k is a constant, and, thus, n_f scales the same. Since n_o is proportional to pressure, and assuming that n_e is independent of pressure, we get

$$n_v \propto \frac{P}{P + k} \tag{75}$$

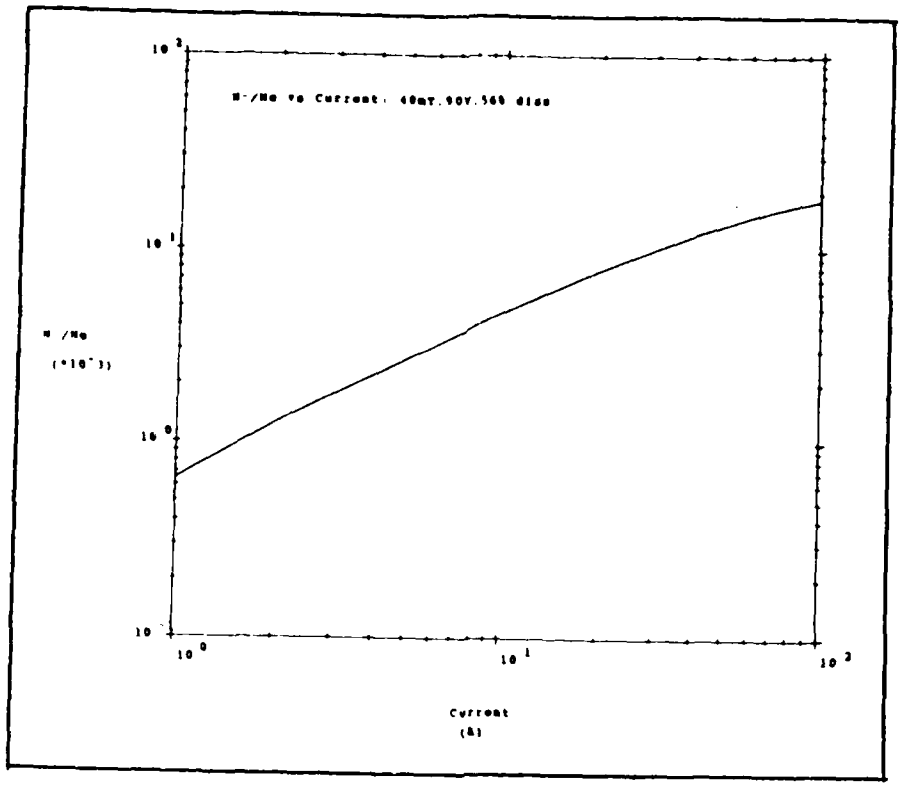

Fig. 13 - The ratio n_-/n_e as a function of discharge current for the same conditions as in Fig. 9.

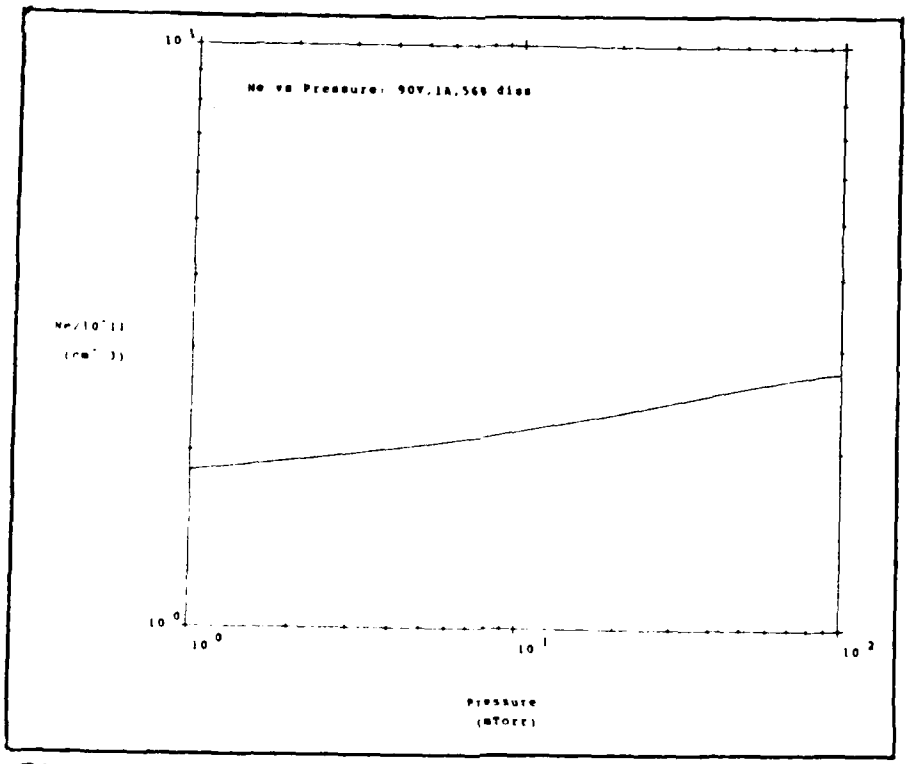

Fig. 14 - Electron density as a function of gas pressure for a 90 V, 1 A, 56% dissociation discharge.

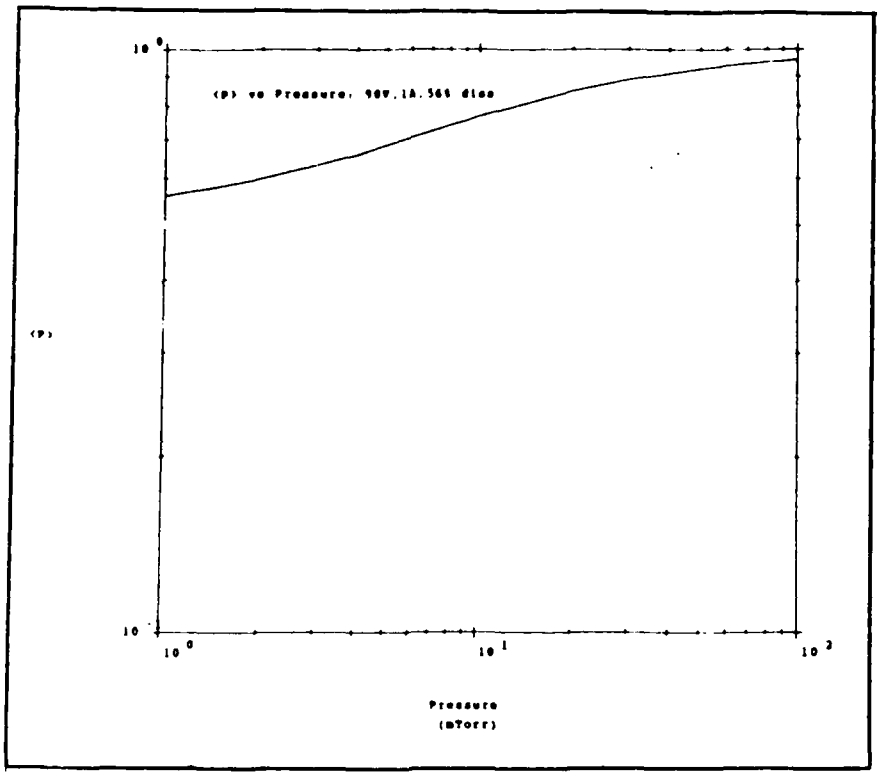

Fig. 15 - $\langle P \rangle$ as a function of gas pressure for the same conditions as in Fig. 14.

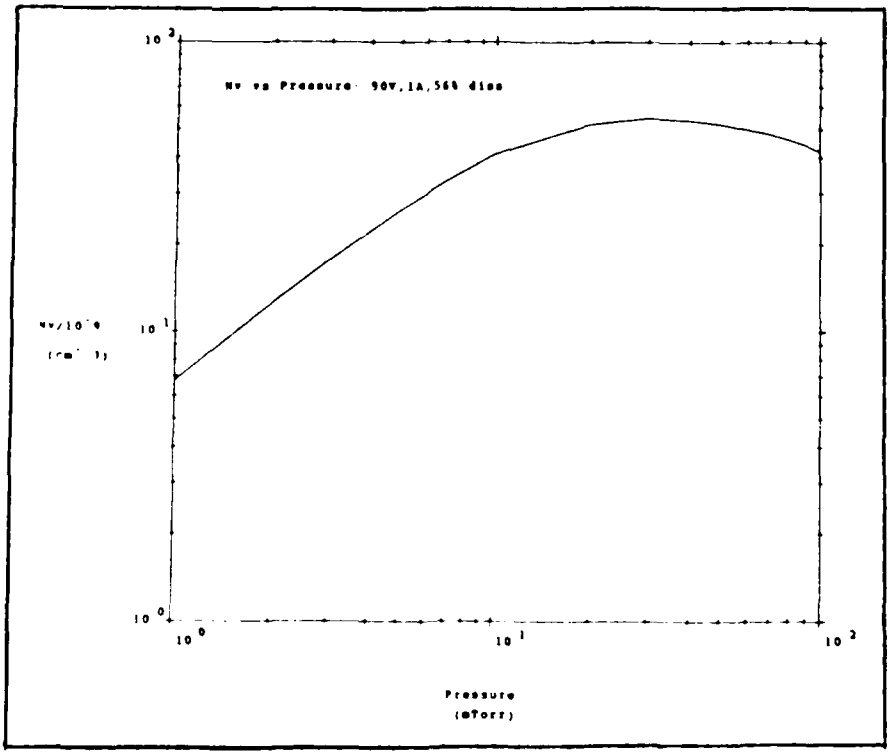

Fig. 16 - Vibrational population as a function of gas pressure for the same conditions as in Fig. 14.

Thus for low pressures the vibrational density should be roughly proportional to pressure and it should saturate at higher pressures. The vibrational density versus pressure is shown in Fig. 16 and it is seen to basically follow the scaling of Eqn. 75.

With the pressure scalings for n_e and n_v it is now easy to determine how the negative ions will scale with pressure in this model. Since $n_{s^-} \propto P$ we have, using Eqn. 65,

$$n_{-} \propto \frac{1}{P + k} \tag{76}$$

Fig. 17 demonstrates this scaling for the negative ions. For high pressure the density is inversely proportional to P, and for low pressures signs of saturation are evident. Actually, the curve in Fig. 17 has a maximum at about 2 mTorr. This maximum has been experimentally observed by Bacal, *et al* [36:22]. The maximum appears to occur from the change in the negative ion production and loss mechanisms. This is represented mathematically by the change from Eqn. 65 to Eqn. 69 at these low pressures.

Using Eqns. 67 & 76 it appears that the H^+ density should be given by

$$n_{s^+} \propto P \tag{77}$$

Looking at Fig. 18, this scaling does not seem to hold. However, as was mentioned earlier, the H^+ density had not reached a steady state value at the time of output from the code, so the above scaling should not be expected to hold for

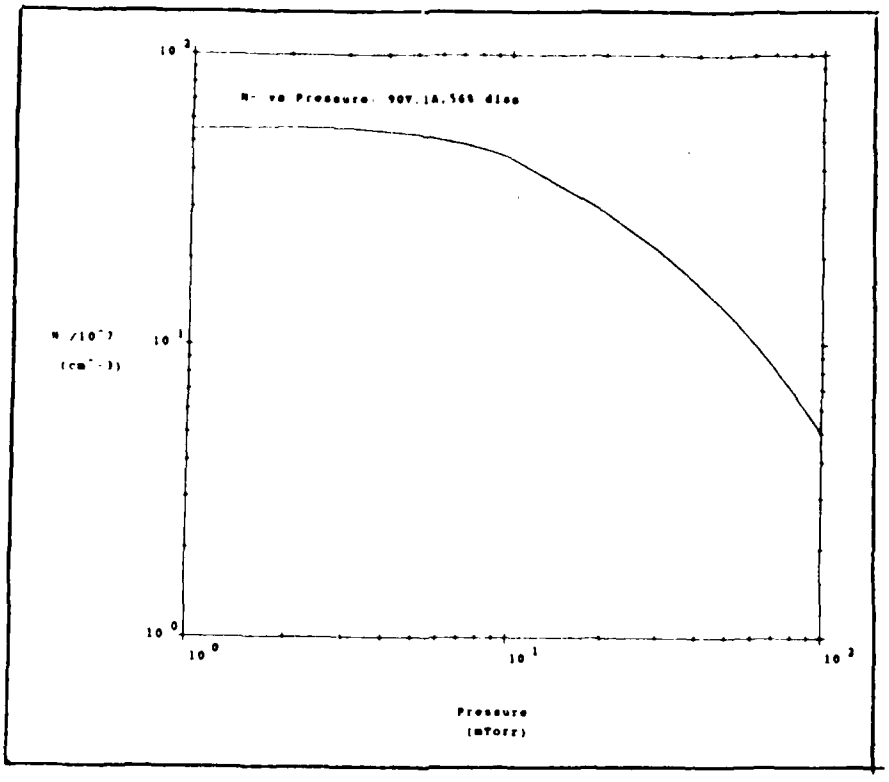

Fig. 17 - Negative ion density as a function of gas pressure for the same conditions as in Fig. 14.

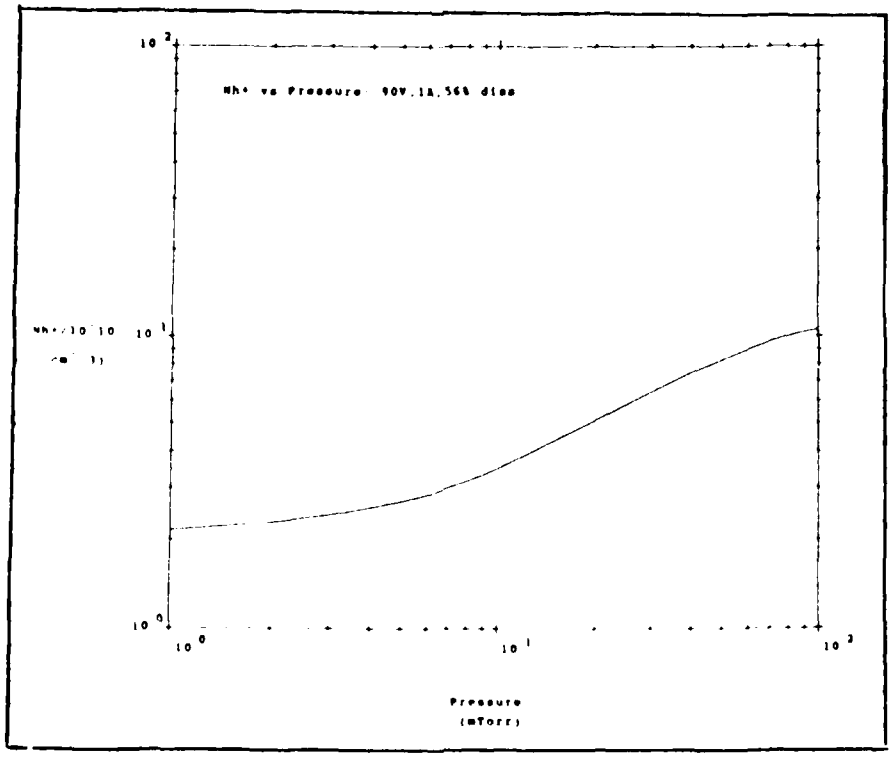

Fig. 18 - H^+ density as a function of gas pressure for the same conditions as in Fig. 14.

the data presented.

Finally, the ratio of negative ions to electrons is expected to follow the same scaling as for n_- (Eqn. 76). This is confirmed in Fig. 19.

Next, we will determine the scaling with discharge voltage.

Scaling with voltage

The electron number density voltage scaling is due to the scaling of the source strength. From Eqn. 29, it is seen that S_o is directly proportional to V. Thus we expect to have

$$n_e \propto V^{1/2} \tag{78}$$

The electron density as a function of discharge voltage is graphed in Fig. 20. The curve in this figure follows the scaling of Eqn. 78 only approximately. Eqn. 78 should only be used as an indication that the electron density is a slowly increasing function of discharge voltage.

If we assume Eqn. 78 is valid in order to analyze the voltage scaling of the rest of the species, then we need to find the scaling of n_f with voltage to see how the vibrational population scales. From Eqn. 32, we find that f_{tail}, and hence, n_f, is directly proportional to the voltage. Combining this with Eqn. 78, we get that n_v scales as

$$n_v \propto V^{1/2} \tag{79}$$

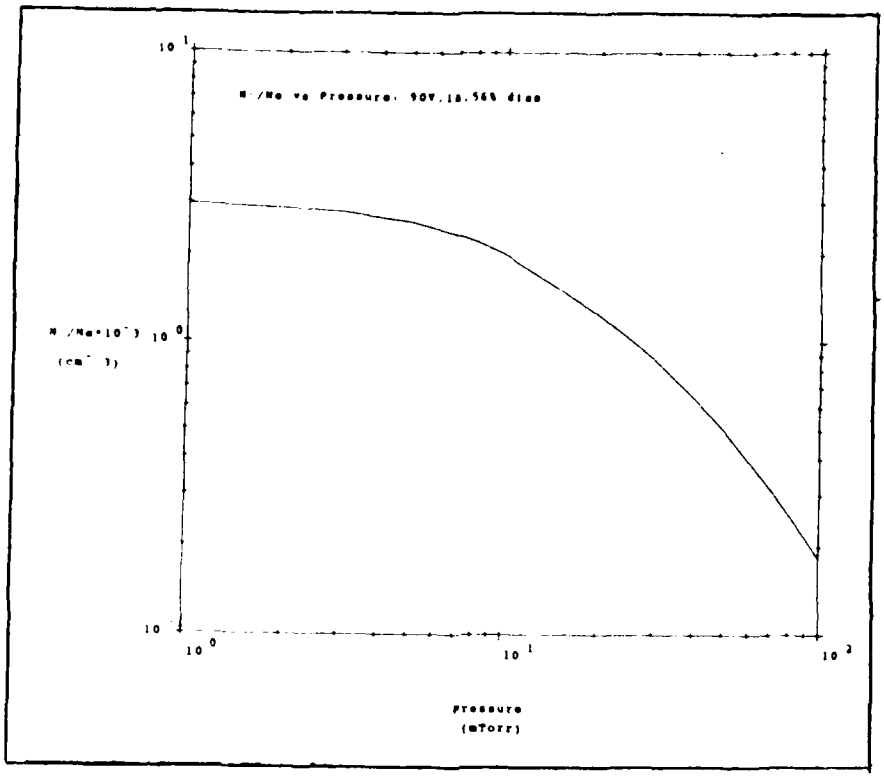

Fig. 19 - The ratio n_-/n_e as a function of gas pressure for the same conditions as in Fig. 14.

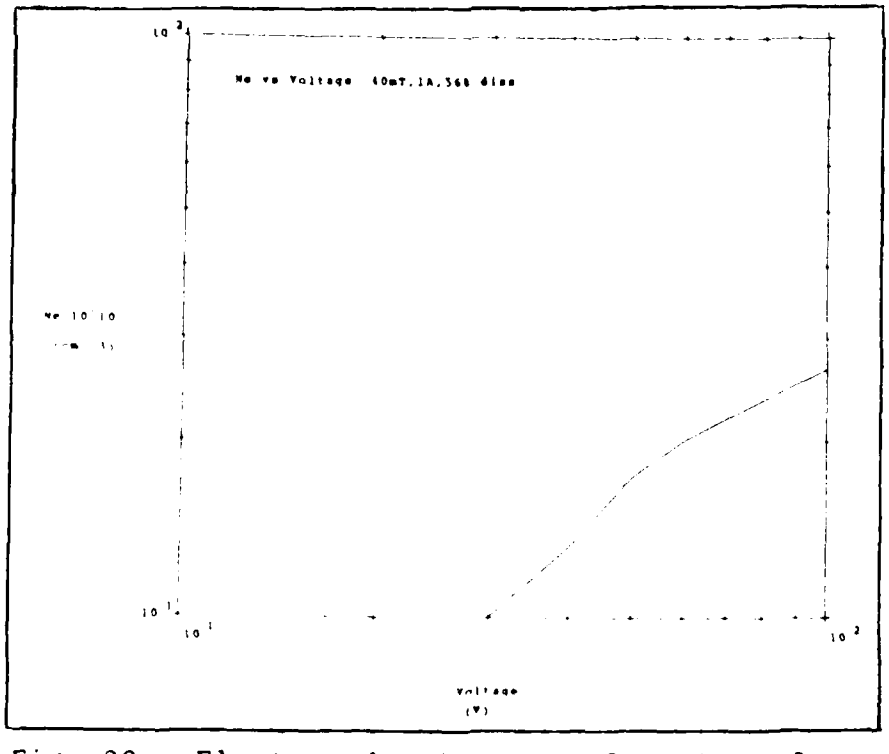

Fig. 20 - Electron density as a function of discharge voltage for a 40 mTorr, 1 A, 56% dissociation discharge.

Fig. 21 shows n_v versus voltage. This graph is roughly represented by Eqn. 79.

Using Eqn. 65 and incorporating Eqns. 78 & 79, we find that

$$n_- \propto V \tag{80}$$

The actual scaling is shown in Fig. 22. This graph basically validates Eqn. 80. The scaling given by this equation has been experimentally shown to exist by Leung, *et al* [9:365]. In that study, it was found that the negative ion density was directly proportional to voltage up to around 120 V, at which point it saturates.

The scaling of the ratio n_-/n_e is found from Eqns. 78 & 80 to be

$$\frac{n_-}{n_e} \propto V^{1/2} \tag{81}$$

This ratio is graphed in Fig. 23. As with the rest of the voltage scalings, Eqn. 81 only approximately duplicates the behavior that the computer code indicates exists. Part of the differences between these equations and what is calculated is that $\langle P \rangle$ is a slowly varying function of V (see Eqns. 35 & 30).

From Eqn. 67, we see that the H^+ density should be independent of the discharge voltage. Fig. 24 indicates that this is not the case. However, the fact that the curve in Fig. 24 is dependent on the voltage is due to n_{H^+} not yet reaching a steady state, as indicated earlier.

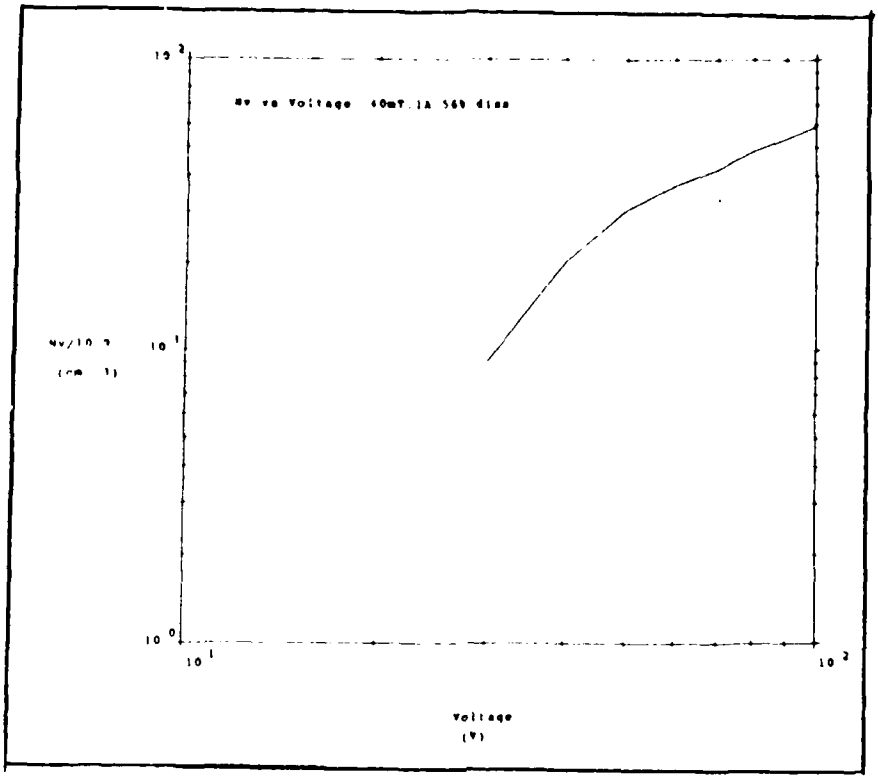

Fig. 21 - Vibrational population as a function of discharge voltage for the same conditions as in Fig. 20.

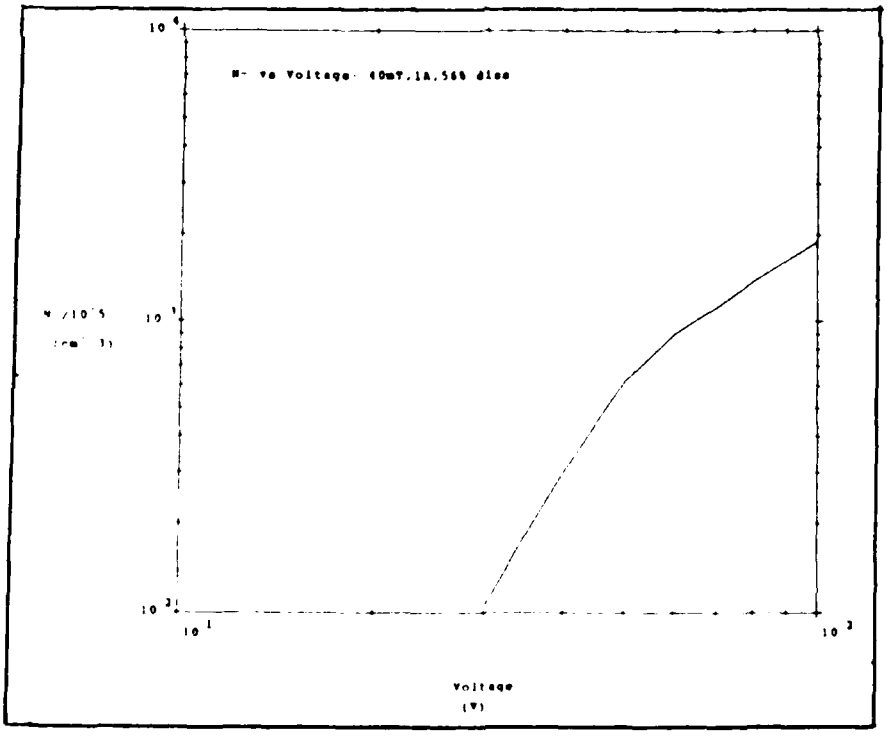

Fig. 22 - Negative ion density as a function of discharge voltage for the same conditions as in Fig. 20.

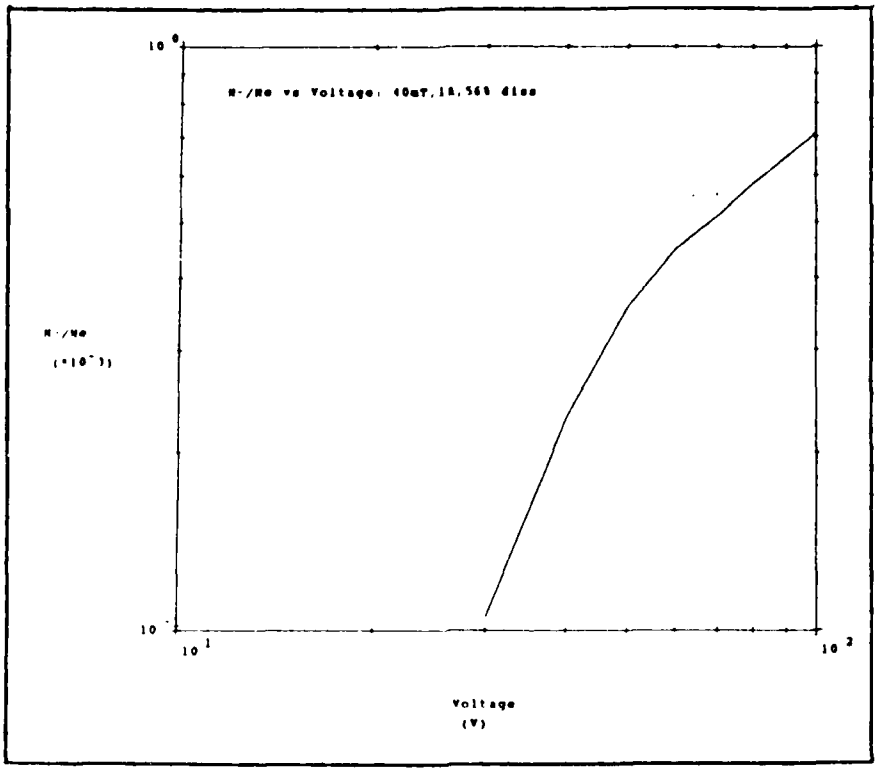

Fig. 23 - The ratio of n_-/n_e as a function of discharge voltage for the same conditions as in Fig. 20.

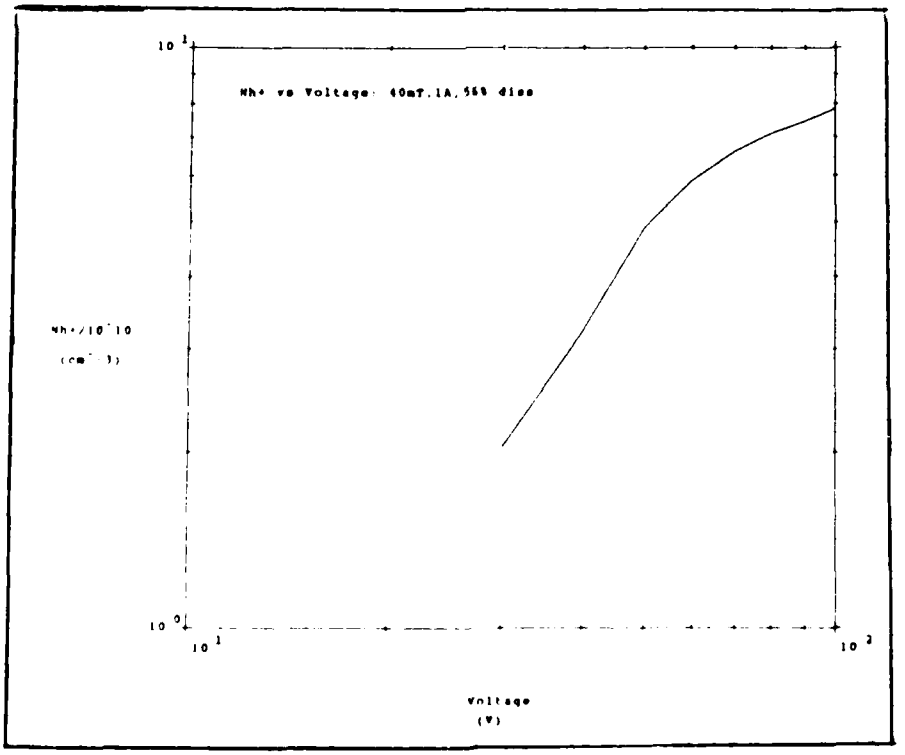

Fig. 24 - H^+ density as a function of discharge voltage for the same conditions as in Fig. 20.

Up to this point, we have discussed the scalings of the species densities with respect to the discharge parameters. Next, we will determine how the electron temperature varies with the discharge parameters.

Electron temperature scaling

Using the energy equation (Eqn. 60) in a steady state and only considering the dominant terms, we find that the electron temperature is given by the balance

$$\langle E_s \rangle S_o \langle P \rangle = n_e n_o E_{vib} R_{vib} + n_e n_+ \langle E \rangle R_{drec} + 2(m_e/M) n_e n_o \langle E \rangle R_{mt} \quad (82)$$

The relative strengths of the terms on the right-hand side of this equation vary depending upon the specific current, pressure, and voltage range the source is being run in. In general, for currents less than 10 A and pressures greater than 10 mTorr, the momentum transfer term will dominate over the recombination term. For higher currents and lower pressures the reverse is true. For all values of the discharge parameters, the vibrational term is the largest, representing anywhere from 50% to 90% of the total contribution from the right-hand side. Since this is true, we will ignore both the momentum transfer term and the recombination term in order to make it easier to see how the electron temperature scales with the discharge parameters. In this case, Eqn. 82 reduces to

$$\langle E_s \rangle S_o \langle P \rangle = n_e n_o E_{vib} R_{vib} \quad (83)$$

We will now make the assumption that

$$R_{vib} \approx R_o e^{-E_o/T_e} \tag{84}$$

This assumption should be valid since the electron temperature is in the neighborhood of E_{vib}. The constants R_o and E_o are determined by fitting R_{vib} to Eqn. 84. Using Eqn. 84 in Eqn. 83, we get

$$\frac{1}{T_e} = \frac{\ln\left[(n_e n_o E_{vib} R_o)/(\langle E_e\rangle S_o \langle P\rangle)\right]}{E_o} \tag{85}$$

We know how all of the terms in Eqn. 85 scale with the discharge parameters, so we find that

$$\frac{1}{T_e} \propto \ln \frac{P}{(I\ V)^{1/2}} \tag{86}$$

Figs. 25-27 show the electron temperature data as functions of current, pressure, and voltage, respectively. It is seen that Eqn. 86 is a good representation for what is observed.

Summary of Scaling Laws

The scaling laws in terms of pressure, current, and voltage are given by

$$n_- \propto \frac{I\ V}{P + k} \tag{87}$$

$$n_e \propto (I\ V)^{1/2} \tag{88}$$

$$n_v \propto \frac{(I\ V)^{1/2}\ P}{P + k} \tag{89}$$

$$n_{H^+} \propto P \tag{90}$$

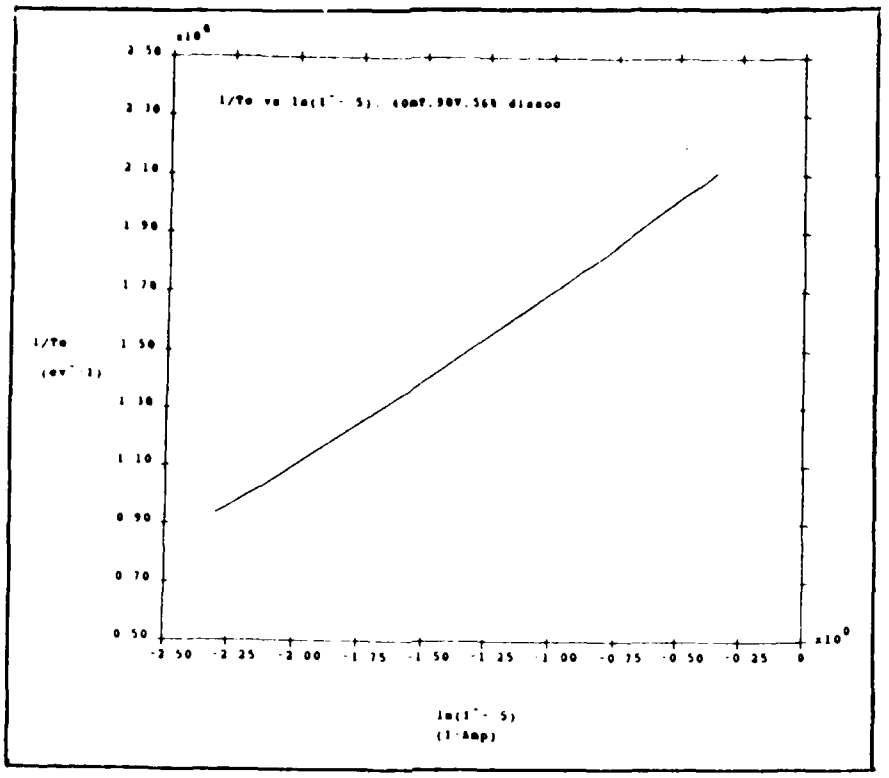

Fig. 25 - T_e^{-1} as a function of ln $(I)^{-1/2}$ for a 40 mTorr, 90 V, 56% dissociation discharge.

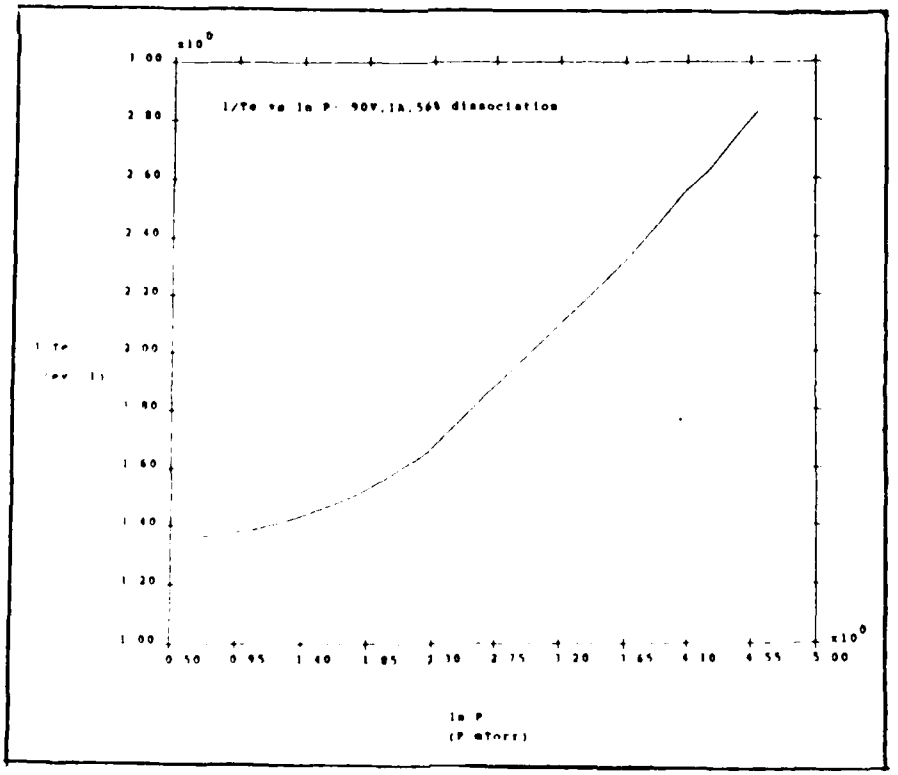

Fig. 26 - T_e^{-1} as a functicn of ln P for a 90 V, 1 A, 56% dissociation discharge.

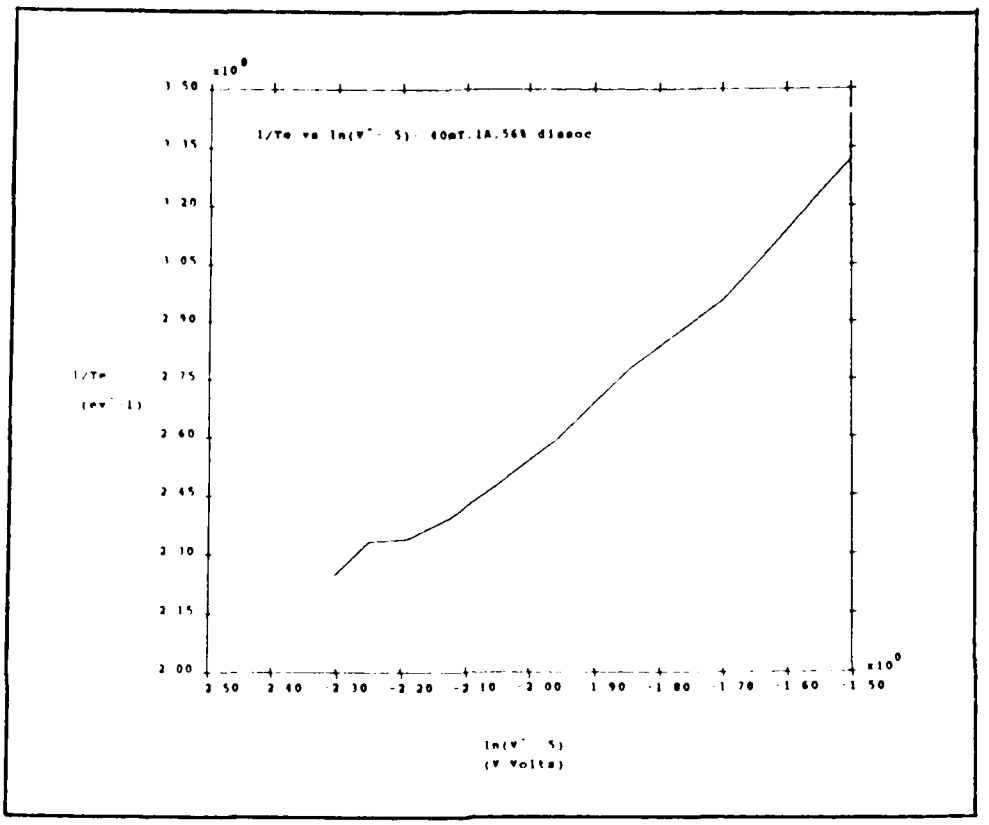

Fig. 27 - T_e^{-1} as a function of ln $(V)^{-1/2}$ for a 40 mTorr, 1 A, 56% dissociation discharge.

and

$$\frac{n_-}{n_e} \propto \frac{(I\ V)^{1/2}}{P + k} \qquad (100)$$

where k is a constant that depends on the gas temperature, the plasma volume, the effective wall loss area, the plasma potential, and the reaction rates for the electronic excitations. These proportionalities, in addition to Eqn. 86, give a means to optimize the production of negative hydrogen ions in a MMIS, with respect to the discharge parameters.

The Optimal Operating Regime for a MMIS

Using the scaling laws predicted by this model, it is easy to determine for which values of the discharge parameters the efficiency of a magnetic multicusp ion source can be optimized. To maximize the production of negative ions, the discharge parameters must be chosen so as to maximize Eqn. 87. It is obvious that this will be for a high current, high voltage, low pressure source. For voltage and current, however, there are optimum values. As it was mentioned earlier, the negative ion density actually saturates for a voltage around 120 V. This then represents the voltage limit for efficient operation. The optimum value for the pressure was found to be between 2 and 4 mTorr.

In addition to Eqns. 86-100 being useful for determining the optimum operating regime for a generic MMIS, they should be useful to the experimentalist in the optimization of his

ion source. He can normalize the above equations to his specific source and see how variations in the discharge parameters will effect his source operation.

Temporal Evolution of Parameters

Before concluding, it is worth mentioning how the densities and electron temperature evolve with time. For a 40 mTorr, 90 V, 1 A discharge most of the species reach a pseudo-steady state within about 2 msec (see Figs. 28-33). For the H^+ density this is not true (Fig. 33); it has not reached a steady state after 20 msec (at which point the code was stopped). Since the H^+ density never truly reached a steady state, the scalings developed above are not exactly seen from the data. None of the other parameters being measured are dependent upon n_{H^+}, so the fact that it has not reached steady state does not affect the other calculations.

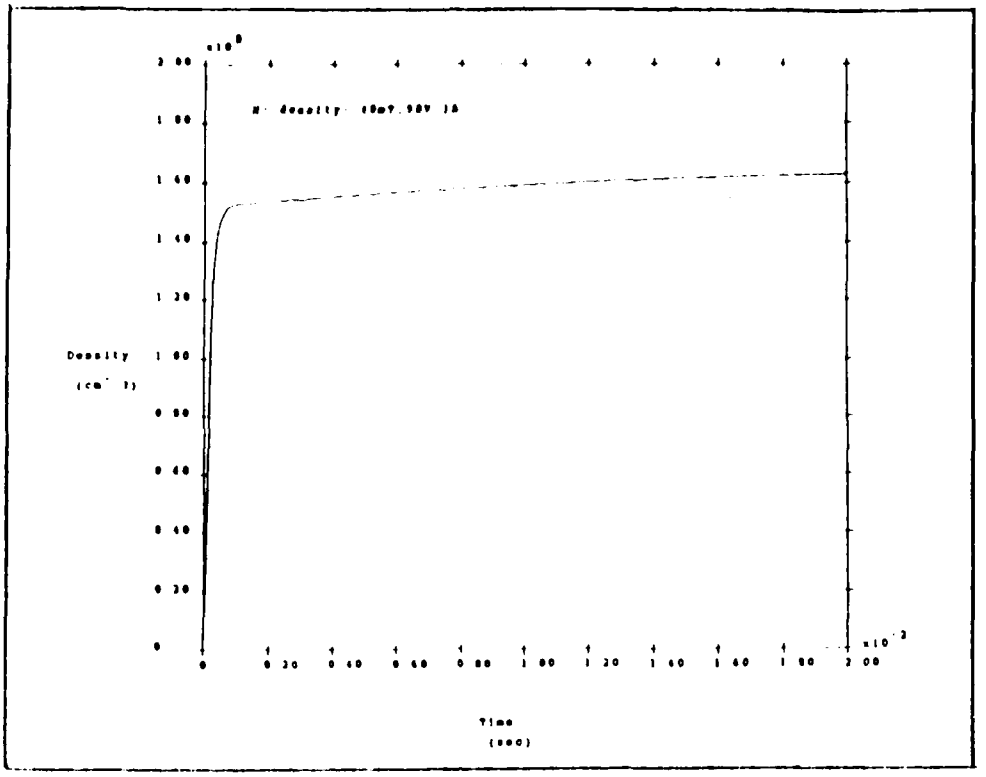

Fig. 28 - Temporal evolution of negative ion density for a 40 mTorr, 90 V, 1 A, 56% dissociation discharge.

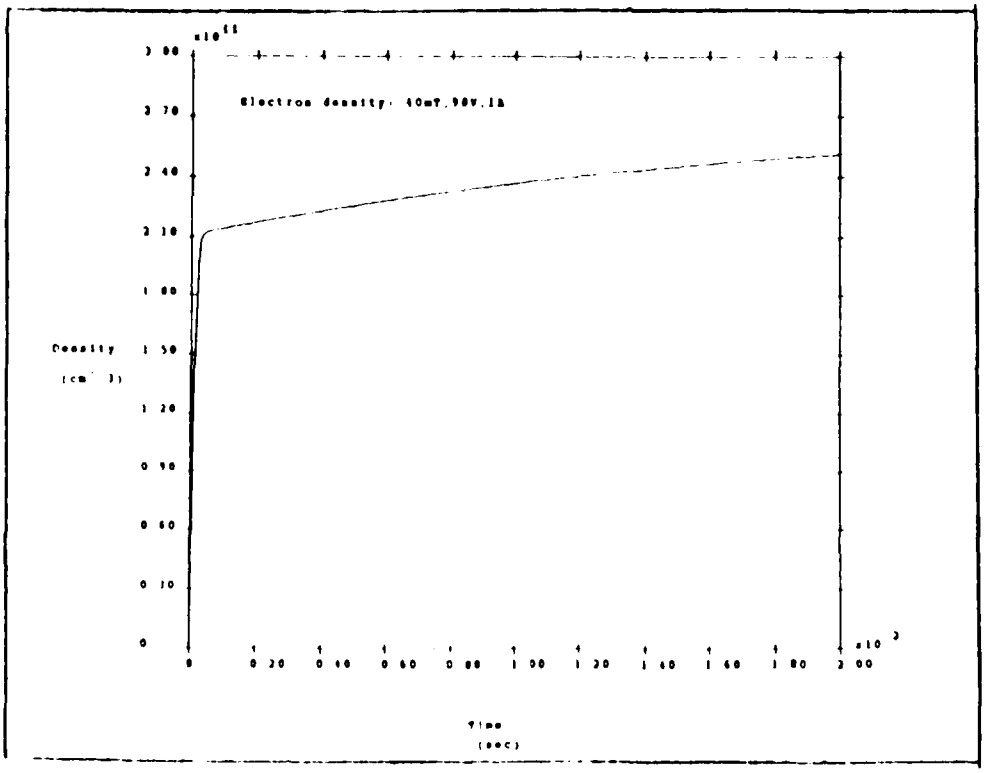

Fig. 29 - Temporal evolution of electron density for the same conditions as in Fig. 28.

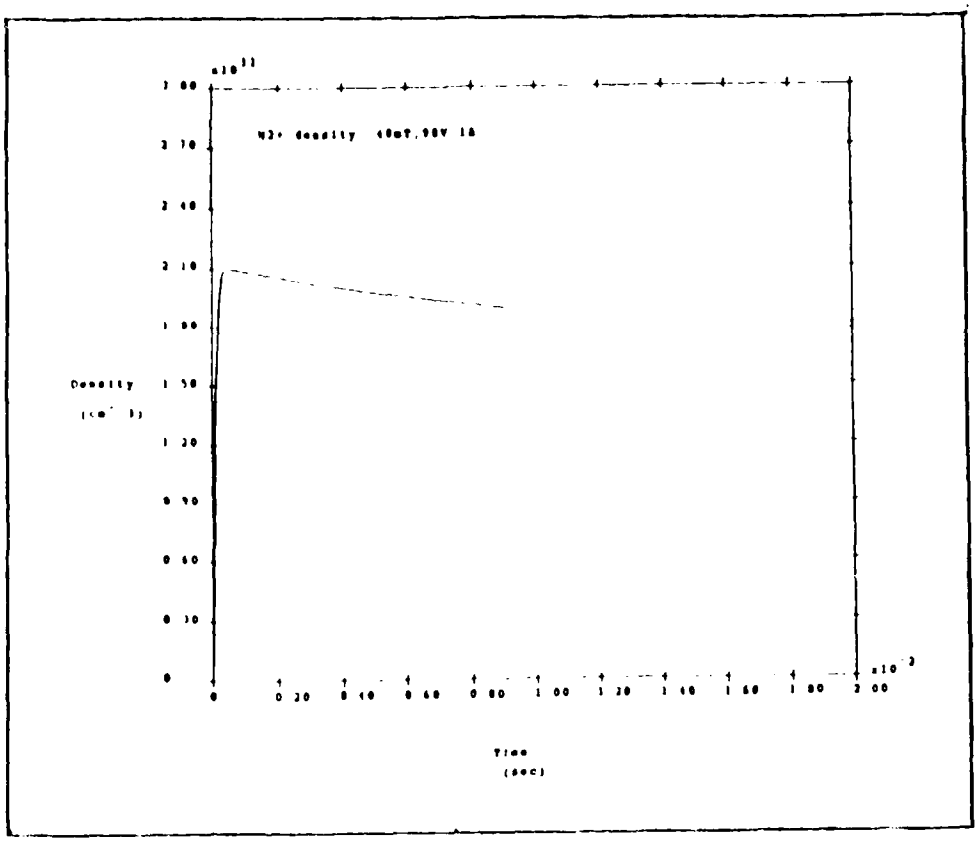

Fig. 30 - Temporal evolution of H_2^+ density for the same conditions as in Fig. 28.

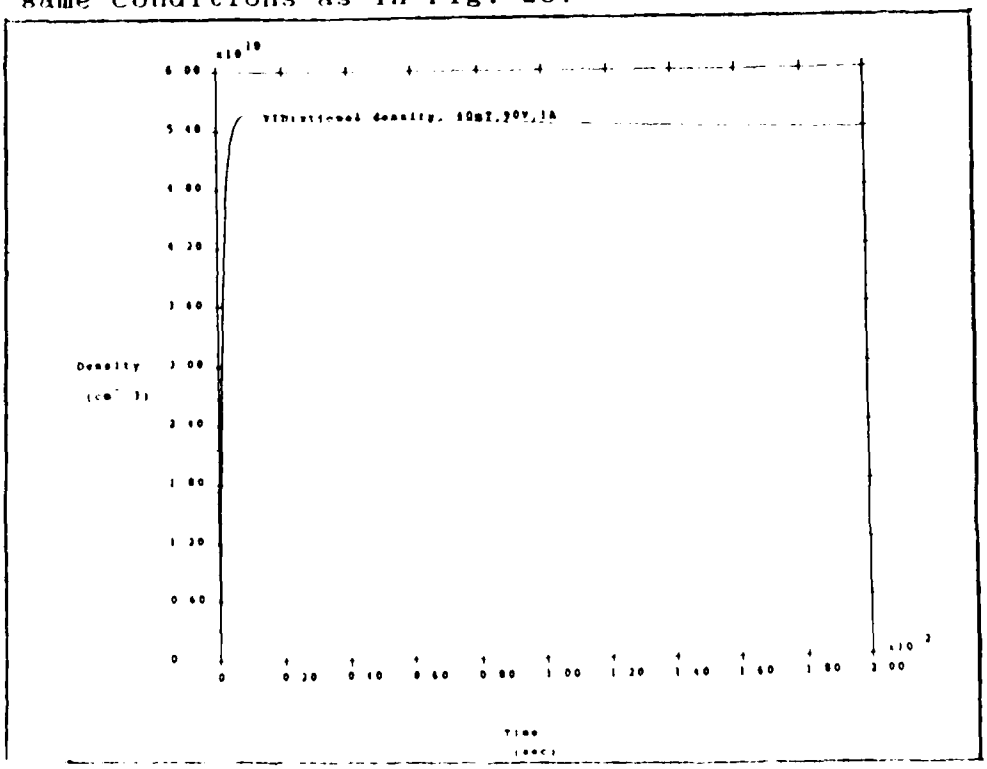

Fig. 31 - Temporal evolution of vibrationally excited hydrogen density for the same conditions as in Fig. 28.

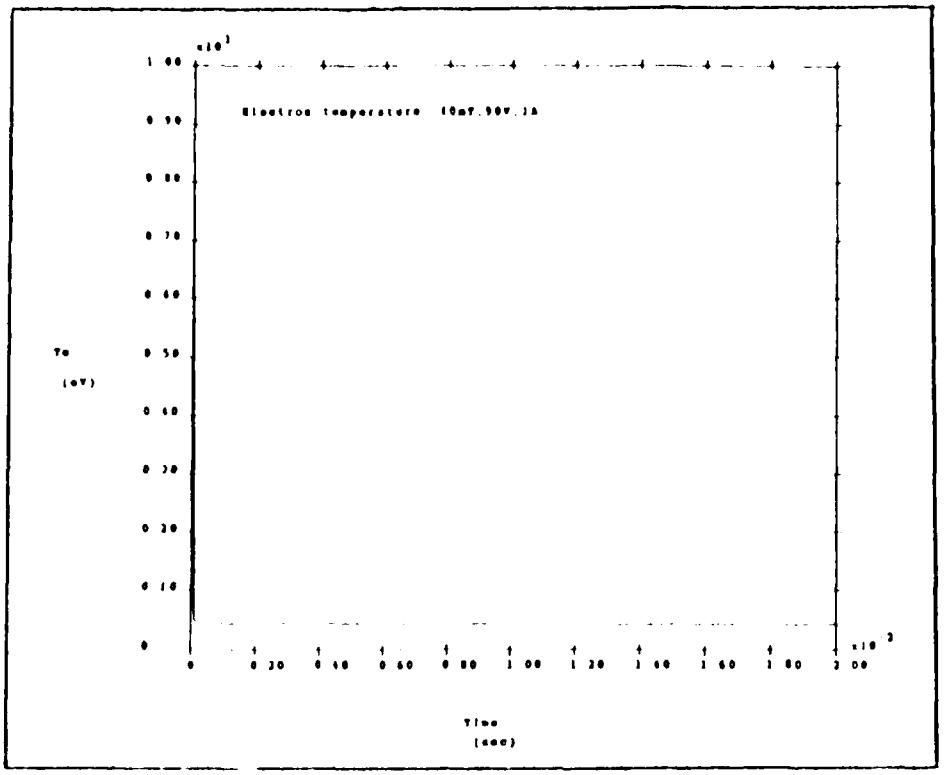

Fig. 32 - Temporal evolution of electron temperature for the same conditions as in Fig. 28.

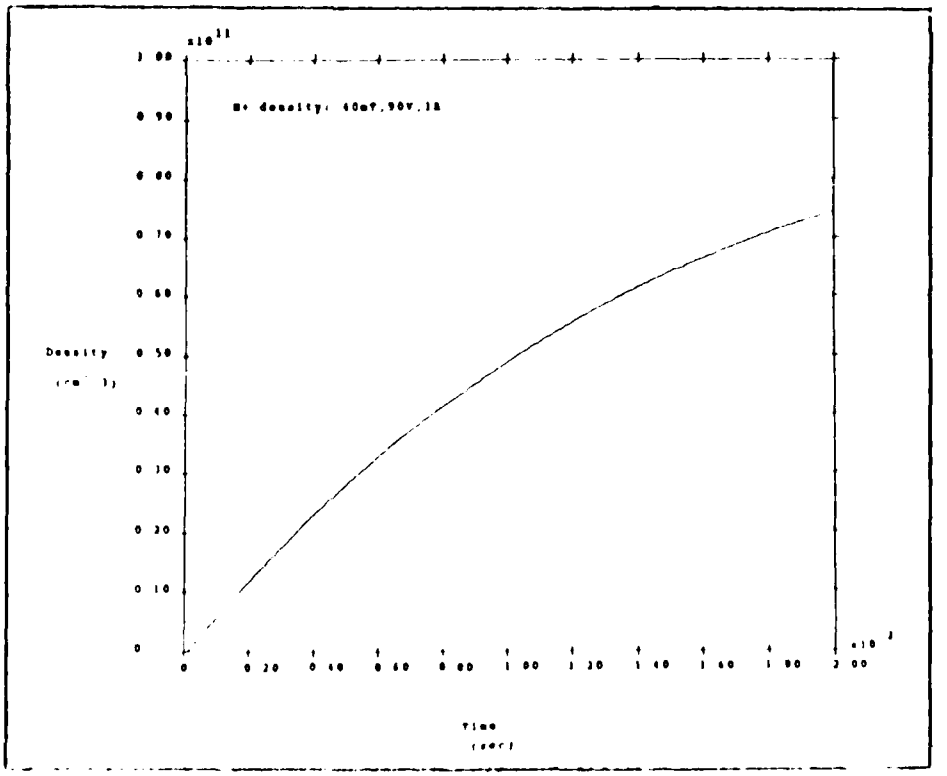

Fig. 33 - Temporal evolution of H^+ density for the same conditions as in Fig. 28.

CHAPTER IV - CONCLUSIONS AND RECOMMENDATIONS

Conclusions

This study has developed a method to model a magnetic mulicusp ion source using self-consistent Maxwellian moments of the Boltzmann equation. The departure from a Maxwellian electron distribution was considered and incorporated into the model by modifying the high energy tail of the distribution using the classical theory of ionization. The distribution tail so derived is found to scale as the ratio of current to pressure, as was previously seen from the complete solution of the Boltzmann equation [10:819-820].

A numerical comparison of the results of this model to previous experimental and theoretical work show that they are in fairly good agreement. The most useful result from this work, however, is the determination of how the various species' densities scale with the discharge parameters.

The scaling laws obtained from this model are supported by several experimental and theoretical studies. In particular, the experimentally observed scaling of negative hydrogen ions with current, pressure, and voltage have been predicted by this model. With these scaling laws it has been determined that for the most efficient production of negative hydrogen ions, the discharge should be run at high currents, pressures around 2-4 mTorr, and voltages around 100-120 V. The scaling laws allow negative ion source users to determine how to vary the discharge parameters most efficiently to

optimize their sources.

Using this model it has been found that negative hydrogen ions are produced through dissociative attachment onto vibrationally excited hydrogen and lost through associative detachment (at the degree of dissociation considered). Slow electrons are produced through ionization by fast electrons and lost through dissociative recombination with H_2^+.

The above results have a positive impact on the use of a MMIS in a neutral particle beam (NPB) weapon system. The low pressure operation indicates that the negative ion beam will have a low emittance, which is highly desired. Also, the low pressure operation will simplify the construction of a space-worthy system. If it is assumed that the discharge current is around 1000 A, as in Holmes' source at Culham Laboratory [5], then it is seen that the power required for continuous operation is around 100 kW. Depending upon the projected duty cycle, this power requirement could be substantially reduced. The size of Holmes' source is 55 x 31 x 20 cm^3 - easily small enough that all of the size limitations in a NPB system will be imposed upon the accelerator and not the ion source. Thus, it is apparent that a MMIS will make an efficient ion source for a space-based NPB weapon system.

Comparison to a typical surface ion source, the Penning discharge, shows that, while having a lower negative ion current, the MMIS has a lower emittance. For instance a typical Penning discharge ion source [37:S80] produces a

current of 140-180 mA with an emittance of about .07 cm-mrad. A typical MMIS [5:234,35:684] produces a current of about 1 mA with an emittance of around .03 cm-mrad. The factor of 2 difference in emittances indicates that the NPB from a MMIS will have roughly twice the effective range as a NPB from a surface source. If it is assumed that the current delivered by the Penning source is the minimum allowed for a weapon system to be considered lethal, then the beam delivered by the MMIS cannot be considered lethal. However, it has been determined [37:S79] that the total beam energy (and hence beam current) required for use in discrimination may be a factor of around 100 less than required for lethality. Therefore, a MMIS is an excellent option for use in a NPB discrimination system.

A final factor in favor of volume sources over surface sources is the use of cesium in the latter. The cesium, being highly reactive, will decrease the useful lifetime of the surface source. A volume source does not have this problem.

Recommendations

To improve the results obtained, several things can be done with this model. First, all of the runs were made with a dissociation of 56% (taken from the value in Bretagne, *et al* [10]). Adding a self-consistent dissociation into the model by considering the appropriate dissociation chemistry would probably improve the numerical results obtained

tremendously.

Second, the plasma potential was always taken to be 2 V (except for the 2 mTorr, 50 V, 5 A discharge). Bretagne, *et al*, [32:1206-1207] have shown that a variation in the plasma potential dramatically effects the Maxwellian portion of the EEDF. The present model could be improved by adding a self-consistent calculation of the plasma potential based on the balance of charged particles falling on the chamber walls. This calculation would be complex due to the nature of the multicusp field at the wall.

Finally, this model ignored the presence of H_3^+, which is actually the dominant ionic species found in many multicusp discharges [7:1802]. It is indicated by Bruneteau [15:381] that for a 4 mTorr discharge, $H^- - H_3^+$ mutual neutralization is the dominant loss mechanism for negative ions, being a factor of 10 larger than the losses due to associative detachment. In addition, she indicates that H_3^+ ions play an important role in the production of vibrationally excited hydrogen. Thus, inclusion of the plasma chemistry for H_3^+ should improve the calculations of this model significantly.

The next logical step would be to expand the approach to include the spatial variation of the densities and electron temperature. This could possibly be accomplished by not only using the continuity equation and energy equation, but also the momentum moment of the Boltzmann equation. With this adaptation to the model, it would be easier to analyze what

is going on in both the production region and the extraction region of a tandem MMIS.

APPENDIX A - THE CLASSICAL THEORY OF IONIZATION AND THE THOMSON DISTRIBUTION

In this appendix, the classical theory of ionization will be developed. This development will lead to the expression for the Thomson distribution of secondary electrons used in Chapter II. The development used is that given by Thomson and Thomson in Ref. 28, pages 96-98 and 200.

We will regard the ionization of a molecule by an electron as a collision between two particles - the electron and one of the electrons in the molecule. Ionization occurs when the molecular electron receives energy greater than or equal to the ionization energy from the incident electron. Although we will be concerned with the collision between two electrons, the following development is for any incident charged particle.

Let M be the mass of the incident particle and let E be its charge. Assume that its velocity before the collision is v_o and let b be the impact parameter for the collision. In addition, let m and -e be the mass and charge of the molecular electron.

During the collision, the center of mass of the two-particle system moves with a uniform velocity given by

$$v_{c.m.} = \frac{m}{M + m} v_o \qquad (A-1)$$

In the center of mass (c.m.) system the particles move in hyperbolic orbits (see Fig. A-1). Let v_1 and b_1 be the

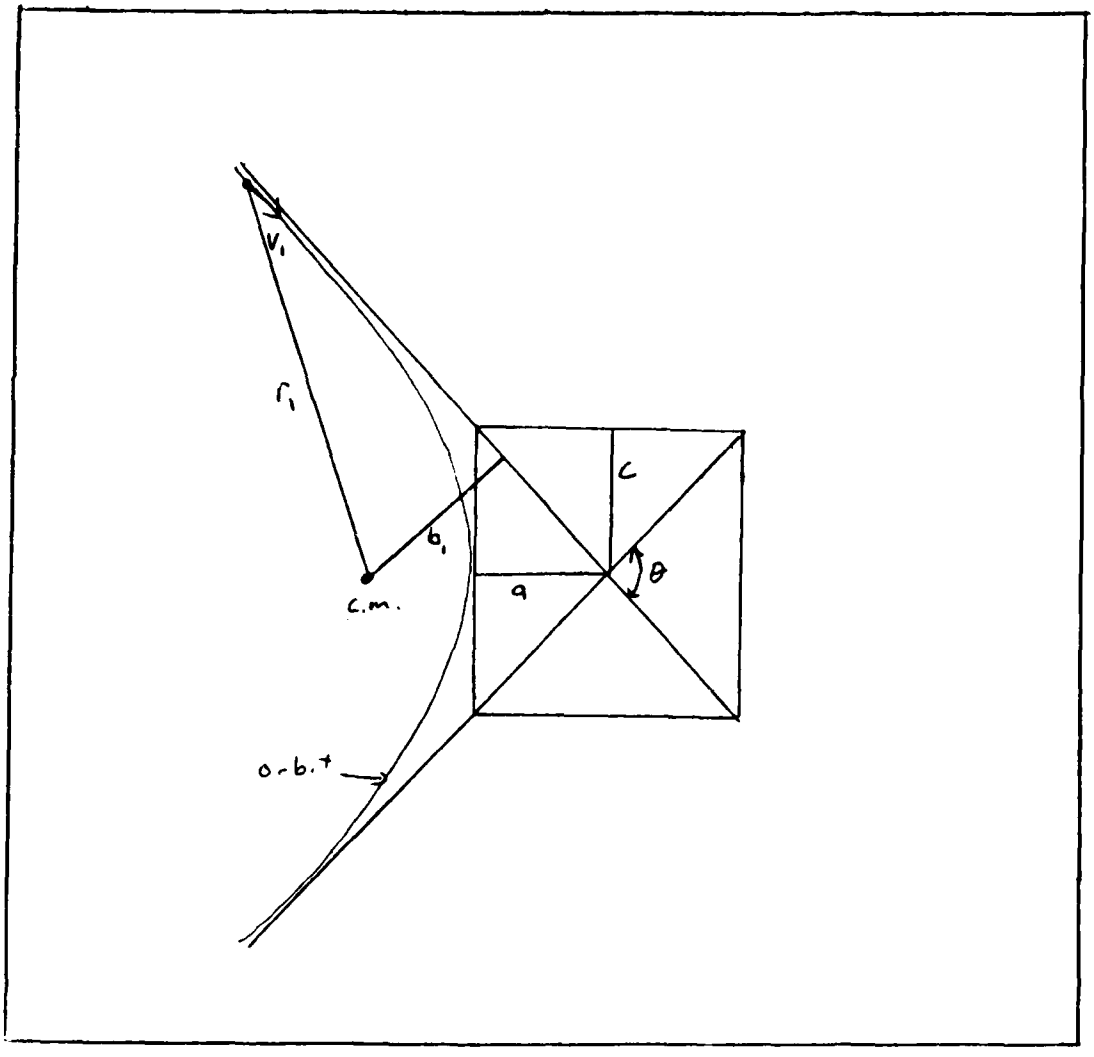

Fig. A-1 - Hyperbolic orbit of incident particle in center of mass frame.

initial velocity and impact parameter of M relative to the c.m. We then have

$$v_1 = \frac{m}{M + m} v_0 \qquad \text{(A-2)}$$

and

$$b_1 = \frac{m}{M + m} b \qquad \text{(A-3)}$$

Let r_1 be the distance of M from the c.m. at any time. Then the force acting on M is given by

$$F = \frac{e E m^2}{(M + m)^2 r_1^2} \qquad \text{(A-4)}$$

and is directed towards the c.m.

If θ is the angle between the asymptotes of the hyperbola then

$$\tan (\theta/2) = c/a \qquad \text{(A-5)}$$

where a and c are the axes of the hyperbola. It is a property of hyperbolae that $c = b_1$. In addition, if μ is the acceleration of M at a unit distance from the c.m.,

$$\mu = \frac{e E m^2}{M (M + m)^2} \qquad \text{(A-6)}$$

then $v_1^2 = \mu/a$, or

$$a = \frac{e E m^2}{v_1^2 M (m + M)^2} \qquad \text{(A-7)}$$

Using Eqns. A-5 and A-7 we then have

$$\tan(\theta/2) = \frac{b_1 v_1^2 M (M+m)^2}{e E m^2} \qquad \text{(A-8)}$$

or, with Eqns. A-2 and A-3,

$$\tan(\theta/2) = \frac{b v_0^2 m M}{e E (M+m)} \qquad \text{(A-9)}$$

After the collision, the component of the velocity of M parallel to v_0 is

$$v_t = \frac{M v_0 - m v_0 \cos\theta}{M+m} \qquad \text{(A-10)}$$

and the component perpendicular to v_0 is

$$v_n = \frac{m v_0 \sin\theta}{M+m} \qquad \text{(A-11)}$$

Therefore, the total kinetic energy of M after the collision is given by

$$E_k = 1/2\ M v_t^2 + 1/2\ M v_n^2$$

or

$$E_k = \frac{1}{2} \frac{M v_0^2}{(M+m)^2} [\, M^2 + m^2 - 2 m M \cos\theta \,] \qquad \text{(A-12)}$$

The energy transfered to the molecular electron is then the change in kinetic energy of the incident particle:

$$Q = 1/2\ M v_0^2 - E_k$$

or

$$Q = \frac{(1+\cos\theta)\, m M^2 v_0^2}{(M+m)^2} \qquad \text{(A-13)}$$

Now

$$1 + \cos\theta = 2\cos^2(\theta/2) = 2\,[1 + \tan^2(\theta/2)]^{-1}$$

so we get, using Eqn. A-9,

$$Q = \frac{2\,e^2\,E^2}{m\,v_o^2}\,\frac{1}{b^2 + d^2} \qquad \text{(A-14)}$$

where

$$d = \frac{e\,E\,(M + m)}{m\,M\,v_o^2}$$

Eqn. A-14 thus represents the transfer of energy from the incident particle to the molecular electron.

It should be noted at this point that the above calculations were made with the assumption that the electrons in the molecule are free to move. If the forces holding the molecular electron are small enough that the period for a small oscillation of the electron about an equilibrium point is large compared to the duration of the collision, then the electron can be considered free. Therefore, to be able to use the above energy transfer calculation, the incident particle must be sufficiently fast. A 90 V electron is moving at about 6×10^8 cm/sec. If the distance over which a collision occurs is on the order of one Bohr radius, then the collision time is approximately 10^{-17} sec - short enough that this classical approach should be valid for the present work.

Now that the energy transfer in the collision is known, it is necessary to find the energy distribution of the

molecular electrons. The chance of a transfer of energy between Q and Q + dQ, f(Q)dQ, is equal to the chance $2\pi nb\ db$ that b is between b and b + db, n being the number density of electrons in the molecule. Therefore, we have

$$f(Q)\ dQ = 2\ \pi\ n\ b\ db \qquad \text{(A-15)}$$

now $2\ b\ db = db^2$, so

$$f(Q)\ dQ = \pi\ n\ \frac{db^2}{dQ}\ dQ \qquad \text{(A-16)}$$

From Eqn. A-14 we get

$$\frac{db^2}{dQ} = -\ \frac{2\ e^2\ E^2}{m\ v_o^2}\ \frac{1}{Q^2} \qquad \text{(A-17)}$$

Putting this in Eqn. A-16 and ignoring the minus sign we have

$$f(Q)\ dQ = \frac{2\ \pi\ n\ e^2\ E^2}{m\ v_o^2}\ \frac{1}{Q^2}\ dQ \qquad \text{(A-18)}$$

Therefore, for an incident electron, the distribution for the molecular electron is

$$f(Q) = \frac{2\ \pi\ n\ e^4}{m\ v_o^2\ Q^2} \qquad \text{(A-19)}$$

If we regard the production of secondary electrons in a MMIS as a case of ionization, we are then saying that an electron emitted from the cathode will collide with an H_2 molecule causing ionization. The molecular electrons will then have a distribution given by Eqn. A-19. Since the secondary electrons have to do work equal to the ionization

energy, E_I, to escape the molecule, the distribution of energy for the secondary electrons will be given by

$$f_{thom}(E) = \frac{A}{(E + E_I)^2} \qquad (A\text{-}20)$$

The constant A can be found by requiring normalization of the above distribution:

$$\int_0^V A\,(E + E_I)^{-2}\,dE = 1 \qquad (A\text{-}21)$$

This gives, with straight-forward integration,

$$A = E_I\,(1 + E_I/V) \qquad (A\text{-}22)$$

Thus, the Thomson distribution of secondary electrons is

$$f_{thom}(E) = \frac{E_I\,(1 + E_I/V)}{(E + E_I)^2} \qquad (30)$$

APPENDIX B - MOMENT EQUATION CODE

In this appendix, the numerical solution of the moment equations is discussed. After this a listing of the computer code is given. A brief schematic of the numerical process is given in Fig. B-1.

Calculation of Reaction Rates

Maxwellian-averaged reaction rates as a function of average electron energy, defined by Eqn. 4, were calculated once at the beginning of the study and stored in ASCII files. These files are then referenced each time the main computer code is run.

In order to calculate the reaction rates, the $\sigma_i(E)v(E)$ data was fit using natural cubic splines [30:122]. The integration in Eqn. 4 was then carried out over the range of the data, for average electron energies ranging between .01 eV and 1000 eV. The integration was performed using Simpson's adaptive quadrature [30:174-175].

The Numerical Solution of the Moment Equations

The main computer code, MOMEQN, uses the above calculated Maxwellian reaction rates in order to calculate the time evolution of the number densities and electron temperature by simultaneously solving the moment equations, represented by Eqns. 43-47 and 50.

As further input to the program, MOMEQN reads two ASCII

files - 'process', and 'init'. The file 'process' contains a line of data for each plasma reaction that was considered in this model. The first element of each line is a character string mnemonic refering to the reaction. The second element is either a 1 or a 0, indicating whether (1) or not (0) that particular reaction is active during the current run. The third element is a real number equal to the threshold energy for the reaction. The file 'init' contains all of the other operating data, such as the discharge current, voltage, pressure, plasma volume, initial values of the densities, etc.

After all of the above data is entered into the program, MOMEQN calls the subroutine DTAIL to calculate the high energy tail of the EEDF. This is accomplished by first fitting the $\sigma_i(E)v(E)$ data with natural cubic splines. Then $f_{tail}(E)$ is calculated using Eqn. 32, starting at $E = V - E_I$. The rest of the distribution is calculated for successively lower energies, using the knowledge of what the distribution is for higher energies.

Once this distribution is calculated, MOMEQN calls the subroutine ELECTRONIC in order to calculate the reaction rates averaged over the tail of the distribution, which will be used in the vibrational density equation. These reaction rates are determined by using Simpson's adaptive quadrature to perform the integration in Eqn. 39. The particular reactions for which rates are calculated at this point are the electronic excitations and H_2 ionization.

Next, MOMEQN calls the subroutine THOMSON, which calculates the average energy of the source (Eqn. 53) and the average probability of no wall collisions (Eqn. 59). These integrals are again calculated using Simpson's adaptive quadrature.

At this point, MOMEQN is ready to start the integration of the moment equations. This is accomplished by first setting the time variable to 0, and then calling the subroutine RKF45. This subroutine integrates the moment equations from the previous time to the present time and outputs the answer. The time variable is then incremented and RKF45 is called again. This process continues until one of two conditions is met: 1) the number densities and electron temperature all have reached a steady state, or, 2) the time variable has reached a maximum, user-specified, value. Condition 1 is numerically determined to be achieved if the values of all the number densities and the electron temperature have not changed by more than a set factor (10^{-4}) for four consecutive time steps. If this condition is met, the values have reached a steady state, as far as the computer code is concerned.

The subroutine RKF45

The subroutine RKF45 integrates a system of coupled first order differential equations by using two Runge-Kutta-Fehlberg integration schemes. One is of order 4 and the other is order 5. The two results obtained are compared to

get an estimate of the error in the answer. This estimate is then used for step size control.

The Runge-Kutta-Fehlberg algorithm calculates the value of the various plasma parameters by using the following formula:

$$y_{j,n+1} = y_{j,n} + \sum_{i=1}^{6} \gamma_i \; k_{j,i} \qquad \text{(B-1)}$$

where

$$k_{j,i} = h_n \; y'_j \left(y_{j,n} + \sum_{m=1}^{i-1} \beta_{i\,m} \; k_{j,m} \; , \; t_n + \alpha_i \; h_n \right) \qquad \text{(B-2)}$$

and where $y_{j,n}$ is the estimate for the j-th plasma parameter (electron density, ion densities, or electron temperature) at the n-th time step, y' is the corresponding derivative, h_n is the step-size for the n-th time step, t_n is the time, and α, β, and γ are coefficients that were found by Fehlberg. He found one set of γ's that makes the estimate given by Eqn. B-1 order 4 and another set of γ's that makes it order 5.

The majority of the code in RKF45 is used to determine the optimum step-size, h, for the current time.

Implementation

The program MOMEQN was written in FORTRAN 77 and ran on a VAX 11/785 under Berkeley 4.3 BSD UNIX. Typical run-times varied between 10 minutes and 1 hour, depending upon the system load. It is quite possible that many improvements

could be made on this code to make it run more efficiently. The present form of the code was written for readability.

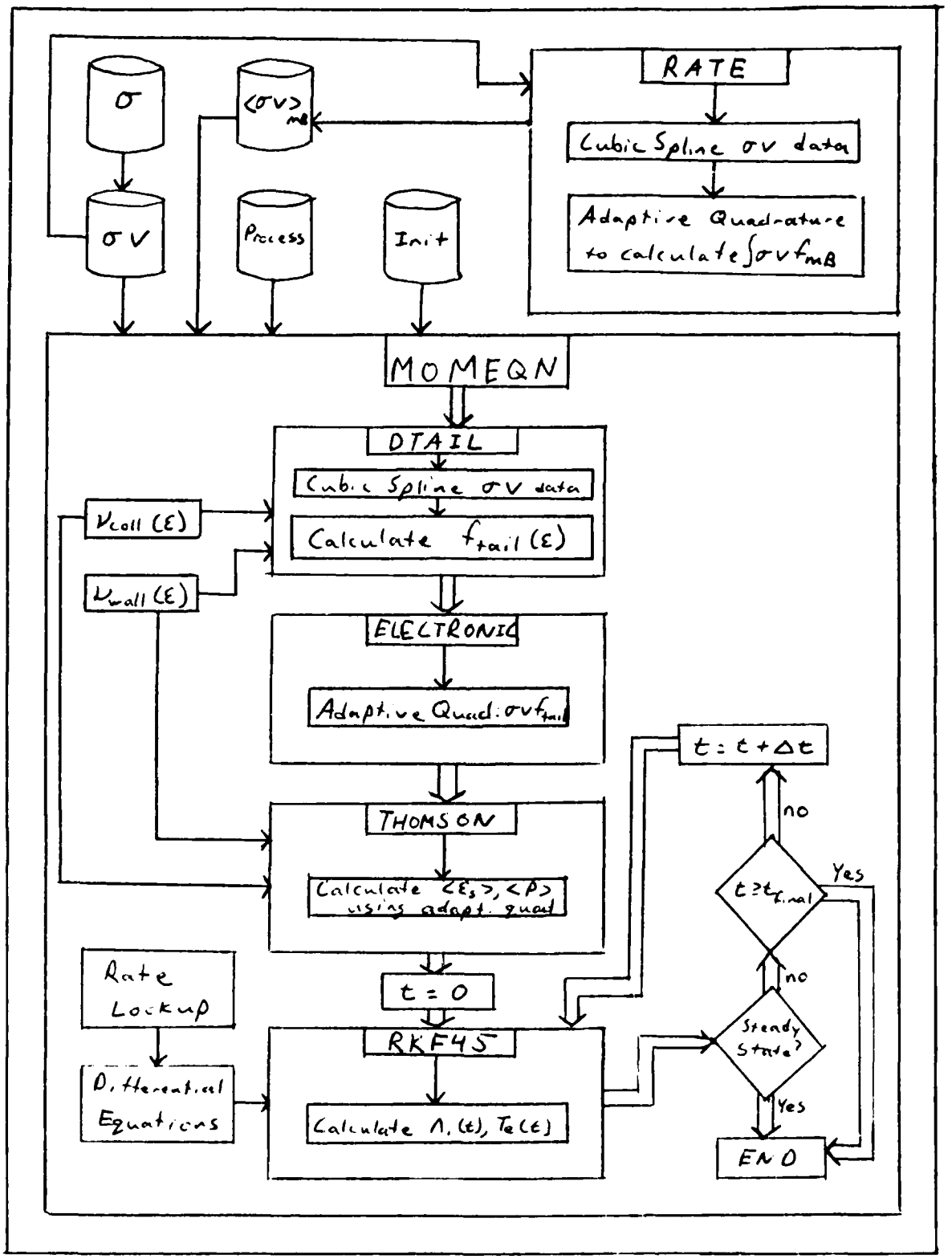

Fig. B-1 - Wiring diagram for computer codes used in numerical solution of moment equations.

```
c*****************************************************************
c
c
c       A SELF-CONSISTENT MOMENT EQUATION SOLVER FOR A
c               MAGNETIC MULTICUSP HYDROGEN DISCHARGE
c
c
c       Written by David E. Bell, 2Lt, USAF
c
c
c       SYNOPSIS:  This program solves the time-dependent
c       moment equations developed in Chapter II for a given
c       set of initial conditions.  It outputs the time
c       evolution of the ionic species and the electron
c       temperature.
c
c*****************************************************************

c*****************************************************************
c
c       VARIABLE LIST:
c
c on - array indicating whether or not (1/0) a process is on
c th - array containing the thresholds for the processes (eV)
c press - pressure of the discharge (Torr)
c volt - discharge voltage (V)
c curr - discharge current (A)
c dt - time increment for output (sec)
c y - array whose elements represent:
c     1 - number density of electrons (cm^-3)
c     2 - number density of negative hydrogen ions (cm^-3)
c     3 - number density of positive H2 ions (cm^-3)
c     4 - number density of positive H ions (cm^-3)
c     5 - average electron temperature (eV)
c     6 - number density of vibrationally excited H2 (cm^-3)
c nho - ratio of H to H2 in plasma
c no - density of H2 (cm^-3)
c nh - density of H (cm^-3)
c so - source strength
c ens - average energy of the source
c m1 - mass of an electron (kg)
c m2 - mass of a hydrogen atom (kg)
c t - time variable (sec)
c tout - next time of output (sec)
c tfinal - time to quit program (sec)
c temp - H2 temperature (eV)
c relerr - relative error allowed in output
c abserr - absolute error allowed in output
c work - array used by rkf45 for various things
c vol - plasma volume of source (cm^3)
c area - effective wall loss area of plasma source (cm^2)
c vp - plasma potential (V)
c iwork - array used by rkf45 for various things
c iflag - flag used by rkf45 to indicate progress. Values:
```

```
c         -2 - single successful step in direction of tout
c          2 - integration reached tout. Successful return.
c          3 - relative error too small, has been increased
c          4 - more than 3000 derivative evaluations needed
c          5 - solution vanished - cannot test relative error,
c              absolute error must be nonzero to continue
c          6 - requested accuracy unobtainable, error
c              tolerance increased
c          7 - RKF45 is inefficient for this problem
c          8 - invalid input parameters :
c              neqn.lt.0
c              t=tout and iflag.ne.+1 or -1
c              relerr or abserr .lt. 0
c              iflag.eq.0 or .lt.-2 or .gt.8
c neqn - number of differential equations in system (6)
c file - character array with file names for the processes
c sav - array used to save y() data for checking convergence
c flag - logical variable used in testing convergence
c ss - counter used in testing convergence
c length - average distance to wall (cm)
c xsect - sigma*vel data for electronic excitations
c nxsect - number of data points for each excitation in xsect
c a,b,c,d - cubic spline data for xsect
c tail - reaction rate coefficient for electronic states
c        averaged over tail of distribution
c rates - array holding Maxwellian reaction rate data
c ftail - array representing the tail of the distribution
c
c*****************************************************************

      external diffeq
      real on(27),th(27),press,volt,curr,dt,y(6),nho,no,nh,
     &     so,ens,m1,m2,t,tout,tfinal,temp,relerr,abserr,
     &     work(39),vol,rates(27,561,2),area,vp,sav(6),
     &     length,xsect(9,50,2),a(9,50),b(9,50),c(9,50),
     &     d(9,50),tail(8),ftail(0:100)
      integer iwork(5),iflag,neqn,ss,nxsect(9)
      logical flag
      character*7 file(27)

      common so,no,nh
      common/ener/ens,m1,m2
      common/onoff/on,file
      common/freq/th,rates,tail
      common/geom/area,vol,vp
      common/recom/y,temp,length
      common/power/volt,curr
      common/sigv/xsect,nxsect
      common/splin/a,b,c,d
      common/dist/ftail

c
c  Input rate coefficient data from files
c
```

```
      call process(on,th,file,rates,xsect,nxsect)
c
c  Input initial operating conditions
c
      call init(press,volt,curr,tfinal,dt,y(1),y(2),y(3),
     &          y(4),nho,temp,vol,area,length,vp,relerr,
     &          abserr)
      no=8.3216e14*press/temp/(1.+nho)
      nh=nho*no
      sav(1)=y(1)
      y(1)=1.e11

c
c  Calculate tail of EEDF
c
      call dtail(ftail)
c
c  Calculate rate coefficients for electronic excitations
c
      call electronic
c
c  Calculate average energy of source and source strength
c
      call thomson(ens,volt,so)
      y(1)=sav(1)
      so=so*curr/1.6022e-19/vol*volt/(2.*15.427)
      y(5)=ens
      m1=9.1095e-31
      m2=2.*1.6726e-27
c
c  Set-up output files
c
      call files

c
c  Start integration of equations
c
      t=0.
      iflag=1
      tout=t
      neqn=6

 10   call rkf45(diffeq,neqn,y,t,tout,relerr,abserr,iflag,
     &          work,iwork)
      call output(t,y)

      goto (80,20,30,40,50,60,70,80),iflag

c
c  Successful step in integration
c
 20   tout=t+dt

c
```

```
c  Check for convergence of answer
c
        flag=.true.
        do 21 i=1,6
        if(y(i).eq.0.)then
            flag=(abs(sav(i)-y(i)).lt.abserr/10.).and.flag
          else
            flag=(abs(sav(i)-y(i))/y(i).lt.relerr/10.).and.flag
          endif
 21     continue
        if(flag)then
             ss=ss+1
           else
             ss=0
           endif

        do 23 i=1,5
 23     sav(i)=y(i)

c
c  Four consecutive times of little change in output
c    constitutes convergence
c
        if(ss.eq.4)goto 22

        if(t.lt.tfinal)goto 10

c
c  Completed successful run of program - output summary
c
 22     call endout(y)
        stop

c
c  Errors in RKF routine handled here
c

 30     write(6,31)t,relerr,abserr
 31     format(' Tolerances reset at time ',1pe9.3/
     &          ' Relative error = ',1pe8.2/
     &          ' Abserr = ',1pe8.2)
        goto 10

 40     write(6,41)t
 41     format(1x,'Over 3000 function evaluations at time ',
     &          1pe9.3)
        goto 10

 50     abserr=1.e-9
        write(6,31)t,relerr,abserr
        goto 10

 60     relerr=10.*relerr
        write(6,31)t,relerr,abserr
```

```
            iflag=2
            goto 10

   70       write(6,71)t
   71       format(1x,'RKF45 is inefficient for this problem.'/
     &              'Time = ',1pe9.3)
            iflag=2
            goto 10

   80       write(6,81)t
   81       format(1x,'Improper call at time ',1pe9.3)
            stop

            end

c*****************************************************************
c
c       This subroutine opens the file 'process' and reads
c       it to determine what processes are active for the
c       current run (on), the threshold energy for the
c       processes (th), and the names of the files that
c       contain the rate look-up data (file).  The rate data
c       is then entered into the array rates() which is used
c       by the function rate() to determine the rate
c       coefficient for a given energy.  This subroutine also
c       enters the cross-section*velocity data as a function
c       of energy for the electronic excitations.
c
c       The file 'process' is made up of 27 records of the
c       form:
c
c       file       1. (on/off)    12.0 (threshold)
c
c*****************************************************************

            subroutine process(on,th,file,rates,xsect,nxsect)
            real on(27),th(27),rates(27,561,2),d2,d3,xsect(9,50,2)
            integer nxsect(9)
            character*7 file(27)
            character*40 d1

            open(unit=15,file='process',status='old')

            do 1 i=1,27
    1       read(15,*)file(i),on(i),th(i)

            close(unit=15)

            do 5 i=1,27

c
c  the extension .rat is used to indicate average rate data
c
            open(unit=15,file=file(i)//'.rat',status='old')
```

```
c
c  first five lines of files are descriptive labels used for
c   graphing purposes only
c  sixth line contains the number of data pairs
c  seventh line contains xmin,xmax
c  eigth line contains ymin,ymax
c
        do 2 j=1,5
 2      read(15,*)d1
        read(15,3)n
 3      format(i3)
        read(15,*)d2,d3
        read(15,*)d2,d3

        do 4 j=1,n
        read(15,*)d2,d3
        rates(i,j,1)=d2
        rates(i,j,2)=d3
 4      continue

        close(unit=15)

 5      continue

        do 6 i=1,9

c
c  the extension .vel is used to denote cross-
c  section*velocity data
c
        open(unit=15,file=file(i)//'.vel',status='old')

        do 7 j=1,5
 7      read(15,*)d1
        read(15,3)nxsect(i)
        read(15,*)d2,d3
        read(15,*)d2,d3

        do 8 j=1,nxsect(i)
 8      read(15,*)xsect(i,j,1),xsect(i,j,2)

        close(unit=15)

 6      continue

        return
        end

c*****************************************************************
c
c       This subroutine opens the file 'init' and reads in
c       the initial operating conditions of the discharge.
c
c*****************************************************************
```

```
      subroutine init(press,volt,curr,tfinal,dt,ne,nm,np,
     &                nhp,nho,temp,vol,area,length,vp,
     &                relerr,abserr)
      real press,volt,curr,tfinal,dt,ne,nm,np,nhp,nho,temp,
     &     vol,relerr,abserr,area,vp,length

      open(unit=15,file='init',status='old')

      read(15,*)press
      read(15,*)volt
      read(15,*)curr
      read(15,*)tfinal
      read(15,*)dt
      read(15,*)ne
      read(15,*)nm
      read(15,*)np
      read(15,*)nhp
      read(15,*)nho
      read(15,*)temp
      read(15,*)vol
      read(15,*)area
      read(15,*)length
      read(15,*)vp
      read(15,*)relerr
      read(15,*)abserr

      close(unit=15)
      return
      end

c*****************************************************************
c
c       This subroutine sets up the output files for the
c       number densities of tne ionic species and the
c       electrons and the electron temperature.  They are
c       set up in the correct format to be used by 'graph'.
c       The program 'graph' takes a data file and produces a
c       file that is in the correct format to be plotted
c       either on a Benson printer or on a Laser printer.
c       The first 5 lines of the data file must be blank or
c       contain labels for the plot. The next line must
c       contain the number of data points in i3 format.  The
c       next two lines are the minimum and maximum values for
c       the x range and the y range.  The rest of the lines
c       contain the data points.
c       Another file ('all') is set up for output in a more
c       readable format.
c
c*****************************************************************

      subroutine files
      character*1 line(80)
```

```
      open(unit=10,file='ne',status='new')
      open(unit=11,file='nm',status='new')
      open(unit=12,file='np',status='new')
      open(unit=13,file='nhp',status='new')
      open(unit=14,file='en',status='new')
      open(unit=16,file='nv',status='new')
      open(unit=20,file='all',status='new')

      write(10,*)'Electron density'
      write(11,*)'H- density'
      write(12,*)'H2+ density'
      write(13,*)'H+ density'
      write(14,*)'Electron temperature'
      write(16,*)'Vibrational density'

      do 1 i=10,13
      write(i,*)'Time'
      write(i,*)' (sec)'
      write(i,*)'Density'
      write(i,*)' (cm^-3)'
1     continue
      write(16,*)'Time'
      write(16,*)' (sec)'
      write(16,*)'Density'
      write(16,*)' (cm^-3)'

      write(14,*)'Time'
      write(14,*)' (sec)'
      write(14,*)'Temperature'
      write(14,*)' (eV)'

      do 3 i=10,14
      write(i,2)999
2     format(i3)
      write(i,*)0.,0.
      write(i,*)0.,0.
3     continue

      write(20,4)
4     format('TIME',9x,'Ne',11x,'N-',11x,'N+',11x,'Nh+',
     &       10x,'Te')
      do 6 i=1,80
      line(i)='='
6     continue
      write(20,5)(line(i),i=1,80)
5     format(80a)

      return
      end

c*************************************************************
c
c     This subroutine calculates the rate coefficients for
c     the electronic excitations based on the modified
```

```
c       Thomson.
c
c*****************************************************************

        subroutine electronic
        real xsect(9,50,2),tol,a(9,50),b(9,50),c(9,50),d(9,50),
     &       rates(27,561,2),tl(200),a2(200),h2(200),fa(200),
     &       fc(200),fb(200),s(200),k2(200),fd,fe,s1,s2,v(8),
     &       th(27),ion,volt,curr,vol,area,vp,tail(8)
        integer nxsect(9)

        common/splin/a,b,c,d
        common/sigv/xsect,nxsect
        common/freq/th,rates,tail
        common/geom/area,vol,vp
        common/power/volt,curr

        tol=1.e-3
        ion=15.427

        do 1 k=1,8

        tail(k)=0.

        i=1
        tl(i)=10.*tol
        a2(i)=xsect(k,1,1)
        h2(i)=(xsect(1,nxsect(k),1)-xsect(k,1,1))/2.
        fa(i)=felect(k,xsect(k,1,1))
        fc(i)=felect(k,xsect(k,1,1)+h2(i))
        fb(i)=felect(k,xsect(k,nxsect(k),1))
        s(i)=h2(i)*(fa(i)+4.*fc(i)+fb(i))/3.
        k2(i)=1.

5       if(i.le.0)goto 4

        if(tl(i).lt.1.e-6)tl(i)=1.e-6
        fd=felect(k,a2(i)+h2(i)/2.)
        fe=felect(k,a2(i)+3.*h2(i)/2.)
        s1=h2(i)*(fa(i)+4.*fd+fc(i))/6.
        s2=h2(i)*(fc(i)+4.*fe+fb(i))/6.
        v(1)=a2(i)
        v(2)=fa(i)
        v(3)=fc(i)
        v(4)=fb(i)
        v(5)=h2(i)
        v(6)=tl(i)
        v(7)=s(i)
        v(8)=k2(i)

        i=i-1

        if(abs(s1+s2-v(7)).lt.v(6))then
            tail(k)=tail(k)+s1+s2
```

```
                else
                  if(v(8).ge.200)then
                      write(6,*)'Integration failed in ELECTRONIC'
                      stop
                    else
                      i=i+1
                      a2(i)=v(1)+v(5)
                      fa(i)=v(3)
                      fc(i)=fe
                      fb(i)=v(4)
                      h2(i)=v(5)/2.
                      tl(i)=v(6)/2.
                      s(i)=s2
                      k2(i)=v(8)+1.

                      i=i+1
                      a2(i)=v(1)
                      fa(i)=v(2)
                      fc(i)=fd
                      fb(i)=v(3)
                      h2(i)=h2(i-1)
                      tl(i)=tl(i-1)
                      s(i)=s1
                      k2(i)=k2(i-1)
                    endif
                  endif

            goto 5

     4      continue

     3      continue
     1      continue

            return
            end

c*****************************************************************
c
c       This subroutine performs natural cubic splines on the
c       cross-section data for the electronic excitations.
c
c*****************************************************************

            subroutine spline(data,num,a,b,c,d)
            real data(9,50,2),a(9,50),b(9,50),c(9,50),d(9,50),
     &           h(50),alpha(50),l(50),mu(50),z(50)
            integer num(9)

            do 10 k=1,9
            do 20 j=1,num(k)
            a(k,j)=data(k,j,2)
     20     continue
     10     continue
```

```
            do 1 k=1,9

            do 2 i=1,num(k)-1
 2          h(i)=data(k,i+1,1)-data(k,i,1)

            do 3 i=2,num(k)-1
            alpha(i)=3.*(a(k,i+1)*h(i-1)-a(k,i)*(data(k,i+1,1)
     &                -data(k,i-1,1))+a(k,i-1)*h(i))/(h(i-1)*h(i))
 3          continue

            l(0)=1.
            mu(0)=0.
            z(0)=0.

            do 4 i=2,num(k)-1
            l(i)=2.*(data(k,i+1,1)-data(k,i-1,1))-h(i-1)*mu(i-1)
            mu(i)=h(i)/l(i)
            z(i)=(alpha(i)-h(i-1)*z(i-1))/l(i)
 4          continue

            l(num(k))=1.
            z(num(k))=0.
            c(k,num(k))=0.

            do 5 j=num(k)-1,1,-1
            c(k,j)=z(j)-mu(j)*c(k,j+1)
            b(k,j)=(a(k,j+1)-a(k,j))/h(j)-h(j)*(c(k,j+1)
     &           +2.*c(k,j))/3.
            d(k,j)=(c(k,j+1)-c(k,j))/(3.*h(j))
 5          continue

 1          continue

            return
            end

c*****************************************************************
c
c       This function represents the distribution function
c       for the tail multiplied by sigma*velocity.
c
c*****************************************************************

            real function felect(i,e)
            real e,ion,ftail(0:100),distrib

            common/dist/ftail

            ion=15.427

            distrib=(e-float(int(e)))*
     &           (ftail(int(e)+1)-ftail(int(e)))+ftail(int(e))
```

```
      felect=sv(i,e)*distrib

      return
      end

c*****************************************************************
c
c     This function uses the spline data calculated by
c     spline to calculate sigma*vel as a function of energy.
c     This routine is used by fcoll and felect.
c
c*****************************************************************

      real function sv(i,en)
      real en,xsect(9,50,2),den,a(9,50),b(9,50),c(9,50),
     &     d(9,50)
      integer nxsect(9)

      common/sigv/xsect,nxsect
      common/splin/a,b,c,d

      if((en.lt.xsect(i,1,1))
     &     .or.(en.gt.xsect(i,nxsect(i),1)))then
          sv=0.
          return
        endif

      do 1 j=1,nxsect(i)-1
      if(en.ge.xsect(i,j,1).and.en.lt.xsect(i,j+1,1))goto 2
 1    continue
      j=nxsect(i)

 2    den=en-xsect(i,j,1)

      sv=a(i,j)+b(i,j)*den+c(i,j)*den**2+d(i,j)*den**

      return
      end

c*****************************************************************
c
c     This function calculates the
c     rate as a function of energy
c
c*****************************************************************

      real function f
      real en,no,s
      common

      f=0.

      d
```

AD-A188 858 A MOMENT APPROACH TO MODELING NEGATIVE ION SOURCES(U) 2/2
AIR FORCE INST OF TECH WRIGHT-PATTERSON AFB OH SCHOOL
OF ENGINEERING D E BELL DEC 87 AFIT/GEP/ENP/87D-2
UNCLASSIFIED F/G 20/7 NL

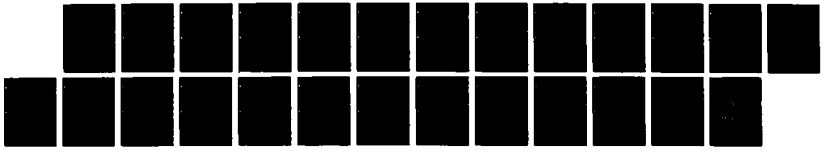

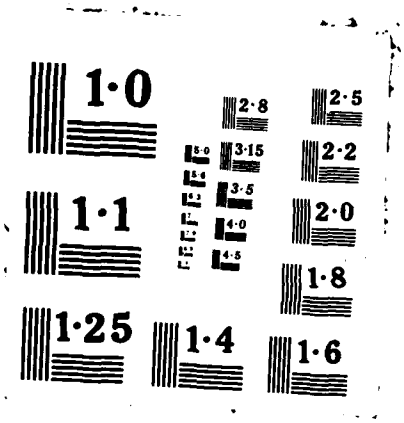
1·0
1·1
1·25
1·4
1·6
1·8
2·0
2·2
2·5
2·8
3·15
3·5
4·0
4·5

```
            fcoll=fcoll+sv(i,en)

    1       continue

            fcoll=no*fcoll

            return
            end

c***********************************************************************
c
c       This function calculates the rate of loss of primary
c       electrons to the walls of source.  Formula is from
c       Bretagne, et al [10:813].
c
c***********************************************************************

            real function fwall(en)
            real en,area,vol,no,vp,so,nh

            common so,no,nh
            common/geom/area,vol,vp

            if(en.lt.vp)then
                fwall=0.
              else
                fwall=6.e7*area/vol*sqrt(en)*(1.-vp/en)/4.
              endif

            return
            end

c***********************************************************************
c
c       This subroutine calculates the tail of the
c       distribution.
c
c***********************************************************************

            subroutine dtail(ftail)
            real ftail(0:100),volt,curr,th(27),rates(27,561,2),
     &           tail(8),area,vol,vp,ion,a(9,50),b(9,50),c(9,50),
     &           d(9,50),xsect(9,50,2),x,y,xp,yp,no,nh,so
            integer nxsect(9),flag

            common so,no,nh
            common/power/volt,curr
            common/freq/th,rates,tail
            common/geom/area,vol,vp
            common/splin/a,b,c,d
            common/sigv/xsect,nxsect

            call spline(xsect,nxsect,a,b,c,d)
```

```
      ion=15.427
      flag=0

      do 1 i=100,0,-1

      en=float(i)

      if(en.gt.volt-ion)then
          ftail(i)=0.
          goto 1
        endif

      sum=0.
      do 2 j=1,9
      k=i+int(th(j)+.5)
      if(k.gt.100)k=100
      sum=sum+ftail(k)*sv(j,en+th(j))
2     continue
      sum=no*sum

      x=fcoll(en)
      y=fwall(en)
      if((flag.eq.0).and.(x+y.eq.0.))then
          xp=fcoll(en+1.)
          yp=fwall(en+1.)
          flag=1
        endif
      if(flag.eq.1)then
          x=xp
          y=yp
        endif
      ftail(i)=(ion*1.+ion/volt)*curr/1.6022e-19/vol*volt
     &          /(2.*ion)/(en+ion)**2+sum)/(x+y)

1     continue

      return
      end

c*********************************************************************
c
c     This subroutine outputs the current data to the
c     output files.
c
c*********************************************************************

      subroutine output(t,y)
      real t,y(6),telec

      write(10,*)t,y(1)
      write(11,*)t,y(2)
      write(12,*)t,y(3)
      write(13,*)t,y(4)
```

```
      telec=2.*y(5)/3.
      write(14,*)t,telec

      write(20,1)t,y(1),y(2),y(3),y(4),telec
 1    format(6(1pe9.3,4x))

      return
      end

c*****************************************************************
c
c     This subroutine represents the system of differential
c     equations to be solved.
c
c*****************************************************************

      subroutine diffeq(t,y,yp)
      real t,y(6),yp(6),so,no,nh,ens,m1,m2,r(27),th(27)
      real rates(27,561,2),tail(8)
      common so,no,nh
      common/ener/ens,m1,m2
      common/freq/th,rates,tail

      do 1 i=1,27
 1    r(i)=rate(i,y(5))

      if(y(5).ge.1000.)write(6,*)'Energy > 1000 -- ',y(5)

c
c  electron continuity
c
      yp(1) = so + r(9)*y(1)*no + r(19)*y(1)*no
     &         + r(13)*y(1)*nh - r(18)*y(1)*y(6)
     &         - r(26)*y(1)*y(3) - r(15)*y(1)*y(3)
     &         - r(16)*y(1)*y(4) + r(22)*y(1)*y(2)
     &         + r(24)*y(2)*nh - r(12)*y(1)*y(3) + r(23)*nh*y(2)

c
c  negative ion continuity
c
      yp(2) = r(18)*y(1)*y(6) + r(25)*y(1)*no
     &         + r(26)*y(1)*y(3) - r(21)*y(4)*y(2)
     &         - r(22)*y(1)*y(2) - r(24)*nh*y(2)
     &         - r(23)*nh*y(2)

c
c  H2+ continuity
c
      yp(3) = so + r(9)*y(1)*no - r(12)*y(1)*y(3)
     &         - r(26)*y(1)*y(3) - r(15)*y(1)*y(3)

c
c  H+ continuity
c
```

```
      yp(4) = r(19)*y(1)*no + r(13)*y(1)*nh + r(25)*y(1)*no
     &         + r(26)*y(1)*y(3) - r(16)*y(4)*y(1)
     &         - r(21)*y(4)*y(2)

c
c  energy equation
c
      yp(5) = - r(1)*no*th(1) - r(2)*no*th(2) - r(3)*no*th(3)
     &         - r(4)*no*th(4) - r(5)*no*th(5) - r(6)*no*th(6)
     &         - r(7)*no*th(7) - r(8)*no*th(8)
     &         - r(10)*no*th(10) - r(11)*no*th(11)
     &         - r(14)*no*th(14) - r(9)*no*th(9)
     &         - r(13)*nh*th(13) + ens*so/y(1)
     &         - r(20)*2.*m1/m2*y(5)*no - y(5)/y(1)*yp(1)

      yp(5) = yp(5) - r(12)*y(3)*y(5) - r(15)*y(3)*y(5)
     &          - r(16)*y(4)*y(5) - r(18)*y(6)*y(5)
     &          - r(22)*y(2)*y(5) - r(23)*y(2)*nh/y(1)*y(5)
     &          - r(24)*y(2)*nh/y(1)*y(5)

c
c  vibrational population continuity
c
      yp(6) = (tail(1) + tail(2) + tail(3) + tail(4)
     &         + tail(5) + tail(6) + tail(7) + tail(8))*no
     &         - r(18)*y(1)*y(6) - r(17)*y(6)/10.
     &         - r(27)*y(6)*nh

      return
      end

c**********************************************************************
c
c       Fehlberg Fourth-Fifth Order Runge-Kutta Method
c
c       Written by H.A. Watts and L.F. Shampine
c                  Sandia Laboratories
c                  Albuquerque, NM
c       As published in
c             Forsythe, G.E., Malcolm, M.A., & Moler, C.B.,
c               COMPUTER METHODS FOR MATHEMATICAL
c               COMPUTATIONS, Prentice-Hall, NJ, 1977,
c               pp.135-147.
c
c       This subroutine, in conjunction with RKFS and FEHL,
c       performs a fourth order and a fifth order Runge-Kutta
c       routine on the system of differential equations.  It
c       uses the output from these two calculations to
c       estimate the error involved in the answer it gives.
c       If the error is too great, it reduces the time step
c       and tries again.  The process continues until an
c       answer with tolerable error is returned or the code
c       decides that too much work is being done.  For a more
c       detailed explanation of the routine see the above
```

```
c       book.
c       It should be noted that the routine is incorporated
c       exactly as it was given in Forsythe,et al.  As such
c       it is very general.  It is possible to specialize the
c       routine for use solely by this code, but that was
c       deemed unnecessary and undesirable for future
c       expansion of the model.
c
c*****************************************************************

        subroutine rkf45(f,neqn,y,t,tout,relerr,abserr,iflag,
     &                   work,iwork)
        integer neqn,iflag,iwork(5)
        real y(neqn),t,tout,relerr,abserr,work(3+6*neqn)
        external f
        integer k1,k2,k3,k4,k5,k6,k1m

        k1m=neqn+1
        k1=k1m+1
        k2=k1+neqn
        k3=k2+neqn
        k4=k3+neqn
        k5=k4+neqn
        k6=k5+neqn

        call rkfs(f,neqn,y,t,tout,relerr,abserr,iflag,work(1),
     &          work(k1m),work(k1),work(k2),work(k3),work(k4),
     &          work(k5),work(k6),work(k6+1),iwork(1),iwork(2),
     &          iwork(3),iwork(4),iwork(5))

        return
        end

        subroutine rkfs(f,neqn,y,t,tout,relerr,abserr,iflag,
     &              yp,h,f1,f2,f3,f4,f5,savre,savae,nfe,kop,
     &              int,jflag,kflag)
        logical hfaild,output
        integer neqn,iflag,nfe,kop,int,jflag,kflag
        real y(neqn),t,tout,relerr,abserr,h,yp(neqn),f1(neqn),
     &       f2(neqn),f3(neqn),f4(neqn),f5(neqn),savre,savae
        external f
        real a,ae,dt,ee,eeoet,esttol,et,hmin,remin,rer,s,
     &       scale,tol,toln,u26,epsp1,eps,ypk
        integer k,maxnfe,mflag
        real amax1,amin1
        data remin/1.e-12/
        data maxnfe/3000/

        if(neqn.lt.1)goto 10
        if((relerr.lt.0.).or.(abserr.lt.0.))goto 10
        mflag=iabs(iflag)
        if((mflag.eq.0).or.(mflag.gt.8))goto 10
        if(mflag.ne.1)goto 20
```

```
      eps=1.
5     eps=eps/2.
      epsp1=eps+1.
      if(epsp1.gt.1.)goto 5
      u26=26.*eps
      goto 50

10    iflag=8
      return

20    if((t.eq.tout).and.(kflag.ne.3))goto 10
      if(mflag.ne.2)goto 25

      if((kflag.eq.3).or.(int.eq.0))goto 45
      if(kflag.eq.4)goto 40
      if((kflag.eq.5).and.(abserr.eq.0.))goto 30
      if((kflag.eq.6).and.(relerr.le.savre)
     &    .and.(abserr.le.savae))goto 30
      goto 50

25    if(iflag.eq.3)goto 45
      if(iflag.eq.4)goto 40
      if((iflag.eq.5).and.(abserr.gt.0.))goto 45

30    stop

40    nfe=0
      if(mflag.eq.2)goto 50

45    iflag=jflag
      if(kflag.eq.3)mflag=iabs(iflag)

50    jflag=iflag
      kflag=0

      savre=relerr
      savae=abserr

      rer=2.*eps+remin
      if(relerr.ge.rer)goto 55

      relerr=rer
      iflag=3
      kflag=3
      return

55    dt=tout-t

      if(mflag.eq.1)goto 60
      if(int.eq.0)goto 65
      goto 80

60    int=0
      kop=0
```

```
      a=t
      call f(a,y,yp)
      nfe=1
      if(t.ne.tout)goto 65
      iflag=2
      return

65    int=1
      h=abs(dt)
      toln=0.
      do 70 k=1,neqn
      tol=relerr*abs(y(k))+abserr
      if(tol.le.0.)goto 70
      toln=tol
      ypk=abs(yp(k))
      if(ypk*h**5.gt.tol)h=(tol/ypk)**.2
70    continue
      if(toln.le.0.)h=0.
      h=amax1(h,u26*amax1(abs(t),abs(dt)))
      jflag=isign(2,iflag)

80    h=sign(h,dt)

      if(abs(h).ge.2.*abs(dt))kop=kop+1
      if(kop.ne.100)goto 85

      kop=0
      iflag=7
      return

85    if(abs(dt).gt.u26*abs(t))goto 95

      do 90 k=1,neqn
90    y(k)=y(k)+dt*yp(k)
      a=tout
      call f(a,y,yp)
      nfe=nfe+1
      goto 300

95    output=.false.

      scale=2./relerr
      ae=scale*abserr

100   hfaild=.false.

      hmin=u26*abs(t)

      dt=tout-t
      if(abs(dt).ge.2.*abs(h))goto 200
      if(abs(dt).gt.abs(h))goto 150

      output=.true.
```

```
      h=dt
      goto 200

150   h=.5*dt

200   if(nfe.le.maxnfe)goto 220

      iflag=4
      kflag=4
      return

220   call fehl(f,neqn,y,t,h,yp,f1,f2,f3,f4,f5,f1)
      nfe=nfe+5

      eeoet=0.
      do 250 k=1,neqn
      et=abs(y(k))+abs(f1(k))+ae
      if(et.gt.0.)goto 240

      iflag=5
      return

240   ee=abs((-2090.*yp(k)+(21970.*f3(k)-15048.*f4(k)))+
     &     (22528.*f2(k)-27360.*f5(k)))
250   eeoet=amax1(eeoet,ee/et)

      esttol=abs(h)*eeoet*scale/752400.

      if(esttol.le.1.)goto 260

      hfaild=.true.
      output=.false.
      s=.1
      if(esttol.lt.59049.)s=.9/esttol**.2
      h=s*h
      if(abs(h).gt.hmin)goto 200

      iflag=6
      kflag=6
      return

260   t=t+h
      do 270 k=1,neqn
270   y(k)=f1(k)
      a=t
      call f(a,y,yp)
      nfe=nfe+1

      s=5.
      if(esttol.gt.1.889568e-4)s=.9/esttol**.2
      if(hfaild)s=amin1(s,1.)
      h=sign(amax1(s*abs(h),hmin),h)

      if(output)goto 300
```

```
            if(iflag.gt.0)goto 100

            iflag=-2
            return

 300        t=tout
            iflag=2
            return

            end

            subroutine fehl(f,neqn,y,t,h,yp,f1,f2,f3,f4,f5,s)
            integer neqn
            real y(neqn),t,h,yp(neqn),f1(neqn),f2(neqn),f3(neqn),
           &     f4(neqn),f5(neqn),s(neqn)
            real ch
            integer k

            ch=h/4.
            do 221 k=1,neqn
 221        f5(k)=y(k)+ch*yp(k)
            call f(t+ch,f5,f1)

            ch=3.*h/32.
            do 222 k=1,neqn
 222        f5(k)=y(k)+ch*(yp(k)+3.*f1(k))
            call f(t+3.*h/8.,f5,f2)

            ch=h/2197.
            do 223 k=1,neqn
 223        f5(k)=y(k)+ch*(1932.*yp(k)+(7296.*f2(k)-7200.*f1(k)))
            call f(t+12.*h/13.,f5,f3)

            ch=h/4104.
            do 224 k=1,neqn
 224        f5(k)=y(k)+ch*((8341.*yp(k)-845.*f3(k))+(29440.*f2(k)
           &       -32832.*f1(k)))
            call f(t+h,f5,f4)

            ch=h/20520.
            do 225 k=1,neqn
 225        f1(k)=y(k)+ch*((-6080.*yp(k)+(9295.*f3(k)
           &       -5643.*f4(k)))+(41040.*f1(k)-28352.*f2(k)))
            call f(t+h/2.,f1,f5)

            ch=h/7618050.
            do 230 k=1,neqn
 230        s(k)=y(k)+ch*((902880.*yp(k)+(3855735.*f3(k)
           &     -1371249.*f4(k)))+(3953664.*f2(k)+277020.*f5(k)))

            return
            end

c*************************************************************************
```

```
c
c       This function performs a table look-up to determine
c       the rate coefficient at a given energy, en, and for a
c       given process, p.
c
c                 p                process
c               =====              =========
c                 1                B'1Σ+u
c                 2                B"1Σ+u
c                 3                D1Πu
c                 4                D'1Πu
c                 5                E-F1Σ+g
c                 6                a3Σ+g
c                 7                b3Σ+u
c                 8                c3Πu
c                 9                h2ion
c                 10               h2hn2
c                 11               h2hn3
c                 12               drec
c                 13               hion
c                 14               v0v1
c                 15               h2rec
c                 16               hrec
c                 17               vib-wall deex
c                 18               att
c                 19               (not used)
c                 20               mt
c                 21               mneut
c                 22               edet
c                 23               hdet
c                 24               adet
c                 25               (not used)
c                 26               pdiss
c                 27               V-T relax
c
c*****************************************************************

      real function rate(p,en)
      real en,on(27),th(27),rates(27,561,2),y(6),temp,
     &     length,tail(8)
      integer p,n
      character*7 file(27)
      common/oncff/on,file
      common/freq/th,rates,tail
      common/recom/y,temp,length

      if((on(p).eq.0.).or.(en.le.0.))then
           rate=0.
           return
         endif

      if((p.eq.21).or.(p.eq.23).or.(p.eq.24))then
           rate=rates(p,1,2)
           return
```

```
            endif

          if((p.eq.15).or.(p.eq.16))then
               if(en.gt.1.e7)then
                   rate=0.
                 else
                   rate=8.75e-27/en**(4.5)*y(1)
                 endif
               return
            endif

          if(p.eq.17)then
               rate=1.56e6*sqrt(temp/2.)/length
               return
            endif

          if(p.eq.27)then
               rate=40./8.*1.5e-10*exp(-.1603/temp)
               return
            endif

          if(en.lt..01)then
               rate=0.
               return
            endif

          if(en.le.10.)then
               n=int(en/.05+.5)
               goto 1
            endif

          if(en.le.100.)then
               n=int(en/.5+181.5)
               goto 1
            endif

          if(en.le.1000.)then
               n=int(en/5+361.5)
               if(n.eq.561)n=560
               goto 1
            endif

          rate=rates(p,561,2)
          return

    1     rate=(en-rates(p,n,1))/(rates(p,n+1,1)-rates(p,n,1))*
         &      (rates(p,n+1,2)-rates(p,n,2))+rates(p,n,2)

          return
          end

c*************************************************************
c
c       This subroutine calculates the effect of wall
```

```
c       collisions on the average energy of the source by
c       modifying the Thomson distribution by  a survival
c       probability.  It also calculates the source strength.
c
c*****************************************************************

        subroutine thomson(ens,volt,so)
        real ens,volt,tol,integral(3),tl(200),a3(200),h(200),
     &       fa(200),fc(200),fb(200),s(200),l(200),fd,fe,s1,
     &       s2,v(8),so,eps,epsp1

c
c  eps is machine epsilon, or the limit of machine accuracy.
c  It is calculated to be used as a minimum allowed error
c  tolerance.
c
        tol=1.e-2
        eps=1.
 10     eps=.5*eps
        epsp1=eps+1.
        if(epsp1.gt.1.)goto 10
        eps=20.*eps

        do 100 j=1,3

        integral(j)=0.

        do 1 i=1,200
        tl(i)=0.
        a3(i)=0.
        h(i)=0.
        fa(i)=0.
        fc(i)=0.
        fb(i)=0.
        s(i)=0.
        l(i)=0.
 1      continue

        fd=0.
        fe=0.
        s1=0.
        s2=0.
        do 2 i=1,8
 2      v(i)=0.

        i=1
        tl(i)=10.*tol
        a3(i)=0.
        h(i)=volt/2.
        fa(i)=ft(0.,j)
        fc(i)=ft(h(i),j)
        fb(i)=ft(volt,j)
        s(i)=h(i)*(fa(i)+4.*fc(i)+fb(i))/3.
        l(i)=1.
```

```
3       if(i.le.0)goto 100

        if(tl(i).lt.eps)tl(i)=eps

        fd=ft(a3(i)+h(i)/2.,j)
        fe=ft(a3(i)+3.*h(i)/2.,j)
        s1=h(i)*(fa(i)+4.*fd+fc(i))/6.
        s2=h(i)*(fc(i)+4.*fe+fb(i))/6.
        v(1)=a3(i)
        v(2)=fa(i)
        v(3)=fc(i)
        v(4)=fb(i)
        v(5)=h(i)
        v(6)=tl(i)
        v(7)=s(i)
        v(8)=l(i)

        i=i-1

        if(abs(s1+s2-v(7)).lt.v(6))then
             integral(j)=integral(j)+s1+s2
           else
             if(v(8).ge.200)then
                write(6,*)'Integration failed in Thomson'
                stop
              else
                i=i+1
                a3(i)=v(1)+v(5)
                fa(i)=v(3)
                fc(i)=fe
                fb(i)=v(4)
                h(i)=v(5)/2.
                tl(i)=v(6)/2.
                s(i)=s2
                l(i)=v(8)+1.
                i=i+1
                a3(i)=v(1)
                fa(i)=v(2)
                fc(i)=fd
                fb(i)=v(3)
                h(i)=h(i-1)
                tl(i)=tl(i-1)
                s(i)=s1
                l(i)=l(i-1)
              endif
           endif

        goto 3

100     continue

        ens=integral(1)/integral(2)
        so=integral(2)/integral(3)
```

```
      return
      end

c
c  This function is the integrand used in the routine thomson
c
      real function ft(e,j)
      real e,p,x

      if(j.eq.3)then
          ft=1./(e+15.427)**2.
          goto 2
        endif

      x=fwall(e)
      y=fcoll(e)
      if(x.eq.0.)then
          p=1.
        else
          p=1.-x/(x+y)
        endif

      ft=p/(e+15.427)**2.
      if(j.eq.1)ft=ft*e

 2    return
      end

c*********************************************************************
c
c     This subroutine outputs various pieces of information
c     at the end of the run in order to better understand
c     what is going on in the discharge.
c
c*********************************************************************

      subroutine endout(y)
      real y(6),telec,r(27),cp,cn,pin,pout,th(27),ens,so,no,
     &     nh,m1,m2,rates(27,561,2),telec,relectron,tail(8),
     &     distrib,area,vol,vp,volt,curr,ftail(0:100)

      common so,no,nh
      common/ener/ens,m1,m2
      common/freq/th,rates,tail
      common/geom/area,vol,vp
      common/power/volt,curr
      common/dist/ftail

      telec=2.*y(5)/3.
      write(20,1)y(1),y(2),y(3),y(4),y(6),telec
1     format(//20x,'SUMMARY'//'Electron density = ',1pe10.3/
     &                        'H- density       = ',1pe10.3/
     &                        'H2+ density      = ',1pe10.3/
```

```
     &                          'H+ density       = ',1pe10.3/
     &                          'H2(v) density    = ',1pe10.3/
     &                       'Electron Temperature = ',0pf6.3)
        write(20,13)y(2)/y(1)
 13     format(/'N-/Ne ratio  = ',1pe10.3)
        write(20,12)no,nh,so,ens
 12     format(/'H2 density   = ',1pe10.3/
     &          'H density    = ',1pe10.3/
     &          'Source strength = ',1pe10.3/
     &          'Average energy of source = ',0pf6.3)

c       Charged particle balance

        cp=y(3)+y84r
        cn=y(1)+y(2)
        write(20,2)cp,cn
 2      format(//'CHARGED PARTICLE BALANCE'/
     &         'Total POSITIVE charge density = ',1pe10.3/
     &         'Total NEGATIVE charge density = ',1pe10.3/)

c       Rate coefficients

        write(20,4)
 4      format(//'RATE COEFFICIENTS IN STEADY STATE')
        do 3 i=1,27
 3      r(i)=rate(i,y(5))
        write(20,9)'Dissociative Recombination = ',r(12)
        write(20,9)'Vibration                  = ',r(14)
        write(20,9)'Recombination - H2         = ',r(15)
        write(20,9)'Recombination - H          = ',r(16)
        write(20,9)'Dissociative Attachment    = ',r(18)
        write(20,9)'Momentum Transfer          = ',r(20)
        write(20,9)'Mutual Neutralization      = ',r(21)
        write(20,9)'Detachment by e            = ',r(22)
        write(20,9)'Detachment by H            = ',r(23)
        write(20,9)'Associative Detachment     = ',r(24)
        write(20,9)'Polarized Dissociation     = ',r(26)
        write(20,9)'V-T relaxation             = ',r(27)
        relectron=(tail(1)+tail(2)+tail(3)+tail(4)
     &             +tail(5)+tail(6)+tail(7)+tail(8))/y(1)
        write(20,9)'Total electronic - tail    = ',relectron
        relectron=r(1)+r(2)+r(3)+r(4)+r(5)+r(6)+r(7)+r(8)
     &            +r(10)+r(11)
        write(20,9)'Total electronic - MB      = ',relectron
 9      format(a,1pe10.3)

c       Power balance

        write(20,5)
 5      format(//'POWER PARTITION')
        pout=0.
        pin=ens*so/y(1)
        x=0.
        do 6 i=1,8
```

```
 6      x=x+r(i)*th(i)
        x=(x+r(10)*th(10)+r(11)*th(11))*no
        write(20,10)'e-beam power input          = ',pin
 10     format(a,1pe10.3)
        write(20,11)'power into electronic       = ',x,x/pin*100
        pout=pout+x
        x=no*th(14)*r(14)
        write(20,11)'power into vibrational      = ',x,x/pin*100
        pout=pout+x
        x=y(3)*y(5)*r(12)
        write(20,11)'power into diss rec         = ',x,x/pin*100
        pout=pout+x
        x=no*th(9)*r(9)
        write(20,11)'power into H2 ionization    = ',x,x/pin*100
        pout=pout+x
        x=nh*th(13)*r(13)
        write(20,11)'power into H ionization     = ',x,x/pin*100
        pout=pout+x
        x=y(3)*y(5)*r(15)
        write(20,11)'power into recombination    = ',x,x/pin*100
        pout=pout+x
        x=y(4)*y(5)*r(16)
        write(20,11)'power into recomb of H      = ',x,x/pin*100
        pout=pout+x
        x=y(6)*y(5)*r(18)
        write(20,11)'power into diss att         = ',x,x/pin*100
        pout=pout+x
        x=2.*m1/m2*y(5)*no*r(20)
        write(20,11)'power into momentum trans   = ',x,x/pin*100
        pout=pout+x
        x=y(2)*y(5)*r(22)
        write(20,11)'power into detach by e      = ',x,x/pin*100
        pout=pout+x
        x=y(2)*nh/y(1)*y(5)*r(23)
        write(20,11)'power into detach by H      = ',x,x/pin*100
        pout=pout+x
        x=y(2)*nh/y(1)*y(5)*r(24)
        write(20,11)'power into assoc det        = ',x,x/pin*100
        pout=pout+x
 11     format(a,1pe10.3,2x,0pf7.2,'%')

        write(20,8)pin,pout
 8      format(/'Total power input =',1pe10.3/
     &          'Total power output =',1pe10.3)

c
c  this section of code outputs the EEDF into the file
c  dist.out in the correct format to be used by 'graph'
c
        open(unit=15,file='dist.out',status='new')
        write(15,*)'Electron distribution'
        write(15,*)'Energy'
        write(15,*)' (eV)'
        write(15,*)'ftot(e)'
```

```
      write(15,*)'cm-3eV-1'
      write(15,'(i3)')101
      write(15,*)0.,100.
      write(15,*)0.,2.*y(1)
      do 20 i=0,100
      en=float(i)
      distrib=sqrt(4/3.14159)*y(1)/telec**(3./2.)
     &          *exp(-en/telec)
      distrib=distrib+ftail(i)
21    write(15,*)en,dist
20    continue

      return
      end
```

REFERENCES

[1] Limpaecher, R., & MacKenzie, K.R., "Magnetic Multipole Containment of Large Uniform Collisionless Quiescent Plasmas", Rev. Sci. Instrum., 44, 726-731, (1973).

[2] Holmes, A.J.T., "Role of the Anode Area in the Behavior of Magnetic Multipole Discharges", Rev. Sci. Instrum., 52, 1814-1823, (1981).

[3] Leung, K.N., Kribel, R.E., Goede, A.P.H., & Green, T.S., "Primary Electron Confinement Measurement in a Multipole Device", Phys. Letters, 66A, 112-114, (1978).

[4] Green, T.S., Holmes, A.J.T., & Nightingale, M.P.S., "A Model for H^- Volume Production Ion Sources", Proc. 4th Int Symp on Production & Neutralization of Negative Ions and Beams, AIP Conf Proc. 158, 208-218, (1986).

[5] Holmes, A.J.T., Lea, L.M., Newman, A.F., & Nightingale, M.P.S., "Extraction of H^- and D^- Ions from a Large Magnetic Multipole Source", Rev. Sci. Instrum., 58, 223-234, (1987).

[6] Bacal, M., Bruneteau, A.M., Graham, W.G., Hamilton, G.W., & Nachman, M., "Pressure and Electron Temperature Dependence of H^- Density in a Hydrogen Plasma", J. Appl. Phys., 52, 1247-1254, (1981).

[7] Goede, A.P.H., & Green, T.S., "Operation Limits of Multipole Ion Sources", Phys. Fluids, 25, 1797-1810, (1982).

[8] Holmes, A.J.T., Dammertz, G., & Green, T.S., "H^- and Electron Production in a Magnetic Multipole Source", Rev. Sci. Instrum., 56, 1697-1702, (1985).

[9] Leung, K.N., Ehlers, K.W., & Pyle, R.V., "Optimization of H^- Production in a Magnetically Filtered Multicusp Source", Rev. Sci. Instrum., 56, 364-368, (1985).

[10] Bretagne, J., Delouya, G., Gorse, C., Capitelli, M., & Bacal,M., "Electron Energy Distribution Functions in Electron-Beam-Sustained Discharges : Application to Magnetic Multicusp Hydrogen Discharges", J. Phys. D, 18, 811-825, (1985).

[11] Bailey, W., & Jones, R., "Electron Energy Distributions in Magnetic Multicusp Hydrogen Discharges", Proc.

4th Int Symp on Production and Neutralization of Negative Ions & Beams, AIP Conf Proc. 158, 16-25, (1986).

[12] Fukumasa, O., & Saeki, S., "Numerical Studies on Volume Production of Negative Ions in Hydrogen Plasmas", J. Phys. D: Appl. Phys., 18, L21-L26, (1985).

[13] Wadehra, J.M., "Rates of Dissociative Attachment of Electrons to Excited H_2 and D_2", Appl. Phys. Lett., 35, 917-919, (1979).

[14] Peart, B. & Dolder, K.T., "Collisions Between Electrons and H_2^+ Ions: VI. Measurements of Cross Sections for the Simultaneous Production of H^+ and H^-", J. Phys. B: Atom. Molec. Phys., 8, 1570-1574, (1975).

[15] Bruneteau Mordin, Anne-Marie, "Etude sur l'Ion Negatif d'Hydrogene dans des Decharges a Basse Pression", PhD dissertation, University of South Paris - Centre d'Orsay, 1983 (Orsay order no. 2740). (in French)

[16] Walton, D.S., Peart, B., & Dolder, K.T., "A Measurement of Cross Sections for Detachment from H^- by a Method Employing Inclined Ion and Electron Beams", J. Phys. B: Atom. Molec. Phys., 4, 1343-1348, (1971).

[17] Dalgarno, A., & Browne, J.C., "The Associative Detachment of H and H^-", Astrophys. Journal, 149, 231-232, (1967).

[18] Moseley, J., Aberth, W., & Peterson, J.R., "$H^+ + H^-$ Mutual Neutralization Cross Section Obtained with Superimposed Beams", Phys. Rev. Letters, 24, 435-439, (1970).

[19] Peart, B., Grey, R., & Dolder, K.T., "Measurement of Cross Sections for the Mutual Neutralization of H^+ and H^- Ions", J. Phys. B:Atom. Molec. Phys., 9, L369-L372, (1976).

[20] Rapp, D., & Englander-Golden, P., "Total Cross Sections for Ionization and Attachment in Gases by Electron Impact. I. Positive Ionization", J. Chem. Phys., 43, 1464-1479, (1965).

[21] de Heer, F.J., McDowell, M.R.C., & Wagenaar, R.W., "Numerical Study of the Dispersion Relation for e^- - H Scattering", J. Phys. B: Atom. Molec. Phys., 10, 1945-1953, (1977).

[22] Peart, B. & Dolder, K.T., "Collisions Between Electrons

and H_2^+ Ions: V. Measurements of Cross Sections for Dissociative Recombination", J. Phys. B: Atom. Molec. Phys., 7, 236-243, (1974).

[23] Golant, V.E., Zhilinsky, A.P., & Sakharov, I.E., Fundamentals of Plasma Physics, John Wiley & Sons, NY, (1980).

[24] Bretagne, J., Capitelli, M., & Gorse, C., "Modeling of Electron Energy Distribution Functions and Vibrational Distributions in Volume H^- Ion Sources", Proc. 4th Int Symp on Production & Neutralization of Negative Ions & Beams, AIP Conf Proc 158, 48-58, (1986).

[25] Arrighini, G.P., Biondi, F., & Guidotti, C., "A Study of the Inelastic Scattering of Fast Electrons from Molecular Hydrogen", Molec. Phys., 41, 1501-1514, (1980).

[26] Chung, S., & Lin, C.C., "Application of the Close-Coupling Method to Excitation of Electronic States and Dissociation of H_2 by Electron Impact", Phys. Rev. A, 17, 1874-1891, (1978).

[27] Gorse, C., Bretagne, J., Bacal, M., Capitelli, M., "Vibrational Excitation and Negative Ion Production in Magnetic Multicusp Hydrogen Discharges", Chem. Phys., 93, 1-12, (1985).

[28] Thomson, J.J., & Thomson, G.P., Conduction of Electricity through Gases, Vol. 2, Cambridge University Press, Cambridge, (1933).

[29] Forsythe,G., Malcolm, M., & Moler, C., Computer Methods for Mathematical Computations, Prentice-Hall, Englewood Cliffs, NJ, (1977).

[30] Burden, R.L. & Faires, J.D., Numerical Analysis, 3ed, Prindle, Weber & Schmidt, Boston, (1985).

[31] Seshadri, S.R., Fundamentals of Plasma Physics, American Elsevier Publishing Co. Inc., NY, 1973.

[32] Bretagne, J., Delouya, G., Capitelli, M., Gorse, C., & Bacal, M., "On the Electron Energy Distribution Functions in Low-Pressure Magnetic Multicusp Hydrogen Discharges", J. Phys. D: Appl. Phys., 19, 1197-1211, (1986).

[33] Péalat, M., Taran, J., Taillet, J., & Bacal, M., Report ONERA No. 28/7131 PY, (1981).

[34] Leung, K.N., Ehlers, K.W., & Bacal, M., "Extraction of

Volume-Produced H^- Ions from a Multicusp Source", Rev. Sci. Instrum., 54, 56-61, (1983).

[35] York, R.L., Stevens, R.R., Jr., Leung, K.N., & Ehlers, K.W., "Extraction of H^- Beams from a Magnetically Filtered Multicusp Source", Rev. Sci. Instrum., 55, 681-686, (1984).

[36] Bacal, M., Bruneteau, A.M., & Nachman, M., "Negative Ion Production in Hydrogen Plasmas Confined by a Multicusp Magnetic Field", J. Appl. Phys., 55, 15-24, (1984).

[37] "APS Study: Science and Technology of Directed Energy Weapons", Rev. Mod. Phys., 59, Part II, (1987).

VITA

Lieutenant David E. Bell was born on 20 December 1963 in Würzburg, Germany. He graduated from J. M. Hanks High School in El Paso, Texas, in 1982 and attended the University of Texas at El Paso, from which he graduated with honors, receiving the degree of Bachelor of Science in physics in May 1986. Upon graduation, he received a commission in the USAF through the AFROTC program and entered the School of Engineering, Air Force Institute of Technology.

Permanent address: 8338 North Loop
El Paso, Texas 79907

UNCLASSIFIED
SECURITY CLASSIFICATION OF THIS PAGE

REPORT DOCUMENTATION PAGE

Form Approved
OMB No. 0704-0188

1a. REPORT SECURITY CLASSIFICATION UNCLASSIFIED	1b RESTRICTIVE MARKINGS
2a. SECURITY CLASSIFICATION AUTHORITY	3 DISTRIBUTION / AVAILABILITY OF REPORT Approved for public release; distribution unlimited
2b. DECLASSIFICATION / DOWNGRADING SCHEDULE	
4. PERFORMING ORGANIZATION REPORT NUMBER(S) AFIT/GEP/ENP/87D-2	5 MONITORING ORGANIZATION REPORT NUMBER(S)
6a. NAME OF PERFORMING ORGANIZATION School of Engineering	6b OFFICE SYMBOL (If applicable) AFIT/ENP
6c. ADDRESS (City, State, and ZIP Code) Air Force Institute of Technology Wright-Patterson AFB OH 45433-6583	7a NAME OF MONITORING ORGANIZATION 7b ADDRESS (City, State, and ZIP Code)
8a. NAME OF FUNDING / SPONSORING ORGANIZATION	8b OFFICE SYMBOL (If applicable)
8c. ADDRESS (City, State, and ZIP Code)	9 PROCUREMENT INSTRUMENT IDENTIFICATION NUMBER 10 SOURCE OF FUNDING NUMBERS

PROGRAM ELEMENT NO	PROJECT NO	TASK NO	WORK UNIT ACCESSION NO

11. TITLE (Include Security Classification)
A MOMENT APPROACH TO MODELING NEGATIVE ION SOURCES

12. PERSONAL AUTHOR(S)
David E. Bell, B.S., 2d Lt, USAF

13a. TYPE OF REPORT	13b TIME COVERED	14. DATE OF REPORT (Year, Month Day)	15. PAGE COUNT
MS Thesis	FROM _____ TO _____	1987 December	~~116~~ 119

16. SUPPLEMENTARY NOTATION

17. COSATI CODES			18 SUBJECT TERMS (Continue on reverse if necessary and identify by block number)
FIELD	GROUP	SUB-GROUP	
20	09		Negative Ion Source, Moment Model, Scaling Laws, Volume Ion Production, Magnetic Multicusp Ion Source

19 ABSTRACT (Continue on reverse if necessary and identify by block number)

Thesis Advisor: Dr. William F. Bailey
Associate Professor of Engineering Physics

(Abstract on reverse)

20 DISTRIBUTION / AVAILABILITY OF ABSTRACT X UNCLASSIFIED/UNLIMITED ☐ SAME AS RPT ☐ DTIC USERS	21 ABSTRACT SECURITY CLASSIFICATION UNCLASSIFIED
22a NAME OF RESPONSIBLE INDIVIDUAL Dr. William F. Bailey, Associate Professor	22b TELEPHONE (Include Area Code) (513) 255-2012
	22c OFFICE SYMBOL AFIT/ENP

DD Form 1473, JUN 86 Previous editions are obsolete

SECURITY CLASSIFICATION OF THIS PAGE
UNCLASSIFIED

Applications in low energy kinetic studies, high energy accelerator technology and beam heating in fusion studies have fostered experimental and theoretical studies of the volume production of negative hydrogen ions in a magnetic multicusp discharge. In this study, a self-consistent approach based on Maxwellian moments of the Boltzmann equation is presented. The departure of the electron energy distribution from a Maxwellian is also discussed and incorporated. The results of this model for discharge currents ranging from 1-100 A, for pressures ranging from 1-100 mTorr, and for voltages ranging from 20-100 V are compared to previous studies. Finally, scaling laws with discharge current, gas pressure, and discharge voltage are established and used to predict the optimum operating regime for a magnetic multicusp ion source.

END

FILMED

MARCH, 1988

DTIC